UNIVERSITÀ DEGLI STUDI DI MILANO
DEPARTMENT OF MEDICINE

DOCTORAL PROGRAMME IN TRANSLATIONAL MEDICINE

34th CYCLE

Investigating glutamate toxicity associated to *Park2* mutations in pre-clinical models of Parkinson's Disease.

Doctoral dissertation of:

Ilaria TREZZI

Identification Nr. R12457

Supervisor: Prof. Giacomo. P. COMI

Co-supervisor: Dott. Alessio DI FONZO

The Chair of the Doctoral Program: Prof. Chiarella SFORZA

Year 2020-2021

What is diurnal fluctuation? Alleviation after sleep is a reversible process of consumption and restoration of some dopamine-related substance. Heredity and early-onset indicate inborn error in the metabolism, and progression of the disease reflects degeneration and neuronal loss of the substantia nigra. I was convinced that "early-onset parkinsonism with diurnal fluctuation" was a new disease.

(Yamamura Y. The long journey to the discovery of PARK2: The 50th Anniversary of Japanese Society of Neuropathology. Neuropathology. 2010)

ABSTRACT

Background: *Park2* mutations cause Autosomal Recessive Juvenile Parkinsonism (ARJP), characterized by the loss of dopaminergic (DA) neurons in the substantia nigra pars compacta (SNpc). *Park2* encodes for a ubiquitin-ligase protein whose mutation upregulates Gluk2, a subunit of the glutamate kainate receptor (KAR), expressed in SNpc neurons. *Park2* is highly expressed also in astrocytes and KARs upregulation may induce excitotoxicity both in DA neurons and glia, leading to an early synaptopathy, neuroinflamation and neurodegeneration.

Aims and Objectives: 1. To generate *Park2* induced pluripotent stem cells (iPSCs)-derived *in vitro* cellular models; **2.** To characterize *Park2* iPSCs-derived *in vitro* cellular models; **3.** to test glutamate toxicity due to KAR upregulation in *Park2* cellular models.

Materials and Methods: Fibroblasts and lymphocytes from *Park2* patients and age-matched controls were reprogrammed into iPSCs. The iPSCs were further differentiated into dopaminergic neurons, astrocytes and mesencephalic organoids were generated and differentiated. Protein expression profile was analysed through western blot (WB), qPCR and immunofluorescence (IF). Electrophysiology assessment was performed on dopaminergic neurons and midbrain organoids in order to better functionally profile these models.

Results: Gluk2 levels resulted significantly increased in PARK2 midbrain organoids compared to CTR both at WB ($p < 0.001$) and qPCR analyses ($p < 0.001$). Gluk2 levels resulted also significantly enhanced in PARK2 astrocytes both at WB ($p < 0.05$) and qPCR analyses ($p < 0.05$). TH mRNA and protein levels were significantly increased both in PARK2 dopaminergic neurons (WB $p < 0.01$; qPCR $p < 0.0001$; IF $p < 0.0001$) and midbrain organoids (WB $p < 0.01$; qPCR $p < 0.0001$; IF $p < 0.0001$) compared to CTR. Glial fibrillary acidic protein (GFAP), a marker of reactive astrocytes, resulted enhanced

in PARK2 astrocytes and especially in PARK2 midbrain organoids (WB $p < 0.001$; IF $p < 0.01$). EAAT2, the astrocytic glutamate transporter resulted reduced in mutated lines (WB $p < 0.01$). Calcium-imaging and HD-MEAs show an oscillatory augmented reactivity in PARK2 midbrain organoids.

Conclusions and perspectives: Gluk2 expression was enhanced in PARK2 astrocytes and midbrain organoids, confirming the previous finding that *Park2* mutations lead to KAR upregulation (Maraschi A, 2014). Neuronal reactivity was also found increased in PARK2 midbrain organoids at electrophysiology assessment, maybe linked to glutamate dysregulation. Two innovative findings emerged from this study. First of all, that TH expression resulted increased in PARK2, supporting previous finding that stated an augmented dopamine turnover and a reduced dopamine re-uptake (Jiang H., 2012). This is an impairment that happens early in the neurodegenerative process and that could consequently lead to an excessive oxidative stress and consequent neurodegeneration. The second original result is that PARK2 is associated to an increased astrocytic reactivity and a possible dysfunction of astrocytic glutamate transporter EAAT2. This finding means that astrocytes play a key role in neurodegeneration although it is not clear whether they contribute to the initiation or propagation of it. Their increased reactivity could be the consequence of a glutamate toxicity or glutamate toxicity could result from reactive astrocytes dysfunction, not able to process the excessive glutamate influx. Further studies are required in order to establish *Park2* role in TH expression regulation, in astrocytic reactivity induction and in glutamate toxicity.

CONTENTS

1. Introduction

1.1 Parkinson's Disease

Parkinson's Disease (PD) is the second most common neurodegenerative disorder after Alzheimer's Disease (AD) and it affects 2-3 % of the population above 65 years of age. Its prevalence is higher in Europe, North and South America (Kalia LV, 2015). PD is generally viewed as a slowly progressive neurodegenerative disorder and the majority of cases, considered sporadic, are caused by a combination of genetic and environmental factors that promote the neurodegenerative process. Age is considered by far the most important risk factor for the developing of PD. As a matter of fact, PD prevalence and incidence increase exponentially with age, reaching a peak after 80 years of age. Gender is also an established risk factor, with the male having a 1.5 times higher risk of developing the disease.

The main hallmark of PD is the progressive loss of dopaminergic neurons located in the substantia nigra pars compacta (SNpc) of the midbrain. In particular, the ventral tier of the SNpc is the most affected one. This area contains those neurons that project to the dorsal putamen of the striatum. The resultant dopamine deficiency within the basal ganglia leads to a movement disorder characterized especially by bradykinesia and rigidity.

PD motor features typically include beside bradykinesia and muscular rigidity, rest tremor and postural and gait impairment. These motor features are heterogeneous and this has led to the classification of different disease's subtypes (Gibb WR, 1988). From the clinical point of view, we can define two major subtypes: a tremor dominant-PD and a non-tremor dominant PD. The last one subtype displays two different forms: an akinetic-rigid syndrome and a postural instability disorder. There is also a third group of patients which have a mixed and indeterminate phenotype with different motor symptoms of comparable severity. All those different subtypes have a variable prognosis; tremor-dominant PD

often has a slower rate of progression and less functional disability than non-tremor-dominant PD (Jankovic J, 1990). The clinical diversity and the various progression rate rise the hypothesis that they have distinct aetiologies and pathogenesis (Marras C, 2013).

PD is a complex disease characterized also by non-motor symptoms, including olfactory dysfunction, cognitive impairment, psychiatric symptoms, sleep disorders, autonomic dysfunction, pain, and fatigue. These non-motor symptoms can manifest early in the premotor or prodromal phase of the disease, especially impaired olfaction, constipation, depression, excessive daytime sleepiness, and rapid eye movement sleep behaviour disorder (RBD). The premotor phase can be prolonged and the average latency can be 10-20 years (Postuma RB., 2012). The pathogenic process that causes PD involves multiple neuroanatomical areas other than SNpc and it starts during the premotor phase. This prodromal phase represents the correct period where a disease-modifying therapy could be effective in preventing or at least delaying the development of PD.

Progression of PD is marked by worsening of motor symptoms that leads to an advanced stage where complications are related both to the disease and the long-term dopaminergic treatment. In the late-stage of the disease motor symptoms become treatment-resistant and non-motor features are prominent. At this stage axial motor symptoms such as postural instability, freezing of gait, falls, dysphagia, and speech dysfunction prevail. Also dementia becomes prevalent and around 83% of PD patients with a 20-years-history of the disease suffer from it (Hely MA, 2008).

As already anticipated, the majority of cases is sporadic and result of a genetic predisposition combined to environmental risk factors. A meta-analysis that examined 30 different potential risk factors identified 11 environmental factors that significantly altered the risk of PD. Factors increasing the risk (in decreasing order of strength of association) are pesticide exposure, prior head injury, rural living, β-blocker use, agricultural occupation, and well-water drinking (Noyce AJ, 2012). On the other end, there are also environmental factors associated with a decreased risk (in decreasing order of strength of association) such as tobacco smoking, non-steroidal anti-inflammatory drug

use, coffee drinking, and alcohol consumption and calcium channel blocker use. Also urate serum concentration, not taken into consideration in this meta-analyses, is inversely associated with the risk of developing PD especially for men (Cipriani S, 2010).

Although PD is mainly sporadic, monogenic, mendelian mutations account for 5 to 10% of PD cases. The first gene discovered as causative for PD is the alpha synuclein (*SNCA*) which was identified in 1997 (Polymeropoulos MH, 1997). The first mutation identified was the A53T; later studies identified other missense mutations, duplications and triplications of SNCA, confirming the causative role of this gene in PD. Although these mutations are rare, they display an important causative role in autosomal dominant PD (ADPD) because they have a high penetrance. Among ADPD forms mutations in leucine rich repeat kinase 2 (*LRRK2*) gene represents the major causative gene mutations of the disease, causing a typical late onset PD with a benign course. Other genetic cause of ADPD are rarer and among them there are: Vacuolar Protein Sorting 35 (*VPS35*) gene, Eukaryotic Translation Initiation Factor 4 Gamma 1 (*EIF4G*) gene, DnaJ Heat Shock Protein Family (Hsp40) Member C13 (*DNAJC13*) gene and Coiled-Coil-Helix-Coiled-Coil-Helix Domain Containing 2 (*CHCHD2*) gene.

Unlike ADPD, which tends to have a late age of onset similar to sporadic PD, recessively inherited parkinsonism (ARPD) is more frequently associated with an earlier onset, typically before 40 years of age. Among the autosomal recessive forms, mutations in Parkinson-disease 2 (*Park2*) are by far the most frequent genetic cause of early onset Parkinson's Disease (EOPD). Ishikawa et al characterized in 1996 a cohort of patients with a familial juvenile parkinsonism, a female predominance, a young onset (mean age-at-onset was 27.8 years) and a slow progression. The phenotype was characterized by bradykinesia, rigidity, mild tremor and other atypical features, especially foot dystonia, and hyperreflexia. No dementia or autonomic features were noted and patients showed an excellent response to levodopa, but with frequent levodopa induced dyskinesias (LID) and wearing off (Ishikawa A, 1996). Matsumine et al identified an associated locus at 6q25.2–27 through linkage analysis (Matsumine H, 1997). Kitada et al then identified the *Park2* gene and protein in 1998 (Kitada T., 1998). The same year Hattori et al identified four homozygous deletional mutations (Hattori N, 1998) in EOPD patients. Among PD

patients with disease onset before age 45 years, *Park2* mutations are seen in up to 50% of familial cases and about 15% of sporadic cases (Lücking CB, 2000) (Periquet M, 2003). Mutations in *PINK1* and *DJ-1* are other less common genetic cause of ARPD and they account, respectively 1–8% and 1–2% of EOPD (Singleton AB, 2013). ARPD are caused by homozygous or compound heterozygous mutations in these three genes. In some patients, only a single heterozygous mutation has been detected (Klein C, 2007) and this represents an intriguing phenomenon that needs further investigation in order to define their causative role in the disease. All the proteins encoded by *Park2*, *PINK1* and *DJ-1* are necessary for the mitochondrial homeostasis. Parkin, which is an E3 ubiquitin ligase, and PINK1, which is a serine-threonine protein kinase, work in concert to degrade damaged mitochondria through a process called mitophagy. Among these three genes, the function of *DJ-1* is less well characterised, but it seems to protect mitochondria from oxidative stress.

There are additional genes that were found implicated in generating atypical PD forms. They were identified from kindreds and patient cohorts and they are: ATPase cation transporting 13A2 (*ATP13A2*) gene, chromosome 9 open reading frame 72 (*C9ORF72*) gene, F-Box Protein 7 (*FBXO7*) gene, phospholipase A2 group VI (*PLA2G6*) gene, DNA polymerase γ subunit 1 (*POLG1*) gene, spinocerebellar ataxia 1 (*SCA1*) gene, spinocerebellar ataxia 3 (*SCA3*) gene, synaptojanin 1 (*SYNJ1*) gene and *RAB39B* (Puschmann, 2013) (Krebs CE, 2013) (Wilson GR, 2014). All these mutations are rare and they cause an atypical parkinsonism characterized by a prominent cognitive impairment, ophthalmologic abnormalities, pyramidal signs and ataxia.

Considering the genetic risk factors for PD, a novel genetic element has been recently discovered and it can be considered the major genetic risk factor for PD. This gene is *GBA*, which encodes β-glucocerebrosidase, the lysosomal enzyme deficient in Gaucher's Disease (GD) (Sidransky E., 2012). Results of a large multicentre study, including more than 5000 patients with PD and an equal number of matched controls showed an odds ratio greater than 5 for any *GBA* mutation in PD patients versus controls (Sidransky E, 2009).

Advances in genomics and bioinformatics have uncovered additional genetic risk factors for PD. In the past decade, genetic association studies have discovered dozens of potential gene loci in PD. These studies included also genome-wide association studies (GWAS) that analysed up to 500.000 common genetic variants, such as single-nucleotide polymorphisms (SNPs), in the human genome of large case-control cohorts. They compared the frequency of these SNPs between people with and without PD. A recent a meta-analysis of European-ancestry PD GWAS revealed that 24 loci are significantly associated to the risk of developing the disease. These loci include *GBA* but also genes that are associated to monogenic forms of PD such as *LRRK2* and *SNCA* (Nalls MA, 2014).

As mentioned before, the neuropathological hallmark of PD is the degeneration of dopaminergic neurons of the SNpc. One major hypothesis that could explain the selective vulnerability of dopaminergic neurons resides in their pacemaker-like properties that lead to frequent intracellular calcium transients with consequent cellular stress and disruption of cellular homeostasis. In PD the neurodegenerative process is not related only to these dopaminergic neurons, but other brain regions are impaired, such as the locus coeruleus, the nucleus basalis of Meynert, the pedunculopontine nucleus, the raphe nucleus, the dorsal motor nucleus of the vagus, the amygdala, and the hypothalamus (Dickson, 2012).

Beside the neurodegeneration of SNpc, another hallmark of PD is the Lewy pathology that consists of round, eosinophilic inclusions with a hyaline core and a pale peripheral halo located inside neurons. These inclusions are made of more than 90 proteins, including α-synuclein aggregates. Misfolded α-synuclein becomes insoluble and tend to aggregate forming intracellular inclusions inside cell bodies (Lewy's bodies) and processes (Lewy's neurites). Lewy pathology is not only found in PD patients' brain but also in the spinal cord and peripheral nervous system, including the vagus nerve, sympathetic ganglia, cardiac plexus, enteric nervous system, salivary glands, adrenal medulla, cutaneous nerves, and sciatic nerve (Beach TG, 2010). The progression of Lewy pathology follows a stereotyped temporal and spatial pattern, described by Braak and colleagues (Braak H, 2003), through six stages. It was described starting in the peripheral nervous system and progressing to the central nervous system following a caudal-to-

rostral direction. Stages 1 and 2 normally correspond with the onset of premotor symptoms, whereas stage 3 happens when nigrostriatal dopamine deficiency starts and it coincides with the development of motor features. Finally stages 4 to 6 are related to an advanced state of the disease with the worsening of both motor, and especially non-motor symptoms, including the development of a cognitive impairment. Dementia and the severity of cortical Lewy pathology are related and possibly also other non-motor symptoms, but this requires further investigation. The aggregation of proteins, other than α-synuclein, could explain the phenotypical variety of PD. For example, there are some PD monogenic forms that do not display Lewy pathology, like patients carrying *Park2* mutations and also a small portion of patients with *LRKK2* mutations. There surly are other proteins and other disease mechanisms that are implicated in PD. One of these could be the neuroinflamation played by activated microglia and astrocytes (Phani S, 2012).

Important advances in the understanding of PD pathogenesis have been made in the last decades. The importance of mitochondria has emerged from toxic models of PD (eg 6-hydroxy-dopamine (6-OHDA) and 1-methyl-4- phenyl-1,2,3,6-tetrahydropyridine (MPTP)) (Bezard E, 2011). There is evidence that PD patients have a decrease in respiratory chain complex I function. Other important contributors to PD is the impaired protein degradation due both to autophagy-lysosomal dysfunction and proteasome-ubiquitin impairment (Cerri S, 2019). There is also a mutual negative influence between protein degradation and α-synuclein aggregation. Aggregated α-synuclein alters protein degradation and impaired protein degradation leads to the aggregation of α-synuclein. Oxidative damage is another mechanism involved in neuronal dysfunction and death in both sporadic and familial PD patients. Researchers have detected in the SNpc of PD patients increased products of oxidative stress, including lipid peroxides, oxidative proteins and oxidative DNA, but also decreased antioxidants like glutathione. Genes related to PD, such as *SNCA*, *LRRK2* and *SYNJ1* code for proteins that are also implicated in vesicle trafficking at the presynaptic membrane, causing an abnormal dopamine (DA) release. More recently it has been found that synaptic vesicle protein, glycoprotein 2C (SV2C), regulates DA homeostasis and when its expression is dysregulated leads to some pathological features of PD (Mallet N, 2019). On top of that neuroinflamation has emerged as an important contributor to neurodegeneration in PD (Hirsch EC, 2021). It is well known, from extensive studies performed on animal models and human brain

samples, that microglia is activated in PD neurodegeneration and in response to inflammatory challenges, it gets functionally polarized towards the classical proinflammatory M1 phenotype (Tang, 2018). M1 microglia alters the BBB permeability and induces brain infiltration by circulating leukocytes, reinforcing the local inflammatory response. More recently the attention has been focused on the role of astrocytes in neurodegeneration. Studies on animal models and midbrain human samples have demonstrated an astrogliopathy (Booth, Hirst, & Wade-Martins, 2017).

The understanding of the pathogenic pathway that leads to neurodegeneration in PD is continually evolving and it implicates research on *in vivo, in vitro* models and human brain samples. Nowadays we have the possibility of generating patient-based cellular models that can be analysed in order to better understand the different mechanisms behind neuronal degeneration.

1.2 Early onset Parkinson's Disease

In the Western world, the majority of PD cases are late onset PD (LOPD) with a mean age of onset around 60s but there is a small percentage of cases, around 3–5%, where symptoms start before the age of 40 (Quinn N, 1987). In Japan, there is a higher percentages of early-onset PD (EOPD) that can be up to 10–14% and this is possibly due to a higher genetic susceptibility. EOPD can be further subdivided into the rare juvenile parkinsonism and young-onset PD (YOPD). Juvenile parkinsonism is characterized by a disease onset below 21 years of age, while the age of onset of YOPD lies between 21 and 40 years, but some studies reported 50 years of age as cut off. Juvenile parkinsonism and YOPD could be mainly distinguished from a clinical, pathological and genetic point of view (Schrag A, 2006). EOPD can be distinguished from LOPD for its unique motor and non-motor features.

It has been well recognized that the younger the age of onset (AAO), the higher the risk of genetic predisposition. As a matter of fact, a family history of PD is reported in 20% of YOPD patients, but only in 6.9% of LOPD patients, and the age-specific risk of PD is 7.8-fold higher in the relatives of patients with YOPD compared to 2.9-fold among the relatives of patients with LOPD.

Motor and non-motor features of EOPD vary according to the causative genetic mutations.

Park 1 (*SNCA*, 4q21-q23) mutations are related to a more rapid progression with the development of early motor fluctuations if compared to sporadic PD. It is also characterized by more severe psychiatric features, especially in case of *SNCA* duplication or triplication (Kasten M., 2013).

The majority of EOPD are due to *Park2* (*PRKN*, 6q26) mutations. As a matter of fact, *Park2* mutation frequency is approximately 50% of patients with recessive YOPD whereas it accounts 8.6% of all early-onset (<50 years) PD cases (Lucking CB., 2000). The phenotype is characterized by a slow rate of progression, even if frequently associated with some atypical features such as prominent involvement of legs with foot dystonia, freezing of gait, disautonomia and marked levodopa sensitivity with motor fluctuations and dyskinesia. On the contrary these patients have less cognitive impairments but impulse control disorder (ICD) might be more severe (Kim & Alcalay, 2017).

Park6 (*PINK1*, 1p36) represents the second more frequent genetic cause of EOPD with homozygous and compound heterozygous mutations accounting for 4-5% of ARPD and 1-2% of sporadic cases (Marongiu R, 2008). Disease-phenotype is characterized by a relatively slow progression rate with clinical features overlapping the ones of *Park2*.

Park7 (*DJ-1*, 1p36) is less frequent than other gene mutations accounting for 0-2% of EOPD. The phenotype associated to this mutation is also similar to *Park2* but it may be more frequently associated with blepharospasm.

The recessively inherited mutations of other genes can cause EOPD but they are rare and associated to atypical features including pyramidal signs, oculomotor palsy, dystonia, cognitive decline and loss of sustained levodopa responsiveness. Among these genes we can consider: *Park9* (*ATPA13A2*, 1p36), that causes the Kufor-Rakeb syndrome, which is an atypical parkinsonism with a severe phenotype characterized by spasticity, dementia and ophthalmoparesis; *Park14* (*PLA2G6*), also related to a juvenile atypical form of parkinsonism with associated dystonia, pyramidal signs and cognitive decline, but also characterised by paramagnetic deposit in basal ganglia; *Park15* (*FBXO7*) that causes a rare form of juvenile parkinsonism with spasticity, tremor, bradykinesia, and postural instability. Other signs/symptoms reported in the affected families are cognitive decline, eyelid apraxia, supranuclear gaze palsy, reduced saccadic movements, gait impairment

and early postural instability. Levodopa usually improve clinical symptoms, but levodopa-induced dyskinesia in these patients are severe.

More recently *GBA* (1q21) has been recognized as the most important genetic risk factor for PD. While homozygous *GBA* mutations are known to cause Gaucher's disease (GD), heterozygous and occasional homozygous mutations in this gene have been found to markedly increase risk for PD, particularly in the Ashkenazi Jewish population. PD patients that carry this mutation have a more rapid progression and cognitive impairment. As *GBA* mutations are very heterogenic, there are mild and severe ones. Severe mutations, include homozygous and compound heterozygous mutations and they are linked to a higher PD rate (15-fold), an earlier onset and a more severe phenotype. *GBA* mutations have a prevalence of 20.3% in EOPD, suggesting that these mutations should be screened also in this group of patients (Petrucci S, 2020).

Although the clinical picture of EOPD resembles the one of LOPD, there is a longer diagnostic latency in EOPD. Initial pathologic features often include foot dystonia and lower limb rigidity, that may be atypical initial symptoms in LOPD. EOPD typically present a mobile-dystonia exercise-induced that mainly affect a foot or a leg. These patients may present dystonic claudication and also writer's cramp. Sometimes they can display also retrocollis, normally responsive to sensory trick. Although dystonia is an important feature of EOPD phenotype, it does not always respond well to levodopa and requires other types of medications, such as anticholinergics, botulin toxin injection and physiotherapy. In some patients, globus pallidus internal (GPi) or subthalamic nucleus (STN) deep brain stimulation can be considered to treat drug-refractory dystonia, even if other parkinsonian symptoms are well controlled with levodopa.

An additional early neuroradiological feature of EOPD is the sparing of caudate at the SPECT-DAT scan compared with the putamen. This is in contrast with LOPD that show a relatively homogenous involvement of both putamen and caudate. As caudate is involved in psychomotor and complex cognitive functions, this could provide an explanation why it is less affected in EOPD.

EOPD often present levodopa-induced dyskinesias which may be caused by a maladaptive plastic response (Warren Olanow C, 2013) or by higher synaptic dopamine turnovers (Sossi V, 2006).

EOPD patients have in general less comorbidities, a slower disease progression, less gait disturbances and delayed falls and freezing. They do not typically develop cognitive impairment later in the disease course even if incidence of depression could be high. They also show a lower frequency of axial symptoms that do not respond to levodopa, such as dysphagia and postural instability. In addition to that they tend to have a higher rate of ICD associated to dopaminoagonist therapy.

In conclusion, EOPD is a unique subgroup of PD patients with a strong genetic predisposition to the disease and peculiar features that distinguish these patients from the LOPD ones. Knowing the causative genes opens up to the possibility of discovering the pathogenic mechanisms behind neurodegeneration in EOPD and possibly idiopathic PD as well.

1.3 *Park 2*: one gene, multiple functions

In 1965 a research group at Nagoya University examined familial cases of EOPD characterized by autosomal recessive inheritance, diurnal fluctuation of symptoms, foot dystonia, good response to levodopa and a benign disease course without dementia (Yamamura, Iida, Soube, & Ando, 1968). At that stage an inborn error of metabolism in some dopamine-related pattern was suspected (Yamamura, 2010). In 1973 a clinical study of four families with EOPD was published in Neurology (Yamamura Y., 1973). These patients had peculiar clinical features such as diurnal fluctuations, mild dystonia mainly affecting the feet, hyperactive tendon reflexes, good response to levodopa, slow progression and no dementia. Patients developed dyskinesias soon after the initiation of levodopa. Autonomic symptoms were only mild when present. Later on a neuropathological study was published in 1994 describing the dramatic dopaminergic neuronal loss in SNpc of a EOPD, without Lewy pathology (Takahashi H, 1994). The neurodegeneration extended also to locus coeruleus but with less extent than the SNpc. These neuropathological hallmarks were confirmed by other study groups the following years (Mori H, 1998) (Matsumine H., 1998b). Based on clinical and neuropathological evidence EOPD was considered a distinct entity with a different pathogenic aetiology. Finally, in 1998 *Park2* gene was cloned and confirmed in 15 families out of 16 (Kitada, 1998) (Yamamura Y, 1998). This was the second familial PD gene discovered after *SNCA*.

The average prevalence of *Park2* mutations in ARPD has been reported around 50% when disease onset was around or before 25 years and around 10% when disease onset was later, around 30-40 years (Klein C., 2007). In one study including100 PD patients with an age at onset below 45 years, 77% of those with very young onset, below 20 years of age, carried at least one *Park2* mutation (homozygous or heterozygous). This percentage dropped to 26% when only patients with disease onset between 20 and 30 years were considered. The percentage further dropped to 2-7% when patients with disease onset between 30 and 45 years were examined. Unfortunately, in this study, homozygous and heterozygous carriers were reported together, and about half of PD patients carrying *Park2* mutations had only one mutation (heterozygote) (Lucking CB, 2000). Other studies

found homozygous or compound heterozygous *Park2* mutations in a lower percentage of patients with EOPD, ranging from 8.2% in Italy, 2.7% in Korea, 2.5% in Poland, to 1.4% in Australia (Sironi F, 2008) (Mellick GD, 2009). *Park2* mutations also explain ~15% of the sporadic cases with onset before 45 (Bonifati, 2012) and act as susceptibility alleles for LOPD forms (2% of cases).

Beside causing EOPD, *Park2* mutations have been linked to other human pathologies, such as AD (Burns MP., 2009), autism (Glessner JT., 2009), multiple sclerosis (Witte ME., 2009) and cancer (Cesari R., 2003), especially ovarian cancer (Bernardini, 2017). It has been reported also linked to leprosy (Mira MT., 2004), type 2 diabetes mellitus and myositis.

Park2 maps to chromosome 6q25.2-q27 (OMIM: 602544, Ensamble: ENSG00000185345) as indicated by linkage to markers D6S305 and D6S253 (Matsumine H, 1997). The former was deleted in one Japanese patient with PD. By positional cloning within this microdeletion, Kitada et al. (Kitada T., 1998) isolated a cDNA clone of 2,960 bp with a 1,395-bp open reading frame, encoding a protein of 465 amino acids with moderate similarity to ubiquitin at the amino terminus and with a ring finger motif at the C-terminus. A 4.5-kb transcript, expressed in many human tissues but particularly abundant in the brain, including the SNpc, was found shorter in the brain tissue of the exon-4-deleted patients. Mutations in the newly identified gene appeared to be responsible for the pathogenesis of EOPD and, therefore, the protein product was designated 'Parkin.'

Park2 gene has 12 exons, spanning for 1,380 kb (Asakawa, 2001). The longest intron, intron 1, is 284 kb. The 5-prime flanking region has no TATA or CAAT box elements, but it has GC- and CpG-rich regions, as do the first exon and first intron. To date 26 human different cDNAs, corresponding to 21 splice variants have been reported. Although equal, these proteins are encoded by different splice variants which probably produce the same protein but with different efficiency.

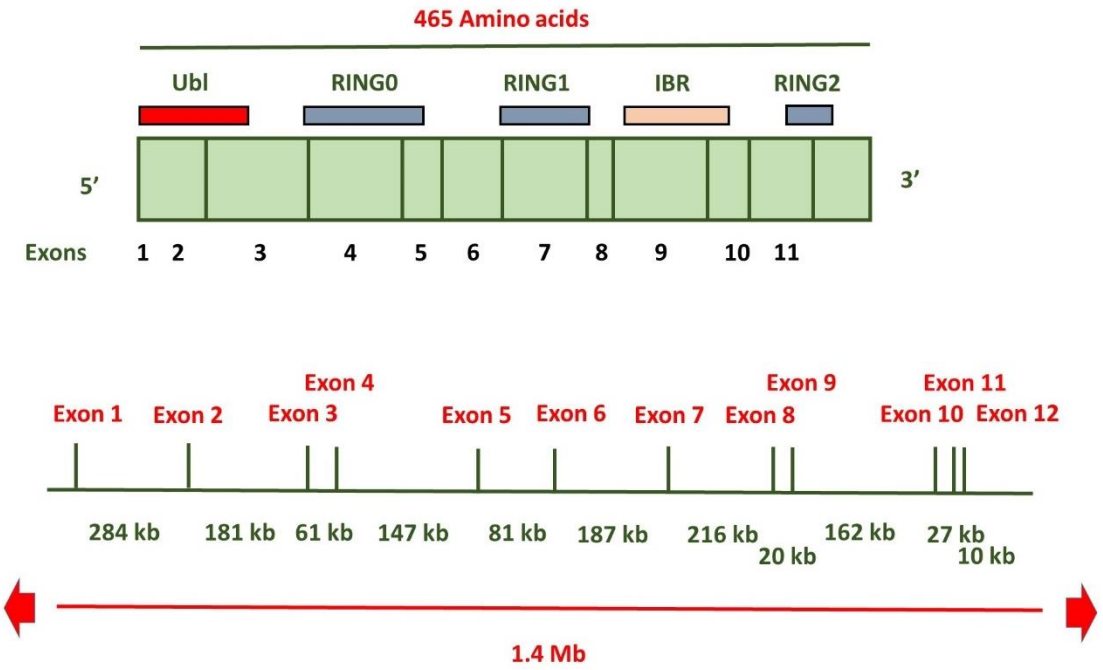

Figure 1. Structure of the *Park2* gene. Above there is a schematic representation of cDNA of the *Park2* gene, whereas below of the whole *Park2* gene. This figure is inspired by the paper of Hattori and Mizuno (Hattori N., 2017).

Park2 mutations, identified till now, mainly lead to Parkin loss of function. Disease-causing mutations include single base-pair substitutions, deletions that could be small (hundreds of nucleotides) or big (thousands of nucleotides), and splice site mutations. Parkin loss of function is obvious when there are deletions spanning several exons. The consequent truncated transcript is destabilized by the nonsense-mediated decay and this causes the absence of protein expression. As a matter of fact, there is little evidence that truncated Parkin is expressed in patients carrying exon deletions. Also missense mutations cause Parkin loss of function and this happens because this kind of mutations decreased Parkin catalytic activity and/or aberrant ubiquitination. Point mutations might also destabilize Parkin, causing its insolubility and rapid proteasomal degradation (Dawson, 2010). Since its discovery in 1998 (Kitada T, 1998), approximately 200 mutations, have been identified, including point mutations and exonic rearrangements. These last ones are more pathogenic than point mutations. Heterozygous mutations have been also reported and these may predispose to LOPD, but their role is still controversial.

To date it is unknown if all Parkin functions are mediated by a single protein or by different isoforms. Alternative splicing of *Park2* produces at least 11 transcript variants encoding for multiple isoforms. This alternative splicing is regulated at transcript and protein level (La Cognata V, 2014). Parkin mRNAs have a different expression and distribution in tissues and cells and this is mirrored at protein level. Parkin distinct isoforms might then perform different functions in different tissues and cells. Parkin isoforms show a different distribution in human aged brain (Pawlyk AC, 2003) and brain regions (Stichel CC, 2000). Emerging evidences support the importance of Parkin splice variant expression changes in disease development. The disease-specific expression profiles of Parkin alternative splice variants suggest a role for splicing deregulation in the development of neurodegenerative disorders. It seems that particularly two splicing variants are significantly overexpressed in PD (Humbert J, 2007). In human frontal cortex of PD patients and controls, two immunoblot bands have been observed, a major one of 52 kDa and a second fainter one of ∼41 kDa immunoblot (Shimura H., 1999). Parkin expression was also observed in Lewy bodies and this might derive from the fact that with aging Parkin may interact with other proteins, altering their properties and leading to the formations of complex protein aggregates, such as Lewy bodies. Those *Park2* mutation that alter its splicing could alter their localization, and lead to a loss of function or gain of function in a time- and cell-specific manner. The alteration of the natural splicing of *Park2* and deregulation in the expression of Parkin isoforms might lead to the selective degeneration of dopaminergic neurons in SNpc of ARPD.

The original Parkin comprises an N-terminal ubiquitin-like (UBQ) domain and two C-terminal in-between ring fingers (IBR) domains. The RING-IBR-RING (RBR) structure is highly conserved and found only in eukaryotes (Beasley, 2007). The UBQ domain serves to target specific substrates for proteasome degradation, whereas the IBR domain has a role in protein quality control. *Park2*-encoded isoforms are structurally different from the original one for the presence/absence of the UBQ domain and for one of or both IBR domains. The UBQ domain, when present, differs in length from the original sequence. There are some isoforms that lack all these domains. As a matter of fact, isoforms could have different structures and domain compositions and this might alter their function.

When Parkin is phosphorylated by casein kinase I (CSNK1A1) and cyclin-dependent kinase-5 (CDK5), it has a reduced solubility and it is prone to form aggregation and to become inactive. Parkin has been found with an enhanced phosphorylation in different brain areas of patients with sporadic PD and this correlated with increased p25 (CDK5R1), an activator of CDK5 (Rubio de la Torre, 2009).

Parkin is a cytosolic component of the multiprotein E3 ubiquitin ligase that targets proteins to proteasome degradation and it has different substrates, indicating that it is a multifunctional protein. Parkin regulates the trafficking and the turnover of a high number of proteins including neurotransmitters. Accumulation of Parkin substrates directed to ubiquitination is critical in the pathogenesis of ARPD. For this reason, it is very important to identify these substrates and clarify their pathogenic roles. Parkin plays a ubiquitin-ligase activity for different targets, that may accumulate in ARPD brains, causing neurodegeneration. It is involved in mitochondrial and microtubular integrity (Cartelli D, 2018), but also in the calcium-kainate exocytosis and it regulates MAOA and MAOB with consequent oxidative stress (Jiang H, 2006). Parkin contribute to all these cellular functions because it targets cytosolic (Synphilin-1, Pael-R, CDCrel-1 and 2a, α-synuclein, p22, and Synaptotagmin XI) (Imai, 2000), nuclear (Cyclin E) (Ikeuchi, 2009), and mitochondrial proteins (MFN1 and MFN2, VDAC, TOM70, TOM40 and TOM20, BAK, MIRO1 and MIRO2, and FIS1) (N. C. Chan, 2011) (Narendra D., 2008).

In the last decades many research groups have addressed their attention on the identification of the pathogenic mechanisms related to *Park2* mutations. Addressing first the attention on mitochondrial dysfunction has been a natural process since it plays a pivotal role in both sporadic and familial forms of PD. As a matter of fact, mitochondrial alterations have emerged also being an effect of *Park2* mutation. Genetic studies in *Drosophila* first suggested *Park2* role in mitochondrial integrity regulation (Greene JC, 2003). This impairment has been widely demonstrated also in Parkin lacking mice and it resulted being related specially to complex I and IV dysfunction (Palacino J. J., 2004) (Casarejos M. J., 2006) (Thomas M., 2007). Parkin is selectively recruited to dysfunctional mitochondria that, in mammalian cells, have a low membrane potential (Narendra D, 2008). After recruitment, Parkin addresses impaired mitochondria to autophagosomes, leading to their selective elimination. In promoting the autophagy of damaged mitochondria, Parkin works in synergy with PINK1, the product of another gene

implicated in ARPD. PINK1 normally accumulates on the outer membrane of damaged mitochondria and activates Parkin's E3 ubiquitin ligase activity by recruiting Parkin to the dysfunctional mitochondria. Then, Parkin ubiquitinates the proteins located on the outer mitochondrial membrane and this triggers a selective autophagy (Pickrell AM, 2015). Parkin ubiquitinates outer mitochondrial membrane proteins such as mitofusins, optic atrophy 1 (OPA1) and Miro and this causes an altered balance between fission and fusion, facilitating the isolation of dysfunctional mitochondria. Parkin and PINK1 contribute, by working together to the repair of mildly damaged mitochondria. Complementary to mitophagy, Parkin and PINK1 promotes the synthesis of new mitochondria and this allows the replacement of damaged mitochondria with new ones (Vincow ES, 2013). Mitochondrial dysfunction has also been assessed in *in vitro* cellular models. Abnormal mitochondrial morphology and increased oxidative stress has been observed in *Park2* iPSCs-derived DA neurons (Imaizumi Y., 2012). This data has been further confirmed by other studies, such as the one of Suzuki et al. that demonstrated impaired mitophagy in iPSCs-derived DA neurons carrying *Park2* mutation (Suzuki S, 2017) and another recent one that showed how knocking out *Park2* gene in human iPSCs leads to increased oxidative stress, dysregulation of mitochondrial and lysosomal function (Ahfeldt T, 2020) and that results in iPSCs-derived DA neurons death. Yokota et al. (Yokota M, 2021) in a very recent publication described functional and structural mitochondrial dysfunction in patient-derived dopaminergic neurons with a tyrosine-hydroxylase reporter (TH-GFP).

Mitochondria fragmentation with ROS increase and loss of mitochondrial membrane potential has been observed in iPSCs-derived progenitor neurons of *Park2* patients, after the exposure to copper (Cu) and cadmium (Cd) but not to manganese (Mn) or mercury (Hg) (Aboud AA, 2015). This study identifies environmental risk factors that could contribute to the development of PD in *Park2* patients.

Also the endoplasmic reticulum (ER)-mitochondria interface is impaired in *Park2* mutations, in particular there is an alteration in the calcium exchange between the two compartments and this results in a defective mitophagy (Gautier CA, 2016). ER are in close proximity to mitochondria in primary fibroblasts from *Park2* knockout (KO) mice and *Park 2* PD compared to controls and also in *Park2* iPSCs-derived DA neurons. The calcium flux from ER to mitochondria is enhanced due to mitofusin2 (Mfn2), a Parkin

substrate, increase. Mfn2 downregulation or Parkin exogenous expression restored a normal calcium transit.

Calcium homeostasis dysregulation has emerged being a great contributor to the development of PD, especially in *Park2* mutations. *Park2*-DA neurons express more T-type calcium channels, but mRNA levels of these calcium channels do not increase after treatment with rotenone (blocker of electron transport chain of mitochondrial complex I), indicating that transcriptional regulation is not a key contributor to the development of calcium dis-homeostasis in *Park2* (Tabata Y, 2018)

Park2 mutations also impair the endocytic pathway because Parkin contribute to the regulation of tubular and multivescicular domains of endosomes, their functions and the formation of exosomes. One study (Song P, 2016) demonstrated that one of Parkin substrates is Rab7, which is a protein implicated in the binding properties of endosomes. A defective regulation of Rab7 causes morphological and functional impairment of endosomes with a decreased endosomal tabulation and association to proteins like vesicle protein sorting 35 (VPS35) and sorting nexin 1 (SNX1). Parkin defect is also associated to an increased release of exosomes. The impairment of this pathway leads to lysosomal dysfunction which is a well-known contributor to neurodegeneration in PD

Another important observation that has been made studying *Park2* iPSCs-derived DA neurons is that *Park2* mutations lead to a reduced neurite length and complexity which renders them particularly vulnerable. This data has been replicated in two independent studies (Ren Y., 2015) (Pu J, 2020). These effects were noted not only on TH+ neurons, but also on TH− neurons. As a matter of fact, *Park2* mutations reduce microtubule (MT) stability through an over-acetylation that leads to a fragmentation of stable MTs in iPSCs-derived neurons. On the contrary, Parkin overexpression stabilizes MTs, rescuing the morphological defects of Parkin-deficient neurons (Ren Y., 2015). As suggested Parkin acts as a regulator of MT system during neuronal aging.

Considering this multiplicity of effects, in humans, *Park2* loss of function mutations mainly produce an early and severe degeneration of dopaminergic neurons of the SNpc

(Poulopoulos M, 2012). This evidence suggests that, among the many cellular processes regulated by Parkin, some are crucial to SNpc dopaminergic neuron function and survival. Parkin is important for neurotransmission modulation of afferent and efferent connections of SNpc dopaminergic neurons. In humans the exact topology of the synaptic connections of SNpc neurons is not fully understood yet, but it is certain that these neurons provide a massive innervation of the striatum (Prensa L, 2009). A single dopaminergic neuron is, indeed, able of forming over 300.000 synaptic connections. The afferent connections to SNpc dopaminergic neurons mainly consist of GABAergic and glutamatergic inputs. GABAergic inputs come from deep brain regions such as the neostriatum, the globus pallidus, and the substantia nigra pars reticulata (SNpr). Glutamatergic inputs derive instead from different cortical regions, as well from deeper brain regions such as the subthalamic and peduncolopontine nuclei. Parkin is a cytosolic protein diffusely located along neuronal axons, soma, and dendrites (Helton TD, 2008). Parkin is also localized on synaptic vesicles and displays a distribution pattern similar to that of synapsin I, another synaptic protein (Kubo SI, 2001) that associates with the cytoplasmic surface of synaptic vesicles. Parkin localizes both at presynaptic and postsynaptic terminals. At presynaptic terminals it associates with synaptic vesicles, whereas at postsynaptic terminals, it associates with postsynaptic density proteins (PSDs). These data concerning Parkin subcellular localization are consistent with the hypothesis that this protein is implicated in regulating synaptic functions (Sassone J, 2017). The evidence that Parkin interacts with synaptic proteins implicated in vesicle release suggests that presynaptic Parkin may be involved in dopamine release. This hypothesis was investigated in parkin-knockout mouse models and an increased spontaneous dopamine release from dopaminergic neurons was found in Parkin-knockout mice aged 3–9 months (Oyama G, 2010). Unfortunately, other studies did not support this hypothesis (Perez FA, 2005). It is worth remembering that Parkin-knockout mice do not develop dopaminergic neuron degeneration and motor impairment and they do not show the clinical aspects that are crucial in ARPD. It is evident that the role of Parkin in controlling dopamine release in human subjects needs to be investigated in human models. Spontaneous dopamine release was found increased in iPSCs-derived DA neurons of patients affected by ARPD (Jiang H., 2012) and overexpression of wild-type Parkin reduced spontaneous dopamine release. Another pathway by which presynaptic Parkin may modulate dopamine is through the binding of the dopamine transporter (DAT) located on the cellular membrane of dopaminergic neurons. This transporter is responsible for the reuptake of dopamine at

synaptic and extrasynaptic sites, reducing dopamine levels at synaptic cleft. At the postsynaptic level Parkin interacts with PSD proteins. In particular, Parkin interacts with PSD-95, which is the best characterized among PSD proteins (Fallon L, 2002). PSD-95 is involved in anchoring synaptic proteins such as NMDAR and AMPA/KAR, but also other ionic channels such as K+ channels. Parkin is then able to modulate their levels at cell surface through the control of their trafficking, anchoring and clustering. Parkin interacts also with Ca2+/CaM-associated serine kinase (CASK) which is an important protein in maintaining the dendritic morphology. Parkin interacts with other postsynaptic proteins. Recently it was discovered that Parkin ubiquitinates a KAR subuint (GluK2) and as a consequence it regulates KAR postsynaptic current (Maraschi A, 2014). As Parkin is localized also in axons, it is possible that Parkin might interact with presynaptic Gluk2, altering also the presynaptic glutamatergic transmission and glutamate reuptake. Another study (Cremer JN, 2015) conducted on Parkin- knockout mice confirmed the finding that Parkin upregulates KAR densities in different cortical areas. This study also demonstrated that in these Parkin models NMDAR levels were increased, whereas AMPAR densities were decreased in different brain regions. Considering that Parkin can alter all the three glutamate receptors, it is evident how this protein is fundamental for glutamatergic transmission and that impairment of this neurotransmission can contribute to neurodegeneration in patients carrying *Park2* mutations.

Park2 mutations seem to impair also GABAergic transmission. A study published by Iwasawa et al. (Iwasawa C, 2019) evaluated changes in the expression of somatostatin (SST), a GABAergic modulator of neurotransmission, in iPSCs-derived GABAergic neurons from *Park2* patients and controls. They found that SST levels significantly decreased in *Park2* neurons as neural maturation progressed. A reduced expression of SST in GABAergic interneurons may partially contribute to the development of PD in *Park2* patient and might also explain their phenotypic differences compared to idiopathic PD.

Another pathogenic mechanism that is a great contributor to neurodegeneration in PD is neuroinflamation. Neuroinflamation is intended as the process involving the synthesis and release of pro-inflammatory mediators and when this process is uncontrolled it can lead or facilitate the development of neurodegeneration. The hypothesis that neuroinflamation may be involved in the pathogenesis of PD has emerged in 1980s where

many studies discovered the role played by oxidative stress and reduced defence mechanisms against free radicals in PD (Hirsch, 1992). Evidence of neuroinflamation in PD has emerged both from neuropathological (McGeer P.L., 1988), neuroimaging (Terada T., 2016) and *in vivo* and *in vitro* studies, as well (Pajares M, 2020). Recent studies indicate that there are some PD-associated genes that influence the immune response of microglia and astrocytes of the CNS, such as *SNCA*, *LRRK2*, but also *PINK1* and *Park2* (Nuytemans K, 2010). *Park2* mutations predispose then to neuroinflamation. Primary human blood-derived macrophages from PD patients carrying *Park2* mutations have high levels of pro-inflammatory mediators, such as NLRP3 and IL-1β when stimulated with lipopolysaccharides and their serum is also enriched with cytokines as IL-6, IL-1β, CCL2 and CCL4. Parkin knock-out mice develop a robust inflammatory phenotype, linked to mitochondria stress (Sliter DA, 2018). In addition to that Parkin expression resulted increased in reactive astrocytes in diseased human brains (Witte ME, 2009) and this indicate that Parkin plays an important role in regulating the glial inflammatory response. Pre-clinical studies show that Parkin augmentation ameliorates disease features in several disease models (Liu B, 2013). A study conducted on iPSCs-derive DA neurons from a patient carrying a *Park2* mutation demonstrated the importance of an anti-inflammatory factor: erythroid 2-related factor 2 (NRF2) that can be increased using the compound NC001-8, an indole derivative. This molecule was able to promote the NRF2 antioxidative pathway, reducing ROS levels. Parkin seems to have a neuroprotective effect on striatal dopaminergic neurons. Further studies are needed to better elucidate *Park2* role in neuroinflamation.

Since the discovery of *Park2* mutations as a causative gene of ARPD, many studies regarding its pathogenic role have been published. The identification of Parkin implication in mitophagy, neurotransmission and neuroinflamation have been fundamental for the understanding of the pathogenesis of ARPD. However, the exact mechanisms through which *Park2* mutations lead to neurodegeneration have been not completely clarified yet. Further studies need to be done, especially on human models, in order to address many questions related to the development of the disease that are still unanswered. Why *Park2* mutations cause an early and dramatic loss of dopaminergic neuros? Why neurodegeneration in *Park2* patients is strictly limited to SNpc, differencing this form from other forms of PD? If *Park2* mutations alter the ubiquitine-proteasomal

system, why *Park2* patients do not develop Lewy body pathology? How can we explain the unique clinical features of *Park2* patients from a pathogenic point of view? How heterozygous *Park2* mutations contribute to the development of PD? Understanding these mechanisms may lead to the development of specific treatments for these patients that could prevent or delay the development of the disease.

1.4 The glutamatergic role of *Park2*

Impaired glutamate homeostasis in the striatum is emerging as a key feature of PD pathology. Glutamate is the major excitatory neurotransmitter in the central nervous system (CNS) and the balance between excitatory and inhibitory transmission is important to make it properly functioning. It is evident that extracellular glutamate levels need to be kept in a physiological range out of which there is an impairment in the neuronal function with consequent neurodegeneration, as it has emerged in Alzheimer disease (AD), amyotrophic lateral sclerosis (ALS), Huntington's disease (HD) and also in PD (Lewerenz J., 2015). In order to have an efficient glutamate transmission, other neuronal and glial receptors and transporters need to function correctly. An important mechanism through which glutamate levels at the synaptic cleft do not exceed is thanks to glutamate reuptake. If there is an extra-cellular glutamate increase, the consequence is an alteration of the synaptic signal with consequent neuronal excitotoxicity and death.

Glutamate is a neurotransmitter released by neurons into the synaptic space where it binds to both ionotropic and metabotropic receptors in order to transmit an excitatory message. Afterwards, glutamate is rapidly removed from the cleft thanks to neuronal and glial high-affinity transporters. Astrocytes play a fundamental role in reducing the synaptic glutamate levels thanks to the enzyme glutamine synthetase (GS) that converts glutamate into the inert glutamine which is then released in the cleft and taken up by neurons as a precursor for glutamate synthesis (Verkhratsky M., 2018). Neurons can reuptake glutamate through five transporters, denominated excitatory aminoacid transporters (EAATs 1-5) (Malik A.R., 2019). EAAT1 and EAAT2 are the most abundant ones in the CNS and they are mainly expressed in astrocytes. Excessive synaptic glutamate accumulation is toxic because glutamate receptors are overstimulated and this causes in the end cellular apoptosis through a Ca2+ overload. Glutamate excitotoxicity contribute to neurodegeneration through the spreading of neuroinflammation.

Glutamate is normally released by neurons at the synaptic cleft where it acts on ionotropic and metabotropic receptors, propagating an excitatory message. At the synaptic cleft

glutamate reaches concentrations above 1 mM for around 10 seconds after an action potential (Moussawi K., 2011). Both neurons and glial cells possess high affinity for glutamate and they rapidly remove it from the extracellular space, reducing its concentration to nanomolar levels. Thanks to glutamate transporters astrocytes clean the cleft from excessive glutamate whereas microglia do not display glutamate transporters at steady state but their expression is induced when they become reactive. When glutamate accumulates at the synaptic cleft over a physiological range it becomes toxic and causes cellular necrosis and apoptosis through a Ca2+ overload. Glutamate ionotropic receptors (iGluRs) are associated with ion channels and are divided into three families: NMDAR (N-methyl-D-aspartate receptors), AMPAR (α-amino-3-hydroxyl-5-methyl-4-isoxazolepropionate receptors), and KAR (kainic acid receptors). AMPAR and KAR are also defined non-NMDA receptors. Metabotropic glutamate receptors (mGluRs) are G-protein coupled receptors that activate biochemical cascades that modify other proteins, leading to changes in synaptic excitability. The term "excitatory toxicity" was proposed in the '80s for the first time to indicate the ability of extracellular glutamate in killing neurons acting on NMDARs (Choi D.W., 1988). Although excitotoxicity has been studied for long, the exact mechanisms leading to neuronal death are still not fully understood. Ionotropic glutamate receptors respond to elevated levels of glutamate at the synaptic cleft with an increase in intracellular Na+, Cl- and Ca2+ levels (Wang Q., 2005). Massive influx of Na+ and Cl- followed by influx of water inside neurons causes cellular necrosis, an acute and traumatic event, whereas Ca2+ influx induces cellular death through apoptosis which is a more controlled and slower process. In contrast, mGluRs are less permeable to glutamate but hyperactivation of type I and V mGluRs induces slower Ca2+ elevation through the release of Ca2+ from endoplasmic reticulum (ER) thanks to the generation of inositol triphosphate (IP3). Intracellular excessive influx of Ca2+ activates catalytic enzymes, causes mitochondrial impairment and release of toxic free radicals. Both magnitude and duration of intracellular Ca2+ overload are important determinants in neuron degeneration. Ca2+ overload activates cellular-death pathways through calcineurin and calpain. Calcineurin acts on proapoptotic BH3 proteins, triggering the intrinsic apoptotic pathway, whereas calpain induces cell death trough mediators such as p53. Ca2+ overload is also responsible for free radicals generation that contribute to mitochondria swelling and disruption with consequent release of Cytochrome C that activates a downstream caspase cascade. Caspases are responsible for DNA damage and fragmentation.

Excitotoxicity mediated by KAR takes place also through autophagic stress which is a form of programmed cell death (PCD) beside necrosis and apoptosis. Autophagy is fundamental for cellular homeostasis as it serves to remove damaged cellular components. If this mechanism is impaired, like in kainate (KA)-mediated excitotoxicity, it accelerates rather than prevent cell death. KA acts both on pre-synaptic and post-synaptic KAR, modulating excitatory signals. KA is a non-degradable analogue of glutamate, 30-fold more potent than glutamate. KAR activation by KA induces membrane depolarization and rise of intracellular Ca2+ levels, activating Ca2+ dependent enzymes such as Cox-2, proteases, kinases, nucleases and phospholipases. This leads to mitochondrial dysfunction and generation of reactive oxygen species (ROS) and reactive nitrogen species (RNS). Intracellular increased ROS levels cause lipid peroxidation, cell membrane damage and further mitochondria damage. Mitochondria disruption is accompanied by the release of mitochondrial factors, such as Cytochrome C, with consequent caspases activation, starting from caspase-9 and 3. This leads to neuronal apoptosis. An excess of KAR stimulation induces also ER disintegration with activation of Bip, Chop and caspase-12 that contribute to cellular apoptosis induction. ER stress acts at an early stage of cell death, prior to Ca2+ dishomeostasis and mitochondrial dysfunction. Intracellular Ca2+ and ROS overload cause mitochondrial swelling with consequent neuronal necrosis. KA-induced neuronal death is accompanied by astrocytes and microglia activation. In KA-induced excitotoxic neurodegeneration, activated microglia release cytokines, chemokines, ROS, RNS, proteases and excitatory amino acids that contribute to neuronal death. Despite the important role played by microglia in KA-induced neurodegeneration, there is no evidence that microglia participate to the initiation of the inflammatory and degenerative process. Activated microglia seems a by-product of KA-toxicity rather than an accomplice. On the other hand, astrocytes, that have always been considered a passive support to neurons, seem to play a dynamic role by modulating synaptic activity and contributing to neurodegeneration. Astrocytes tend to proliferate after KA exposure in *in vivo* experiments on rats (Murabe, et al., 1982) (Bendotti, et al., 2000). Reactive astrocytes produce either anti-inflammatory and pro-inflammatory cytokines and the balance between those factors lead either to neuroprotection or neurodegeneration. Healthy astrocytes remove about 90% of the glutamate released in the CNS. They also release small amounts of glutamate in order to synchronize the firing activity of adjacent neurons. Astrocytes present a more stable membrane potential with higher ratios of Na+/K+, compared to neurons. Astrocytes keep

high levels of ATP, necessary for glutamate uptake. They rapidly convert glutamate into glutamine, keeping a low threshold across the membrane in order to continue uptaking extracellular glutamate. Glutamine is then used by neurons to synthetize new neurotransmitters, such as glutamate or GABA. Glutamate uptake is a highly energy-consuming process, so that astrocytes require a great amount of ATP to maintain this function. As in *Park2* mutations mitochondrial function is compromised, astrocytes might not properly uptake glutamate and convert it into glutamine, contributing to excitotoxicity development. In pathological conditions, astrocytes increase brain damage through the release of proinflammatory molecules and free radicals as well. KA exposure induce an upregulation of GFAP in astrocytes, a marker of astrogliosis (Bendotti C, 2000).

Despite PD has always been described as a dopaminergic disease, it is now accepted that alterations of glutamatergic neurotransmission have a central role in PD development (Blandini F., 1996). Glutamate is the neurotransmitter that modulates fronto-basal circuits in order to allow voluntary movements. In the striatum there are mainly inhibitory spiny projection neurons (SPNs) that receive two different inputs: a dopaminergic input from DA neurons of SNpc and a glutamatergic input from the cerebral cortex and thalamus. These projections directly reach the internal segment of the globus pallidus (GPi) (direct pathway) and indirectly the external segment of the globus pallidus(GPe) and the subthalamic nucleus (STN) (indirect pathway). There is also a direct glutamatergic connexion between STN and SNpc. Nigral DA neurons degeneration cause an impairment of the coordinated activity of the direct and indirect pathways. When the stimulation of the DA receptors (D1R) is decreased, the direct pathway is impaired causing a reduced inhibition of the output signals. On the other side, when the DA receptor (D2R)-mediated stimulation of the indirect pathway is reduced, there is a disinhibition of the STN leading to a glutamatergic overstimulation of the output signals. When the direct and the indirect pathways are unbalanced, the motor thalamic nuclei and consequently the motor cortex are understimulated. SNpc neurons receive glutamatergic inputs from various brain areas, including the cortex, pedunculopontine nuclei, superior colliculus, thalamus, and subthalamic nucleus (Yetnikoff L, 2014). It is clear then that glutamatergic inputs are essential for basal ganglia physiology, but when extracellular glutamate levels are excessively high there is a hyperactivation of ionotropic glutamatergic receptors located on the DA neuron membrane and this results in

excitotoxicity and consequent neuronal death. This could be a key mechanism in neurodegenartion associated to PD (Mehta A, 2013) (Ambrosi G, 2014) because excitotoxicity causes a dopamine deficiency that impair the bursting mode activity of the subthalamic nucleus and this results in a further propagation of glutamate toxicity.

There is increasing evidence suggesting that Parkin contributes to the regulation of glutamatergic excitatory synapses (Helton T. D., 2008). This excitatory hypothesis fits well as a neurodegenerative cause of ARPD and possibly also to sporadic forms of PD. It has been demonstrated that knocking down Parkin enhances synaptic efficacy and leads to glutamatergic synapses proliferation which causes an increased vulnerability to synaptic excitotoxicity. DA neurons display two types of glutamate ionotropic receptors: AMPAR/KAR and NMDAR. Evidence suggests that Parkin specifically regulates the AMPAR/KAR ones (Staropoli JF, 2003). As a matter of fact, DA neurons are more vulnerable to KA treatment, an AMPAR/KAR agonist. This effect could be reverted by overexpressing wild-type Parkin. Parkin loss-of-function causes increased KAR currents with consequent glutamate KAR-mediated toxicity.

KARs are ionotropic glutamate-gated ion channels that modulate synaptic transmission in neuronal circuits. KAR are tetramers made of assembly of four identical subunits (homomers) or mixtures of different subunits (heteromers). KAR tetramers derive from the variable combination of five subuinuts (GluK1-5). These subunits are differently expressed in human brain regions, including SNpc. GluK1-3 subunits are highly expressed in the CA3 region of the hippocampus, in the striatum and in the inner layers of the cortex. In contrast, GluK4 and 5 subunits have a much more restricted distribution, with GluK4 exclusively expressed in the hippocampus (Darstein M, 2003) while GluK5 in the striatum and in the inner/outer layers of the cortex. In the last years the functional and physiological role of kainite receptors in mammalian CNS has been elucidated. What is known is that KAR has both a presynaptic and postsynaptic activity but it has a more limited distribution throughout the brain compared to AMPA and NMDA receptors. KAR induces the NMDA receptor-independent LTP in the CA3 region of the hippocampus and it has a major role in somatosensory synaptic plasticity. KAR alterations cause many psychiatric and neurological diseases, including epilepsy, Huntington’s disease, autism,

schizophrenia, bipolar disorder, depression and more recently also in PD (Maraschi A, 2014).

Recently it was discovered that Gluk2, a KAR subunit, is also a substrate of Parkin and that its ubitiquination from Parkin regulates GluK2 levels and KAR currents. Parkin loss-of-function causes KAR-dependent excitotoxicity *in vitro* and *Park2* mutations correlate with Gluk2 accumulation and excitotoxicity features *in vivo* (Maraschi A, 2014). In this study they first tested the hypothesis that Parkin interacts with KAR Gluk2 in n HEK293T cells that were transfected with GluK2a and Parkin. They found that Parkin co-immunoprecipitated with GluK2a and that GluK2a co-immunoprecipitated with Parkin. Then they tested this hypothesis on human brain samples lysates where they found this co-immunoprecipitation as well. They also found higher levels of Gluk2 in brains from patients with *Park2* mutations and in the *Park2* mouse model Parkin-Q311X. Parkin binds the GluK2 C-terminal cytoplasmic tail and facilitates KAR activation by agonists. Considering that Parkin is located also in axons, it may regulate pre-synaptic GluK2 levels, facilitating glutamate transmission. This paper demonstrated that GluK2 is a Parkin substrate and that the loss of Parkin function increases surface and total GluK2 levels, and consistently increases KAR currents.

EOPD is associated with a massive dopaminergic neuronal loss in the SNpc, a brain region receiving many glutamatergic inputs from different brain areas and for this reason these neurons are very vulnerable to glutamate. This highlights the hypothesis that DA neurons depletion in *Park2* could be the consequence of excitotoxicity.

A recent paper (Regoni M, 2020) showed that the spontaneous firing-frequency sensitivity to UBP310, which is a KAR antagonist, is increased in Parkin-Q311X DA neurons and that means that KAR can modulate DA neuron firing frequency. Parkin-Q311X is a bacterial artificial chromosome (BAC) transgenic mouse that express a C-terminal truncated human mutant Parkin. In this study they decided to use this mouse model instead of Parkin knockout mouse because it displays mild nigrostriatal, cognitive, and noradrenergic dysfunctions. Parkin knockout mouse does not show nigral DA

neurons loss which is the hallmark of PD. As a matter of fact, this Parkin-Q311X mouse model shows dopaminergic neurons degeneration at 6 and 16 month of age. This neurodegeneration was preceded by signs of mitochondrial dysfunction, an extensive cytoplasmic vacuolization, and a dysregulation of spontaneous *in vivo* firing activity. This data suggests that Q311X mouse can recapitulate some key features of EOPD even if it does not display the human phenotype. A better scientific tool that can be used to study monogenic diseases is represented by cellular models that can be obtained straight from patient's samples. These models will be presented in the following chapters.

1.5 Modelling *Park2* through iPSCs

The first PD *in vitro* models were primary neuronal cultures (Cardozo, 1993). These cultures are especially relevant to study DA neuron properties and to challenge these neurons to various stresses for evaluation of neuroprotective agents. As human primary cultures are extremely difficult to obtain, the ones most used are the rat ones, as the dissection of rat embryo mesencephalon is easier and higher amounts of neurons can be obtained.

Primary midbrain cultures present the advantage that they are similar to the *in vivo* situation because they display the interaction between dopaminergic neurons and neighbouring neurons and glia. Unfortunately, they have some relevant limitations, as they are very difficult to maintain and they are composed of a mixture of neuronal and glial cells where DA neurons only represent a small amount, around 5-10%. For this reason, over the years, other PD cell models have been studied. In particular, the neuroblastoma cell line SH-SY5Y and the pheochromocytoma cell line PC12 have been widely used. They produce and release catecholamines, including dopamine, and through specific differentiating protocols they develop neuron-like properties including neurite-like processes. These cell models are easier to maintain but differentiation can be difficult. They can be good models for disease-specific drug development (Falkenburger BH, 2016).

Lund human mesencephalic (LUHMES) cells are one of the most commonly used immortalized cell lines (Lotharius J., 2005). They are generated from 8-week-old human ventral mesencephalic tissue and transformed with a construct expressing the myc oncogene under control of tetracycline. When tetracycline is added they differentiate into non-dividing neurons. These cells display similarities with dopaminergic neurons such as neuronal markers and electrical properties (Scholz D., 2011).

Similar cell lines are the mouse immortalized neuronal progenitor cell line MN9D (Hermanson E., 2003) and the rat immortalized neuronal progenitor cell line CSM14.1 (Haas, 2002). Immortalized cell lines are a homogenous population of continuously proliferating cells and this allows large-scale experiments with reproducible data. In addition to that they can be genetically manipulated and can be frozen at -150°C. This allows the generation and preservation of cellular lines stably expressing a protein of interest. There are some disadvantages using these cell models. First of all, after differentiation they are more delicate to maintain and more difficult to be genetically manipulated; they are also not suitable for all cell suspension techniques. In addition to that they are non-patient-specific which is one of the biggest limitation of this model.

The pioneering work on mouse embryonic stem cells (ESC) (Thomson JA, 1995) set the base for the development of a culturing technique that could lead to the generation of human ESC (hESC) (Thomson J. A., 1998). Theoretically, these cells have the capability to give rise to all somatic cell types present in an embryo and they can be used to be differentiated also in neural and glial cells. Although hESC represent a very interesting model there are many disadvantages in using them. First all they can only be obtained from donated human embryos with all the ethical concern that this involves and as a consequence they also have a limited availability; secondly they can only be used to model embryonic development diseases or diseases that are prenatally diagnosed and this makes this model not suitable for many other diseases including the majority of neurodegenerative diseases.

A revolution in the field of *in vitro* models of human diseases has been made, in 2006, by Takahshi and Yamanaka when they developed an efficient protocol for the generation of iPSCs from somatic cells (Takahashi K, 2006) .This discovery has modified the studying approach to many diseases, including neurodegenerative ones. The inducted expression of four factors, Oct3/4, Sox2, c-Myc, and Klf4 (known as Yamanaka's factors), in somatic cells led to the generation of pluripotent embryonic stem cells. Since Yamanaka's publication (Takahashi K, 2006) different methods have been generated to deliver these factors into the cells (Ring K.L., 2012) (Wang Y, 2011). These cells can be afterwards differentiated in many cell types, including neurons and glial cells (Kim H.S., 2013) (Han

D.W., 2012) (Nolbrant S, 2020). The innovation of this method is the possibility of generating *in vitro* models straight from the patients affected by the disease object of study. Reaching this milestone have widened the understanding of diseases mechanisms, including PD. They also represent a reproducible tool that can be used to test new pharmacological agents.

The generation of DA neurons starting from iPSCs has been reported for the first time in 2011 by Kriks et al. (Kriks S, 2011). In this paper they described a protocol for the differentiation of hESCs and iPSCs into DA neurons. They used a dual-SMAD inhibition to obtain floor plate cells with the optimization of factors such as SHH C25II, Purmorphamine, FGF8b and CHIR99021. Further maturation into DA neurons was obtained using a B27 Neurobasal medium supplemented with ascorbic acid, BDNF, GDNF, TGFbeta3 and dbcAMP. *In vivo* survival and function of these DA neurons was demonstrated using three host species PD models. The transplantation of these DA neurons not only prevented the neurodegeneration but also induced motor improvements.

Three years later Zhang et al. (Zhang P, 2014) published a paper where they described an optimized culture method for the stepwise differentiation of iPSCs to A9 DA neurons, which mimics embryonic DA neuron development. In their protocol, they generated floor plate precursor cells starting from iPSCs and further differentiated them into DA neurons using a small molecule method. These cells could be maintained *in vitro* for several months. They reported few critical steps in the dopaminergic differentiation protocol. First, iPSCs should be completely undifferentiated as a spontaneous differentiation to all three germ layers is always possible in iPSCs cultures. For this reason, it is important to remove the differentiated colonies before starting the protocol. Second, single iPSCs should be plated at an established cell density in order to prevent the detachment of cells during the differentiation.

The generation of iPSCs from somatic cells of patients carrying *Park2* homozygous mutations has been reported in literature since 2012 when the first papers regarding the generation of DA neurons derived from *Park2* iPSCs were published (Sánchez-Danés A,

2012) (Imaizumi Y, 2012). The study (Sánchez-Danés A, 2012) was performed on two *Park2* cell lines and two controls and showed an increase in DA release and a decreased uptake in *Park2* DA neurons. One cell line showed also an augmented level of MAOB with consequent oxidative stress whereas the other not and that was attributed to different mutations (the first one carried a homozygous exon 3 deletion whereas the second one a heterozygous deletion of exon 3 and 5). The analyses performed failed to show that *Park2* mutations lead to mitochondrial dysfunction. Whereas the other study (Imaizumi Y, 2012) was performed on two *Park2* cell lines that were differentiated into DA neurons: one from a patient carrying a deletion in exons 2–3, and the other from a patient carrying a homozygous deletion of exon 6 and 7. Both cell lines showed an increased oxidative stress with abnormal mitochondrial morphology and homeostasis. This study reported also an α-synuclein accumulation only in the first cell line iPSCs-derived DA neurons but the authors attributed it to a different protocol used.

Since these first two publications different papers have been published regarding the capability of generating iPSCs from somatic cell of *Park2* patients and the study of pathogenic mechanisms related to this mutation. In particular, the focus of these studies regarded mitochondrial dysfunction, oxidative stress and neurites alteration.

A detailed profile of *Park2* iPSCs has been performed in 2018 by Marote et al. (Marote A, 2018) who made an accurate analysis on three iPSCs clones carrying a compound heterozygous mutation of *Park2* gene. They expressed common pluripotency markers and could differentiate into the three germ layers. Two other similar characterizations have been published, one in 2019 and one in 2020. The first one (Zanon A, 2019) described one iPSCs line carrying a homozygous exon 3 deletion in *Park2* gene and confirmed the spontaneous differentiation capacity of these cells and their ability in forming EBs containing all the three germ layers (ectoderm, endoderm and mesoderm). The second one (Tariq M, 2020) characterized three iPSCs clones of one *Park2* PD patient carrying a puntiform mutation (p.C253Y). Also in this case it was demonstrated the ability of all clones to generate EBs and to differentiate in the three germ layers.

As already described in the previous chapter, mitochondrial dysfunction has been widely studied in *Park2* in *in vivo* and *in vitro* models. This impairment was first documented in mice and flies lacking Parkin (Palacino J. J., 2004) (Casarejos M. J., 2006) (Thomas M., 2007). Mitochondrial dysfunction has also been assessed in *in vitro* cellular models. As described before, abnormal mitochondrial morphology, impaired mitophagy and increased oxidative stress have been observed in *Park2* iPSCs-derived DA neurons (Imaizumi Y., 2012) (Chung SY, 2016) (Suzuki S, 2017). The study conducted by Chung et al. also reported accumulation of α-synuclein in *Park2* iPSCs-derived DA neurons. Mitochondrial impairment has also emerged from another study (Shaltouki A, 2015) conducted on patient-specific and isogenic *Park2* iPSCs that displayed an altered neuronal proliferation and mitochondrial alterations. The same phenotype was confirmed in isogenic *Park2* null lines. Another recent study confirmed that knocking out *Park2* gene in human iPSCs leads to increased oxidative stress, mitochondrial dysregulation and lysosomal impairment (Ahfeldt T, 2020) consequently resulting in DA neurons death. A very recent publication of Yokota et al. (Yokota M, 2021) also described mitochondrial dysfunction in patient-derived DA neurons. Mitochondria dysfunction has been also recently reported by Okarmus et al. (Okarmus J., 2021) in Parkin knockout iPSCs-derived DA neurons.

Another important observation that has been made studying *Park2* iPSC-derived DA neurons is that these mutations lead to reduced neurite length and complexity (Yong Ren, 2015) (Jiali Pu, 2020). *Park2* mutations destabilize MTs through an over-acetylation (Ren Y, 2015). As suggested Parkin is a MT regulator during neuronal aging. This defective neuritogenesisi has been also reported by Bogetofte et al. (Bogetofte H, 2019) due to the altered function of the binding protein RhoA.

Lysosomal impairment has been reported by Okarmus et al. (Okarmus J, 2020) in two isogenic Parkin knockout iPSCs lines generated from a healthy control. IPSCs have been then differentiated into DA neurons. Parkin KO showed an altered lysosomal morphology with enlarged electron-lucent lysosomes and an increased lysosomal content, exacerbated by mitochondrial stress. These features could be rescued by antioxidant treatment. These

findings might indicate that there is a pathogenic feedback between mitochondria and lysosomes although further studies especially on *Park2* derived iPSCs are mandatory.

Park2 iPSC-derived DA neurons seem to have an alteration in the programmed cell death as it was demonstrated by Konovalova et al. (Konovalova EV, 2015). In this paper they characterized the pro-apoptotic dysfunction in iPSCs-derived DA neurons from a patient carrying compound heterozygous mutations (del202-203AG and IVS1+1G/A) and a control and they found that the mutated line had increased anti-apoptotic factors.

Back in 2012, a study published by Jiang et al. (Jiang H., 2012) demonstrated that *Park2* iPSC-derived DA neurons expressed increased levels of monoamine oxidase (MAO) with consequent increased oxidative stress, and an increased calcium-independent DA release with a reduced DA uptake. MAO-A and MAO-B transcription is increased in *Park2*; MAOs are mitochondrial enzymes responsible for oxidative deamination of dopamine, a process that release a great amount of ROS. *Park2* mutations also reduces the binding sites of DAT. Taken together, these results suggested the key role of Parkin in regulating dopamine utilization and suppressing dopamine oxidation.

Electrophysiological alterations have been observed in midbrain iPSCs-derived DA neurons of *Park2* mutated patients (Zhong P., 2017). In particular, they noted in *Park2* iPSCs-derived DA neurons that dopamine induced a delayed increase in the amplitude of spontaneous Excitatory Postsynaptic Current (sEPSC). This dopamine action was particularly evident when D2-recpetors were inhibited or when D1-receptors were selectively activated. This was able to elicit a large rhythmic bursting of sEPSC. This rhythmic bursting of sEPSC in *Park2* neurons reminds of the oscillatory neuronal activities in basal ganglia of PD patients and PD animal models with differences in frequency and dopamine impact on the oscillation. *Park2* mutations cause presynaptic glutamatergic transmission potentiation through D1-class dopamine receptors, leading to abnormal rhythmic bursting of neuronal activities in basal ganglia, which is known to be a characteristic feature of PD.

The ability to generate functional DA neurons from patient-derived iPSCs constitute a unique opportunity to investigate neurodegenerative pathogenic mechanisms, especially in monogenic forms such as the ones related to *Park2* mutations. Unfortunately, two-dimensional models cannot recapitulate the complexity of human mesenchepalus which is the neurodegenerative focus in PD.

Next step in the investigation of pathogenic mechanisms related to *Park2* mutations is the generation of a three-dimensional model, so called midbrain organoid. A recently published paper by Kano et al. (Kano M, 2020) analysed astrocytic changes in human brains from *Park2* individuals. Few glial fibrillary acidic protein (GFAP) and vimentin-positive astrocytes were observed in the SNpc of these *Park2*-mutated subjects compared to subjects with sporadic PD. They also generated iPSCs-patient derived midbrain organoids and confirmed a decreased number of GFAP-positive astrocytes in *Park2*-mutated organoids compared with age- and sex-matched controls. This three-dimensional cellular model will be introduced in the next chapter.

1.6 Modelling *Park2* through innovative brain organoids

The ability to generate functional dopaminergic neurons from patient-derived iPSCs represents a unique opportunity to investigate pathogenic mechanisms leading to neurodegenerative disorders, especially in monogenic forms such as the one related to *Park2* mutations. Unfortunately, two-dimensional models cannot recapitulate the complexity of human mesenchepalus which is the neurodegenerative focus in PD.

A further step forward in *in vitro* models of neurologic diseases was done in 2013 by Lancaster et al. (Lancaster MA., 2013) with the development of an efficient protocol for the generation of iPSCs-derived three-dimensional neural systems, so called "brain organoids". These extremely innovative models present similarities with real human brain, especially concerning cellular, functional and anatomic features. They also recapitulate some of the most important characteristics of the developing human brain. In addition, they are an unprecedented scientific tool extremely useful for brain disease modelling and personalized drug screening. Brain organoids bridges the gap between traditional 2D *in vitro* models and *in vivo* animal models because they recapitulate the interaction between glial cells and neurons in a spatially organized microenvironment and for this reason they have a great potential for neurological diseases modelling, including neurodegeneration. After aggregation, cells are embedded in a matrix that gives them a structural support, and induce a polarity for the formation of an apicobasal neuroepitelium. These embriod bodies (EBs) embedded in matrix freely float in stirrer flasks and self-organize in brain-like spheres (Lancaster MA., 2013) (Paşca AM, 2015). The original protocol does not use patterned factors in the first phase of organoids generation in order to avoid limitations on specific brain regions identity.

The classic cerebral organoid protocol has been modified through the years, in order to generate more regionally specific 3D cell cultures (Lancaster M.A., 2014) (Lancaster M. A., 2016). Different research groups have demonstrated that it is possible to obtain

specific brain regions through different protocols. Paşca et al. (Paşca AM., 2015), in their study, used a dual-SMAD inhibition through Dorsomrphin and SB-431542 to obtain a neural induction. Neuronal progenitors expressing telencephalic markers such as paired box protein 6 (PAX6) and forkhead box protein G1 (FOXG1) were generated by adding fibroblast growth factor 2 (FGF2) and epidermal growth factor (EGF) without extracellular scaffolding. Further neuronal differentiation was then induced with brain-derived neurotrophic factor (BDNF) and neurotrophic factor 3 (NT3) which enabled the generation of dorsal cortex neural and glial elements. Compared to the original Lancaster's protocol, Paşca et al. were able to generate a 3D brain subregion containing a reduced number of ectodermal derivatives. To obtain homogenous brain organoids, during the first two weeks, EBs were pre-patterned by inhibiting the TGF-β signalling with the activation of Wnt signalling by glycogen synthase kinase 3 (GSK-3β) inhibitor CHIR-99021 (CHIR). This generated forebrain organoids, organized in multi-layers containing neuronal types of all six cortical layers. A similar approach of using a dual-SMAD inhibition (through SB and LDN-193189 (LDN)) was published by Quian et al. (Qian X., 2016) who maintained the Lancaster's method but used miniaturized bioreactors in order to make the production and maintenance of these organoids easier. They patterned the EBs to a hypothalamic fate by activating Wnt and sonic hedgehog (SHH) signalling and applying WNT3a, SHH, and Purmorphamine (PMA) to the culture.

Lancaster et al. (Lancaster MA., 2013) for the first time demonstrated the potential of brain organoids as a model to study neurodevelopment disorders and they generated organoids carrying a mutation causing microcephaly. As a matter of fact, it was suggested that Zika virus (ZIKV) infection was responsible for microcephaly in neonates and for that reason, the first brain organoids, as they recapitulate cortical development, were realized in order to study the pathogenesis of this disease. Thanks to organoids advanced organizational features they were able to demonstrate the link between ZIKV and microcephaly. In addition to this successful application, brain organoids could be used to study other neurological disorders. One example is the study of brain tumour through the generation of so-called "tumouroids" derived from human glioblastoma, the most common and aggressive brain cancer (Dutta D, 2017). These tumoroids present a hypoxic gradient and stem cell heterogeneity that cannot be recreated with 2D cultures. Brain organoids have been used also to study neurodegenerative diseases such as AD (Choi SH,

2014) (Raja WK, 2016). 3D cultures allowed the generation of a pathologic environment able to promote the formation of amyloid-β (Aβ) plaques and neurofibrillary tangles (NFTs), which are the pathological hallmarks of AD. These proteins aggregates cannot be generated using 2D cultured human neurons. Brain organoids could facilitate the study of neurodegenerative disorders because they represent a precise human cellular model. Brain organoids are a better model also to test drugs because they present a metabolism that is similar to human. On top of that, organoids present cell-to-cell interactions and cytoarchitecture that are important to predict the effectiveness of *in vitro* tested compounds in clinical trials. 3D cultures contain mature neurons that establish multiple connections to neuronal and non-neuronal cells in a physiologic environment that is closer to nature. These neurons have morphological and physiological properties similar to those *in vivo*. As a matter of fact, it has been demonstrated that neurons developed in a 3D environment express a wider range of neuronal genes than normally 2D neurons do not express. As synaptic distances in 3D neuronal network are smaller there is a more functional signal transduction (Cullen DK, 2011).

Starting from the original protocols used for the generation of cortical mini-brains, different methods for the generation also of 3D midbrain organoids have been developed (Smits LM, 2019) (Monzel AS, 2017) (Jo J, 2016) (Qian X, 2016) (Kim H, 2019) (Chlebanowska P, 2020). The generation and characterization of midbrain organoids provides an advanced *in vitro* model to study neurodevelopmental and neurodegenerative midbrain disorders. As a matter of fact, these organoids contain a small population of midbrain dopaminergic neurons secerning dopamine. They contain also other types of neural cells, as well as glial cells, including astrocytes and oligodendrocytes. Electrophysiological characterization has been performed and the detection of neuronal activity has been assessed. They last more than bidimensional cellular cultures and this allows the development of the disease phenotype. Initial midbrain-like experiments reported by Qian and Tieng (Qian X., 2016) (Tieng V, 2014) were inspired by Kriks et al. (Kriks S, 2011). The same year another protocol for the generation of midbrain-organoids was published by Jo et al. (Jo J, 2016) followed later by the publication of Kim et al. (Kim H, 2019). Both protocols were based on the findings of Chambers et al. (Chambers SM, 2009). The protocols of Monzel et al. (Monzel AS, 2017) and Smith et

al. (Smits LM, 2019) were based instead on 2D experiments by Reinhardt et al. (Reinhardt P, 2013).

The first step in the generation of midbrain organoids is the induction of a dual-SMAD inhibition. SB was used in all of these protocols to inhibit the Activin/TGF beta signalling pathway; LDN or Nogging were used to obtain the inhibition of the Bone Morphogenetic Proteins (BMP) pathway. To induce neural progenitor cells, CHIR, a potent chemical inhibitor of GSK-3β, was used to activate the WNT signalling pathway (Kirkeby A, 2012). The final patterning, toward midbrain floor plate precursors, was obtained by activating the SHH signalling pathway, using SHH, PMA or smoothened agonist (SAG) (Kriks S, 2011) and FGF8 activators as well. This patterning induces the generation and maturation of midbrain-specific dopaminergic neurons with a gene expression profile similar to human prenatal midbrain samples. To quantify dopaminergic neurons organoids were dissociated and plated as a monolayer and quantification was performed in two ways: or through immunofluorescence or through Fluorescence-activated Cell Sorting (FACS). All these methods used dopaminergic markers, especially TH, even if it is not specific and expressed by other catecholaminergic cells. Another more specific DA neuronal marker is DAT. The percentage of DA neurons found was between 22% and 64% at different timepoints.

There is a limitation in current organoids which is the lack of microvasculature, resulting in limited oxygen and nutrient delivery to the inner part. Recently efforts have been made in trying to find a way of vascularizing them. Transplanting them onto the cortex of the mouse brain induce the outgrowth of murine vessels into the human tissue (Mansour AA, 2018). The possibility of generating *in vitro* functional vasculature-like network in organoids has been demonstrated also starting from ESCs (Cakir B, 2019) and from iPSCs (Pham MT, 2018). The possibility of vascularizing them could prolong their survival allowing the aging process which is fundamental to study many neurodegenerative diseases.

Until now only one paper has been published regarding the generation of midbrain organoids from iPSCs of patients carrying *Park2* mutations (Kano M., 2020). They started their study from the neuropathological evaluation of SN of two patients carrying *Park2* mutation, one idiopathic PD (iPD) and one control. They observed a marked SN depigmentation in the two *Park2* samples with severe neuronal loss, but they did not observe an astrogliosis compared to iPD. iPD had increased intermediate filaments (IF) proteins such as GFAP and vimentin, indicating a reactive phenomenon. To further investigate the effects of *Park2* mutations on astrocytes they generated, using the protocol published by Monzel et al. (Monzel AS, 2017), midbrain organoids that were differentiated until day 35. Midbrain organoids generated from iPSCs of patients carrying *Park2* mutations had a lower percentage of GFAP+ astrocytes compared to controls, although they did not generate comparative iPD midbrain organoids.

It is clear now that *Park2* PD has a different pathogenesis from idiopathic PD and other monogenic forms of PD even if there are some common pathways. Yamamura when first studied patients affected by *Park2* PD was convinced that it was a different kind of disease, and he hypnotized that could be caused by an inborn error in metabolism (Yamamura, 2010). He formulated this hypothesis based on unique clinical aspects of this disease. First of all, disease-onset was very early, in most cases below 20 years of age and often in childhood. Secondly there were diurnal fluctuations with alleviation of parkinsonian symptoms after sleeping, suggesting there might be a reversible process of consumption and restoration of dopamine or some dopamine-related mediator. These are extremely interesting observations and, taking into account all the pathogenic roles played by *Park2* discovered until now, we might consider *Park2* PD a neurodevelopment disorders. In midbrain development of these patients, different mechanisms can lead to the generation of an impaired midbrain neuronal network involving not only dopaminergic neurons but also GABAergic and glutamatergic neurons. For this reason, the right model to study *Park2* pathogenic mechanisms, is the iPSC-derived midbrain organoid, as it recapitulates human midbrain neurodevelopment and can be obtained by patients affected by these mutations.

2. Aims of the study

Parkinson's Disease (PD) associated to *Park2* mutations has a different pathogenesis from idiopathic PD and other monogenic forms of PD even if there are some common pathways. It might be even considered a neurodevelopment disorders where different mechanisms lead to the generation of an impaired midbrain neuronal network involving not only dopaminergic neurons but also GABAergic and glutamatergic neurons.

Solid published data show the role of Parkin in modulating excitatory synapse function (Maraschi A et al., 2014; Fallon L et al, 2002; Helton TD et al., 2008; Staropoli JF et al. 2003). As a matter of fact, *glutamatergic toxicity* has emerged to be an important contributor to neurodegeneration in *Park2*-associated PD, by causing a dysfunction of the glutamate *Kainate Receptor (KAR).* Evidence shows that *Park2* mutations lead to KAR *upregulation* which results in cellular glutamate toxicity and degeneration (Maraschi A, 2014). *Park2* is a gene highly expressed in SNpc neurons and astrocytes and KAR upregulation may result not only in *dopaminergic neurons degeneration* but also in *astrogliopathy*.

The *first aim* of the project is to generate pre-clinical *in vitro* models of *Park2* PD starting from iPSCs of patients carrying *Park2* mutations and controls. Two-dimensional models of dopaminergic neurons and astrocytes and also three-dimensional models, so called "midbrain organoids", were generated and characterized.

The *second aim* of the project is to characterize all these *Park2* cellular models from a molecular and functional point of view in order to assess differences from controls.

The *third aim* of the project is to test KAR upregulation in these pre-clinical *in vitro* models. Neuronal and astroglial KAR levels were quantified and excitotoxicity was assessed through electrophysiology.

These data are essential to elucidate KAR physiological function in basal ganglia, KAR potential pathological role in *Park2* PD and perhaps other forms of PD.

Next step will be to test, for the first time, the effects of a KAR antagonists on *Park2* human midbrain organoids and also its potential neuroprotective effects. The results of this project might lead to the development of new disease-modifying pharmacological tools. Overall, this project may create the rationale for future clinical trials leading to the prevention and cure of a still untreatable disease.

3.Materials and Methods

3.1. PBMCs and fibroblasts isolation

PBMCs are obtained from peripheral blood using a tested protocol in use in our laboratory. Peripheral blood sample is obtained from the patient, kept at room temperature and processed within four hours. An equal volume of blood is added to an equal volume of room temperature PBS 1x (1:1). The volume of the blood mixed with PBS is then drop-by-drop layered on top of an equal volume of room temperature Histopaque-1077 (Sigma, Histopaque, cat. Nr. 10771) and centrifuged at 1000 x g for 30 minutes. After centrifugation, the upper layer is carefully aspirated using a P1000 or a Pasteur pipette to within 0.5 cm of the opaque interface containing mononuclear cells. The upper layer is then discarded. The opaque interface is then carefully transferred into a new falcon containing 10 mL of DMEM 15% FBS, using a P1000 or a Pasteur pipette. The tube is centrifuged at 400 x g for 10 minutes, the surnatant is aspirated and discarded and the pellet is resuspended and plated in a 24-well plate using 1 mL of an hematopoietic medium (Gibco, StemPro™-34 SFM (1X) cat. Nr. 10639011) containing Il-3 (20 ng/mL), IL-6 (20 ng/mL), FLT-3 (100 ng/mL) and SCF (100 ng/mL). PBMCs can be kept in culture at 37°C and CO2 5% for several days, changing the medium every other day and splitting cells when needed. PBMCs can be also frozen in their medium added with 10% DMSO and kept at -80°C for 24/48 hours and then transferred into liquid nitrogen for extended storage.

Fibroblasts are obtained from a 5 mm skin biopsy of the patients using a biopsy punch. The skin sample can be kept in Dulbecco's modified Eagle's medium (DMEM) supplemented with fetal bovine serum (15%), penicillin/streptomycin (1%), and amphotericin B (1%). The skin sample is then transferred into a tissue culture plate and cut into small pieces. A thin layer of DMEM 15% FBS is changed every other day until fibroblast have grown, covering the whole surface of the plate. At this point fibroblasts

can be splitted using Trypsin 1 % and frozen. Fibroblasts can be frozen in their medium (DMEM 15% FBS) added with 10% DMSO, for the first 24/48 hours at -80°C and later transferred into liquid nitrogen. Also the skin biopsy sample can be straightly frozen in the same way, using DMEM 15% FBS with 10% DMSO.

3.2. iPSCs generation, characterization and expansion

In this study 4 iPSCs lines of controls and 4 iPSCs lines of patients carrying *Park2* mutations were used (*see table 1*). These iPSCs lines were obtained by reprogramming patients' fibroblasts and PBMCs.

Table 1. iPSCs lines used in the project

iPSCs line	Mutation	Sex	Age
CTR 1	/	F	newborn
CTR 2	/	M	45
CTR 3	/	M	45
CTR 4	/	F	40
Parkin 1	c.986_987insG (p. V330Rfs*17) hom	F	~40
Parkin 2	c.924C>T (p.R275W) het ; Del exon 6 het	F	~40
Parkin 3	Del exon 3, p.T240M	F	39
Parkin 4	Del exon 4-5 hom	M	45

Fibroblasts and PBMCs were reprogrammed into iPSCs using a commercially available kit (CytoTune-iPS 2.0 Sendai Reprogramming Kit, Thermo Fisher).

Fibroblasts were incubated with reprogramming viral vectors for 24 hr. After another 6 days of culture, cells were detached, plated on feeder-coated 6-well plates, and maintained in a culture medium suitable for pluripotent stem cells (Essential 8 Medium, Thermo Fisher). When colonies appeared, they were transferred to Matrigel-coated culture dishes and expanded.

PBMCs were transduced by adding the reprogramming vectors at appropriate MOI (i.e. KOS: MOI=5, hc-Myc MOI=5, hKlf4 MOI=3) in a total volume of 1 mL. PBMCs were then centrifuge at 2250 rpm for 30 minutes at room temperature and plated in a 12-well tissue culture plate and incubated overnight at 37°C. The following day the viral vectors were removed by centrifugating the cells at 1500 rpm (400 x g) for 10 minutes and resuspending cells in 0.5 mL of complete StemPro-34 medium (Thermofisher, cat. Nr. .10639-011) in a 24-well plate. On day 3 after the reprogramming cells were plated on a 24-well plate coated with feeder or Cultrex in a StemPro-34 medium without cytokines. On the following day the medium was switched to Essential-8 medium (E8, ThermoFisher, cat. Nr. A1517001) and it was changed daily. When colonies appeared, the clones were selected and transferred to Cultrex-coated 6-well plates and expanded.

For the expansion, colonies were detached from the plates using ethylenediaminetetraacetic acid solution (EDTA) 0.5 mM or by picking them using a P20 pipette and plated in new 6-well plates. Colonies were also frozen in a knock out serum (KSR) medium supplemented with 10% DMSO at -80°C for the first 24/48 hours and then transferred to liquid nitrogen for extended storage.

Karyotype analyses were also performed on all clones of generated iPSCs lines. After adding colchicine, cells were processed with a hypotonic solution (0.6% sodium citrate and 0.13% potassium chloride) and fixed with a methanol/acetic acid solution (ratio 3:1). A quinacrine solution was used to obtain Q-banding and cell metaphases were acquired under a fluorescence microscope at 100× magnification; metaphases were analysed with a MetaSystems-Ikaros analytical system. About 30 metaphases from at least two independent cultures were analysed according to the ISCN and to the European General Guidelines and Quality Assurance for Cytogenetics at approximately 300–400 band level.

3.3. iPSCs differentiation into dopaminergic neurons

iPSCs were differentiated toward dopaminergic neurons according to the protocol described by Zhang et al. (Zhang P, 2014) (with slight changes) which, in turn, is based on the protocol described by Kriks et al. (Kriks S, 2011).

Cells were cultured in proper media supplemented with specific factors at proper concentrations as follows. *Day 0:* KSR differentiation medium (81% DMEM, 15% KSR, 100× 1% non-essential amino acids, 100× 1% β-mercaptoethanol, 100× 1% penicillin/streptomycin, 100× 1% amphotericin) supplemented with 10 μM SB431542 and 100 nM LDN-193189. *Days 1 and 2:* KSR differentiation medium supplemented with 10 μM SB431542, 100 nM LDN-193189, 0.25 μM SAG, 2 μM purmorphamine, and 50 ng/mL fibroblast growth factor 8b (FGF8b). *Days 3 and 4:* KSR differentiation medium supplemented with 10 μM SB431542, 100 nM LDN-193189, 0.25 μM Smoothened agonist (SAG), 2 μM purmorphamine, 50 ng/mL FGF8b, and 3 μM CHIR99021. Days 5 and 6: 75% KSR differentiation medium and 25% N2 differentiation medium (97% DMEM, 100× 1% N2 supplement, 100× 1% penicillin/streptomycin, 100× 1% amphotericin) supplemented with 100 nM LDN-193189, 0.25 μM SAG, 2 μM purmorphamine, 50 ng/mL FGF8b, and 3 μM CHIR99021. *Days 7 and 8:* 50% KSR differentiation medium and 50% N2 differentiation medium supplemented with 100 nM LDN-193189 and 3 μM CHIR99021. *Days 9 and 10:* 25% KSR differentiation medium and 75% N2 differentiation medium supplemented with 100 nM LDN-193189 and 3 μM CHIR99021. *Days 11 and 12:* B27 differentiation medium (95% neurobasal medium, 50× 2% B27 supplement, 1% Glutamax, 100× 1% penicillin/streptomycin, 100× 1% amphotericin) supplemented with 3 μM CHIR99021, 10 ng/mL brain-derived neurotrophic factor (BDNF), 10 ng/mL glial cell line-derived neurotrophic factor (GDNF), 1 ng/mL transforming growth factor β3 (TGF-β3), 0.2 mM ascorbic acid, and 0.1 mM cyclic AMP. *From day 13 to the end* of differentiation: B27 differentiation medium supplemented with 10 ng/mL BDNF, 10 ng/mL GDNF, 1 ng/mL TGF-β3, 0.2 mM ascorbic acid, and 0.1 mM cyclic AMP. At 20 DIV cells were split using Accutase.

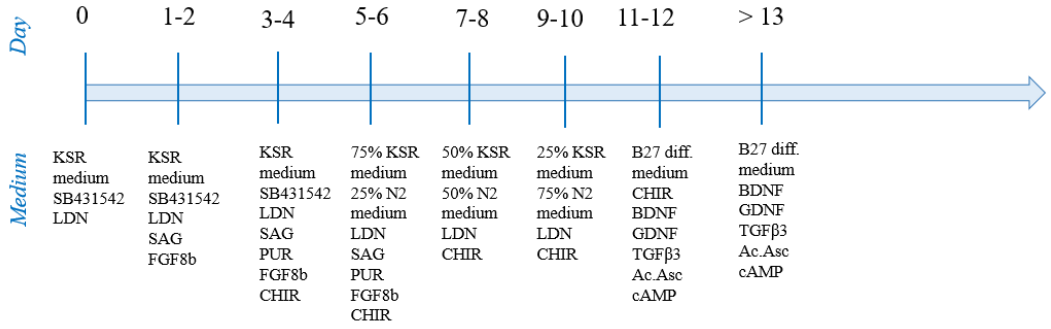

Figure 2. Protocol for iPSCs dopaminergic neurons differentiations (Zhang et al., 2014).

3.4. iPSCs differentiation into mature astrocytes

iPSCs were differentiated into astrocyte following the protocol described by Santos et al. (Santos R, 2017) with mild modifications (*summarized in figure 3*). On day 0 three confluent wells of a 6-well plate were disaggregated using Accutase and resuspended in 15 mL of E8 with 10 uM ROCK and plated into a 100mm ultra-low attachment culture dish (Corning, cat. Nr. 3262). The following day, when embryoid bodies (EBs) were formed, the medium was switched to ScienceCell astrocyte medium plus Nogging (500 ng/ml) and PDGFAA (10 ng/ml). On day 15 medium was switched to ScienceCell medium added with just PDGFAA (10 ng/ml). On day 21 EBs were disaggregated using Trypsin on polyornithin (PORN)–laminin coated plates and kept in ScienceCell medium added with FGF2 20 ng/ml, EGF 20 ng/ml, laminim 1 ug/ml and 10 uM ROCK. The day after the medium was changed without ROCK inhibitor and glial precursor cells (GPCs) were expanded and frozen for few passages. After two weeks of expansion GPCs were differentiated into astrocytes using an astrocyte medium (AM) made of DMEM/F12, Glutamax, N2, B27 supplement added with 10% FBS and LIF (10 ng/ml). LIF was kept for 15 days after which the medium was switched to an AM without factors.

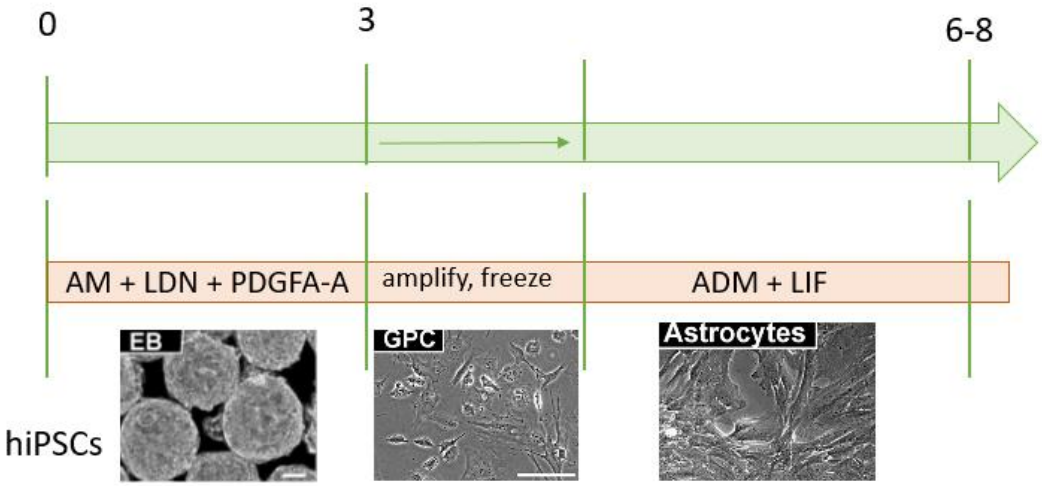

Figure 3. Santos' protocol for iPSCs differentiation into mature astrocytes.

3.5. Midbrain organoids generation and differentiation

Midbrain organoids were generated using a protocol developed in our laboratory which is based on Lancaster protocol (Lancaster MA, 2014) and Zhang protocol (Zhang P, 2014).

iPSCs colonies were grown in one well of a 6-well plate until 70-80% confluency was reached. *On day 0*, cells were detached with 0.5mM EDTA solution and Accutase© (Thermo Fisher). Colonies were then centrifuged at 270 x g for 5 minutes and resuspended in hES medium with 50 uM ROCK and plated at 9,000 live cells/150 µl in each well of a low attachment 96-well U-bottom plate (Corning, cat. Nr. 7007). EBs were fed every other day. 50 µM ROCK inhibitor and 4 ng/ml bFGF were included until EBs began to brighten or were larger than 350-400 µm in diameter. *On day 6*, each EB was transferred to one well of a low attachment 24-well plate containing 500 µl Neural induction medium (NIM). EBs were fed every other day. *On day 10*, EBs were embedded in a drop of Cultrex© (R&D) and transferred into a dish containing Cerebral medium organoid differentiation medium without vitamin A. *On day 14*, embedded organoids were transferred to a spinning bioreactor and starting from this day dopaminergic patterning was obtained following Zhang (Zhang P, 2014) protocol described above for dopaminergic differentiation (*protocol summarized in figure 4*).

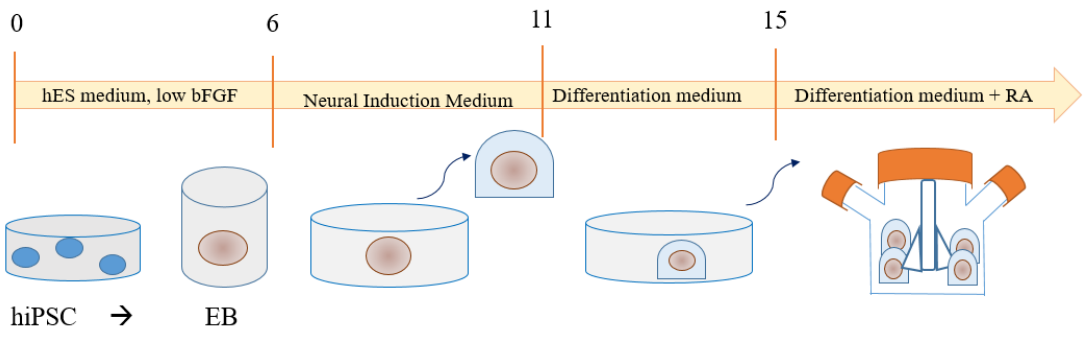

Figure 4. Midbrain organoids differentiation protocol.

3.6. Western blot analyses

WB analyses were performed in collaboration with Jenny Sassone at the Neuropsychopharmacology Unit of San Raffaele Hospital.

Cells were washed in Phosphate Buffered Saline 1X (PBS, Sigma) on ice and scraped. After centrifugation at 13,3 rpm for 1 minute, cells lysates were prepared in ice-cold lysis buffer (50 mM Tris-HCl, pH 7.5, 150 mM NaCl, 1 mM EDTA, 1% NP-40, 0.5% sodium deoxycholate, and 0.1% sodium dodecyl sulfate (SDS)) added with Complete Protease Inhibitor Cocktail (Sigma). Lysates were incubated in ice for 30 min, sonicated in ice for 15 s with the ultrasonic processor UP100H (Hielscher) with a frequency of 30 kHz, and a power output of 80%, and centrifuged at 13,000 rpm at 4°C for 20 min. Proteins in the supernatant were quantified by BCA assay (Thermo Scientific) according to the manufacturer's instructions. Samples were diluted with 3X SDS loading buffer (188 mM Tris-HCl, pH 6.8, 6% SDS, 30% glycerol, and 0.3% bromophenol blue) and 1 M 1,4-dithiothreitol (the final concentration of DTT was 100 mM) and heated to 95°C for 10 min. Protein extracts (20 μg) were separated on NuPAGE 4–12% Bis–Tris gels (Life Technologies) with NuPAGE MOPS SDS Running Buffer (Life Technologies) and the MagicMark XP Standard molecular weight marker (Life technologies). After electrophoresis, gels were transferred onto nitrocellulose membranes (GE Healthcare) for 2 h at 400-mA constant current at 4°C in transfer buffer (25 mM Tris, 192 mM glycine, and 20% methanol). Post-transfer membranes were briefly incubated in Ponceau Solution (Sigma) to visualize proteins, rinsed in Tris-Buffered Saline containing 0.05% Tween-20 (TBS-T), blocked with 5% nonfat dried milk in TBS-T for 1 h at room temperature, and then incubated overnight at 4°C with the following primary antibodies (*see table 2*).

Table 2. WB antibodies list

Antibody	Brand	Cat. Nr.	Dilution
Anti-TUJ1	Promega	G721	1:5000
Anti-Gluk2	Origine	TA310550	1:1000
Anti-Parkin	Sigma	P6248	1:2000
Anti-GAPDH	Santa Cruz	Sc-25778	1:1000
Anti-TH	Millipore	MAB318	1:1000
Anti-DDC	Cell Signaling	13561	1:1000
Anti-EAAT2	Abcam	Ab41621	1:1000
Anti-GFAP	Cell Signaling	3670	1:1000

Membranes were then washed 3 x 10 min in TBS-T, incubated with horseradish peroxidase (HRP)-conjugated secondary antibodies (GE Healthcare-Amersham Biosciences) for 1 h at room temperature, and then washed 3 x 10 min in TBS-T. The antigens were detected using an immunodetection kit (Novex ECL, Invitrogen) according to the manufacturer's instructions. For visualization, we used the Chemidoc Touch Imaging System (BioRad). Band intensity was quantified by densitometry analysis using ImageJ software17. Briefly, the images were converted to an 8-bit format to perform uncalibrated optical density. After conversion, the background was subtracted through the rolling-ball radius method (default setting, ball radius value: 50.0 pixels). Each band was individually selected and circumscribed with the rectangular ROI tool selection. Data were acquired as arbitrary-integrated density values. The final relative expression level was normalized by the internal standard GAPDH.

3.7. Gene expression analyses

RNA extraction was performed from cell/organoid pellets collected in TRI Reagent (Sigma/Aldrich), at different time points. TRI Reagent is a phenol/guanidine isothiocyanate solution that maintains the integrity of RNA during the extraction process by the inhibition of RNAse activity during cells disruption. Every step was performed at 4°C if not otherwise stated. After a mechanical homogenization of the sample with 500 uL of TRI Reagent, 1/5 volume of ice-cold chloroform (Sigma-Aldrich) was added. Samples were vortexed until the two phases mixed together to form an emulsion. After that, samples were centrifuged for 15 min at 4°C at 12.000 g. The mixture was separated in three distinct phases: a lower red-coloured phase containing proteins and denatured DNA, an interphase composed by cellular membrane debris and a colourless upper aqueous phase containing RNA. This third phase was collected in a new tube and ice-cold isopropanol (Sigma-Aldrich) was added in 1:1 ratio, mixing gently. The RNA was precipitated over night at -20°C. The following day, samples were centrifuged 10 minutes at 4°C at 12.000 g. RNA precipitated at the bottom of the tube and supernatant was discarded. RNA pellets were washed twice with 1 mL of ice-cold 75% ethanol (Sigma-Aldrich) without resuspending it. For every wash, samples were centrifuged 5 minutes at 7.500 g at 4°C. After the last one, RNA pellets were suspended in 20 ul DNA/RNA-free water (Sigma/Aldrich) and stored at -80 °C until further use.

RNA was then quantified using NanoDrop One Spectrophotometer (Thermofisher). Measurements were made using 1uL of each sample and nucleic acid concentration was reported in ng/uL and two purity absorbance ratios are expressed (A260/A280 and A260/A230). A purity A260/A280 ratio of ~2 is accepted as “pure” for RNA. A A260/A230 purity ratio between 1.8 and 2.2 is generally accepted as “pure” for RNA. Purity ratios are important indicators of sample quality and an excessive presence of extraction reagents in the sample, such as phenol, can cause “impurity” contributing to an absorbance between 230 nm and 280 nm.

Retrotranscription of extracted RNA was performed with Real-time Polymerase Chain Reaction (qRT-PCR) technique through iScript cDNA Synthesis Kit (Bio-Rad) following manufacturer's instructions. 500 ng of RNA were transferred in a PCR RNAse-free tube and nuclease-free water was added up to 15 µL volume. Then 5 µL of mix solution (4 µL 5X iScript Reaction Mix/Buffer, 1 µL iScript Reverse Transcriptase) were added and the PCR tube containing complete reaction mix was incubated in a thermal cycler using the RT-PCR protocol. Once RT-PCR protocol was completed, cDNA was stored at -20°C until use.

Gene expression was quantified by real-time qPCR on 7500 RealTime PCR System (Applied Biosystems) with TaqMan molecular probes or standard primer-based SYBR green detection with and their respective commercially available TaqMan™ Universal PCR Master Mix (Applied Biosystems) or Power SYBR™ Green PCR Master Mix (Applied Biosystems). Cycle threshold were normalized on reference gene (YWHAZ) and fold change were calculated by ΔΔCt method (*see table 3* for primers list).

Table 3. qPCR primers list

GLUK 2-F	CTTCACTCAGCCGTGCCATT
GLUK 2-R	CGAATGAGACCAGTGCTGTCA
TH-F	TCCAGTGCACCCAGTATATCC
TH-R	AGGCCAATGTCCTGCGAGAA
DAT-F	GTCACCAACGGTGGCATCTA
DAT-R	TGGATGTCGTCGCTGAACTG
YWHAZ-FW	ACTTTTGGTACATTGTGGCTTCAA
YWHAZ-RV	CCGCCAGGACAAACCAGTAT
ALDH1L1-F	GCTCCATCATCTATCACCCGT
ALDH1L1-R	ATCTCCGTGAATGAGGGTCCA
GFAP-F	CTGCGGCTCGATCAACTCA
GFAP-R	TCCAGCGACTCAATCTTCCTC
OCT4-F	GAGAAAGCGAACCAGTATCG
OCT4-R	ACTCGGACCACATCCTTCTC
OCT4-F2	GTGGAGGAAGCTGACAACAA
OCT4-R2	ATTCTCCAGGTTGCCTCTCA
NANOG-F	GATTTGTGGGCCTGAAGAAA
NANOG-R	CTTTGGGACTGGTGGAAGAA

3.8. Immunofluorescence and immunohistochemistry

For IF analyses, DA neurons, astrocytes and midbrain organoids, after a rinse with PBS 1x were fixed with 4% paraformaldehyde (PFA) for 30 minutes. At least three PBs 1x washing were performed of 5-10 minutes each. After being fixed samples were conserved in PBS 1x at 4°C until the IF staining.

For IHC midbrain organoids, after a rinse in PBS 1x, were fixed in formalin 10% for 24 hours.

DA neurons and astrocytes IF was performed at our lab. 2D cultures (DA neurons and astrocytes) were first incubated for 30 minutes at room temperature (RT) with a permeabilization\blocking buffer made of PBS 1X, BSA 3%, NGS 5% and Triton-X 100 0.3%. Samples were then incubated overnight at 4°C with primary antibodies (see table 4) diluted in antibody buffer made of PBS 1X, BSA 3%, NGS 1%, Triton X-100 0.1%. The following day the plates were washed three times in wash buffer (PBS 1X, Triton X-100 0.1%) for 5 minutes each and incubated with secondary antibodies (Alexa Fluor 488, 568, 647, Molecular Probes; 1:500) at RT for one hour. Then cell nuclei were counterstained with 4', 6-diaminidino-2-phenylindole solution (DAPI) for 10 minutes. After two washes with PBS, coverslips were mounted with Dako fluorescence mounting medium (Dako, Carpinteria, CA, USA # S3023), left to dry for 12 hours at room temperature and then stored at 4°C until microscope acquisition.

Midbrain organoids IF was performed at our lab and at Prof. Arianna Bellucci's lab (Molecular and Traslational Medicine Departement, University of Brescia). Midbrain organoids, after being fixed with PFA 4%, were punt in a 15% sucrose solution overnight at 4°C. The following day the solution was changed to a 30% sucrose medium and left at

4°C overnight. The day after the organoids were embedded in O.C.T. (O.C.T. compound, VWR BDH Chemicals, Cat. No. 361603E), freezed with dry ice and conserved at -20°C for a short term or -80°C for longer periods. Samples were cryosectioned at the cryostat (Leica Microsystems) with slice's thickness of 12-15 μm. Sections were let dry at RT overnight and then conserved at -20°C or processed for IF as follows. First samples were treated with permeabilization with 0.5% Triton X-100 in PBS for 15 minutes at RT and then with blocking in 10% NGS + 0.1% Triton X-100 in PBS for 1 hour at RT. Sections were then incubated with primary antibodies (see table 4) in 3% NGS + 0.1% Triton X-100 in PBS overnight at 4°C. The day after they were washed three times in PBS 1X for 5 minutes each and incubated with secondary antibodies in the same solution of primary ones, for 1hour at RT. Secondary antibodies Alexa Fluor goat 488, 568 and 647 conjugates (Invitrogen 1:500) were used. Afterwards, sections were washed two times in 0.1% Triton X-100 in PBS and incubated with DAPI (0.1 μg/mL) nuclear counterstain for 10 minutes at RT and then washed with PBS 1X. Finally, the sections were mounted in Dako and covered with coverslips. Sections were stored at 4°C in dark until image acquisition through wide-field and confocal microscopes.

IHC staining was performed at the Anatomic Pathology Department of Policlinico Hospital of Milan. For IHC staining midbrain organoids, given their small diameter (1-3 mm), were processed using a "cytoblock" procedure, in order to avoid tissue loss and/or crushing. Samples were centrifuged at 1512 x g for 10 minutes in their medium. The pellet was then resuspended in a saline solution and another centrifugation at 1512 x g for 10 minutes was performed. In the meanwhile, Bio-Agar (Bio-Optica 05-9803S) was heathen up into a microwave oven at 90 W until completely liquefied and when cooled down at 50° C it was added to the pellet and placed at 4°C for solidification.

The paraffin-embedded specimens were then cut at 3 μm thickness, placed on glass slides and then stained with hematoxylin & eosin and Schmorl's reaction.

Hematoxylin & Eosin stain was performed with Leica ST5020 automatic stainer and Leica CV5030 automated coverslipper machine as follows: xylene for 2 min, twice; absolute ethanol for 2 min, twice; ethanol 96% for 2 min twice; washed in distilled water for 4 min; Carazzi's Hematoxylin (Bio-Optica, ref. 05-06012/L) for 9 min; washed in tap water for 6 min; eosin 1% (Bio-Optica, ref. 05-10002/L) for 1 min; washed in tap water for 2 minutes; ethanol 96% for 20 sec, twice; absolute ethanol for 20 sec, twice; xylene for 30 sec, twice; mount with xylene-based mounting medium.

Kluver-Barerra staining was performed with Luxol Fast Blue Stain Kit (Myelin Stain) (ab150675) on deparaffinised sections of midbrain organoids put in Luxol Fast Blue solution at 56°C overnight. The following day sections, after being rinsed, were put in Litium Carbonate Solution for 30 seconds and after that in ethanol 70%. The counter-staining was performed in Cresyl Violet Acetate.

Schmorl's reaction was performed as follows. Sections were washed with a freshly prepared solution of 4 ml of 0,4% aqueous potassium ferricyanide and 30 ml of 1% aqueous ferric chloride for 7,5 minutes. After that a wash in running tap water for 10 minutes was performed to ensure that all residual ferricyanide was completely removed from the section. A counterstaining with Kernechtrot solution was done (0,1 gr of nuclear fast red, 5 gr of aluminium sulphate, 100 ml of distilled water prepared as follows: dissolve aluminium sulphate in water; add nuclear fast red and slowly heat to boil and cool; filter and add a grain of thymol as a preservative) for 5 minutes. Sections were then dehydrated, cleared and mounted in synthetic resin.

IHC staining with GFAP and TH (see table 4) was performed on midbrain organoids at selected timepoints, using the automated systems Dako Omnis and Ventana.

Table 4. IF and IHC antibodies list

Antibody	Brand	Cat.Nr.	Dilution	Species
Anti-TH	RD	MAB7566	1:100	Ms
Anti-GFAP	Sigma	G3893	1:200	Ms
Anti-Aldh1l1	Abcam	Ab190298	1:250	Rb
Anti-Gluk2	Abcam	Ab66440	1:100	Rb
Anti-Sox 2	Abcam	Ab97959	1:500	Rb
Anti-TUJ1	Abcam	Ab18207	1:250	Rb
Anti-EAAT2	Abcam	Ab41621	1:250	Rb
Anti-MAP2	Sigma	M4403	1:250	Ms
Anti-Oct4	Cell Signaling	C30A3	1:100	Rb
Anti-Tra-1-60	Cell Signaling	Tra-1-60 (S)	1:500	Ms
Anti-Tra-1-81	Cell Signaling	Tra-1-81 (S)	1:500	Ms
Anti-SSEA4	Cell Signaling	MC813	1:100	Ms
Anti-Nanog	Cell Signaling	D73G4	1:200	Rb
Anti-MBP	Abcam	Ab62631	1:100	Ms

3.9. Image analyses

Image analyses was performed on IF staining both for 2D and 3D cultures.

For astrocytes and dopaminergic neurons analyses a total of 25-30 images at 20 x and oil 40x magnification were taken using a Leica Confocal TCS SP8.

For the analyses of GFAP and TH on midbrain organoids, images were taken using a wide-field microscope at 20x magnification. For each markers four organoids (2 CTR and 2 PARK2), two sections/organoid were analysed and 10 images/section were taken for the quantification. Images were blindly acquired on DAPI.

GFAP staining on organoids was also quantified from Prof. Bellucci's team on the whole organoid section taken at confocal microscope using Imaris (https://imaris.oxinst.com). A ratio of marker positive area on total organoid area was calculated. Two organoids/cell line and two sections/organoid were analysed. Quantification of GFAP was performed on 8 organoids in total (4 CTR and 4 PARK2).

Intensity analyses were performed using the base package of Fiji- ImageJ (https://imagej.net).

DA neurons cell counting was performed manually using the plug-in Cell Counter of ImageJ. Cell counting was performed for TH, TUJ1 and DAPI and TH/DAPI, TUJ1/DAPI and TH/TUJ1 ratios were calculated.

Astrocytes cell counting was performed manually and separately for GFAP and Aldh1l1 using the plug-in Cell Counter of ImageJ. GFAP/DAPI and Aldh1l1/DAPI ratios were calculated. GFAP/Aldh1l1 was not calculated as the staining was performed separately for the two markers.

GFAP, TH and Aldh1l1 signal was analysed using an intensity analyses protocol. RGB images were opened in Fiji-ImageJ and the signal was analysed by splitting the three channels. After duplicating the image, brightness and contrast was adjusted to an optimal state when signal was clear. A region of interest (ROI) was drawn all around the whole image and it was added to the ROI manager. To subtract background signal, a second small ROI was drawn in an area of background and added to the ROI manager. Before analysing the signal, measurements were set in order to analyse only the mean grey value. The final analyses were performed on the original image using the ROI set before. Signal of background was subtracted from signal of the whole image. Before performing a statistical analyses values were normalized by putting the first value of control equal to 1. A ratio of every value and the value of reference was then calculated.

SOX2 which is a transcription factor located in the nucleus of the cell and DAPI were analysed using a nuclear count protocol with Fiji-ImageJ. After splitting the channels, the original image was duplicated and the background was subtracted by setting the rolling ball radius to 50 pixels. The threshold was adjusted by setting the following parameters: default, black and white and dark background. The image was then processed to binary and to watershed and measurements parameters were set to area, mean grey value, min. and max. grey value. Particles were analysed setting a size range from 20 to infinity for images at 20x magnification, and an elliptic shape. The percentage of positive SOX2 cells was calculated as a ratio on DAPI positive cells.

3.10. Electrophysiology

Electrophysiology characterization of DA neurons was performed with whole-cell patch-clamp technique by Dr. Luca Murru at Dr. Passafaro's lab (CNR- Institute of Neuroscience, University of Milano-Bicocca). Recordings took place from DIV 35 to DIV 50 and they were performed at room temperature in Krebs'–Ringer's–HEPES solution containing (in mM): 125 NaCl, 5 KCl, 1.2 MgSO4, 1.2 KH2PO4, 2 CaCl2, 6 glucose, and 25 HEPES (pH 7.4). The composition of the intracellular solution was (in mM)126 K-gluconate, 4 NaCl, 1 EGTA, 1 MgSO4, 0.5 CaCl2, 3 ATP (magnesium salt), 0.1 GTP (sodium salt), 10 glucose, 10 HEPES-KOH (pH 7.3). Patch-clamp electrophysiological recordings were performed with a Multiclamp 700B amplifier (Axon CNS Molecular Devices, USA) and using an infrared-differential interference contrast microscope (Nikon Eclipse FN1). Patch electrodes (borosilicate capillaries with a filament and an outer diameter of 1.5 μm; Sutter Instruments) were prepared with a four-step horizontal puller (Sutter Instruments) and had a resistance of 3–5 MΩ. Series resistance of the recorded DA neuron was always below 20 MΩ. The iPSCs membrane properties were analysed in current-clamp configuration. Briefly, a series of depolarizing current steps were injected into the DA neurons (5 pA per step, 0.5 s duration) to evoke action potential (AP) firing. The membrane properties not directly related to AP firing (input resistance, capacitance and resting membrane potential (RMP)) were analysed in all the DA neurons that showed inward and outward currents, even in absence of AP firing. AP features (threshold, amplitude and half-width) were analysed for the first AP evoked by the smallest current step able to induce AP firing (rheobase). Inward and outward currents were recorded in voltage-clamp configuration. Inward currents were evoked by 5 mV (from -50 to +60 mV) voltage steps (10 ms duration) and neurons were held at −40 mV. Outward currents were evoked through 10 mV voltage steps (1 s duration, from −70 to +40 mV) preceded by 500 ms hyperpolarization pre-pulse (from −70 to -120 mV). Spontaneous post-synaptic currents (sPSCs) were recorded with no blockers in order to investigate DA neurons synaptic activity. sPSCs were analysed for amplitude (pA) and frequency (Hz). Currents were amplified, filtered at 5 kHz and

digitized at 20 kHz. All the analyses were performed offline with Clampfit 10.1 software. For statistical analysis the GraphPad PRISM software (version 9.0.0) has been used.

Electrophysiological characterization of midbrain organoids was performed using different techniques: high-density microelectrode arrays (HD-MEAs) and calcium imaging using two-foton microscopy.

HD-MEAs recordings were performed at the Department Biosystems Science and Engineering of ETH Zürich in Basel by Dr. Manuel Schröter and Dr. Alessio Buccino. HD-MEA recordings were performed on CTR2, CTR3, CTR4, Parkin 1, Parkin 2, Parkin 3 and Parkin 4. At least three organoids/cell line were analysed.

Midbrain organoids were recorded on single- and multi-well planar HD-MEAs provided by MaxWell Biosystems (MaxWell Biosystems, Zurich, Switzerland). The used single-well complementary-metal-oxide-semiconductor (CMOS)-based HD-MEA ("MaxOne") comprises 26,400 platinum microelectrodes (size of electrode: 9.3 × 5.3 μm2) at a 17.5 μm pitch (center-to-center) within a total sensing area of 3.85 × 2.10 mm2 (Ballini et al. 2014; Müller et al. 2015). The MaxOne system allows for simultaneous recordings from up to 1,024 readout electrodes at a sampling rate of 20 kHz; the electrodes can be flexibly selected and reconfigured according to experimental needs. To decrease the impedance and to improve the signal-to-noise ratio, electrodes were coated with platinum black (Müller et al. 2015). Additionally, we used the multi-well system by MaxWell Biosystems ("MaxTwo"). This system comprises 6 HD-MEA wells that are equipped with HD-MEAs featuring the same technical details as previously described for the MaxOne HD-MEA. Recordings with the MaxTwo system were sampled at 10 kHz.

Cross-sectional slices were obtained from 70-day old midbrain organoids. Single organoids were first transferred from maturation medium to ice-cold BrainPhys

(STEMCELL Technologies) using cut 1000 µl pipette tips. Next, cross-sectional 500-µm-thick slices were cut from organoids using a sterile razor blade and collected in six-well plates filled with BrainPhys medium at room temperature. For recovery, slices were housed in a humidified tissue culture incubator for 1h before plating. Before the plating, single- and multi-well HD-MEAs were sterilized in 70% ethanol for 30 minutes and rinsed 3 times with distilled water. To improve tissue adhesion, arrays were coated with 0.05% (v/v) poly(ethyleneimine) (Sigma-Aldrich, St. Louis, MO, USA) in borate buffer (pH 8.5, Thermo Fisher Scientific) for 40 minutes at room temperature, rinsed with distilled water, and left to dry. To attach organoids on HD-MEAs, we adopted procedures developed for organotypic slices (Gong et al. 2015): First, we applied a thin layer of Matrigel (Corning) to the centre of the HD-MEA sensing area and then transferred individual organoid slices from the 6-well plates to the coated HD-MEAs. After positioning the tissue, we placed a tissue "harp" on top of the organoid slice and applied several drops of recording medium (STEMCELL Technologies, #05793) around the organoid. HD-MEAs were then covered with a lid and placed in a humidified incubator at 37°C, 5% CO2/95% air for 30 minutes. Following the incubation, we carefully added more medium. In the following 1-2 days, medium was increased to a final volume of 2 ml per chip. Half of the recording medium was changed every 3-4 days.

In order to probe single-cell and network activity of sliced organoids and to identify neurons on the HD-MEA, we performed a series of activity scans, i.e., sequential high-density recordings covering all electrodes of the array (*see figure 5*). To select recording electrodes, the multi-unit activity (MUA) for each electrode configuration was estimated using a sliding-window, threshold-crossing spike detection algorithm (detection threshold: 5 × the root mean squared error of the noise of the bandpass filtered signal). After the activity scan, and depending on the requirements of each analysis (single-cell or network related features), we selected the readout electrodes based on the online detected activity. HD-MEA recordings of organoids slices started two days after plating. The reported electrophysiological results are based on data obtained from 12 slices (2x6 CTR, 2x6 PARK2 organoids) maintained for about 3 weeks on the HD-MEA.

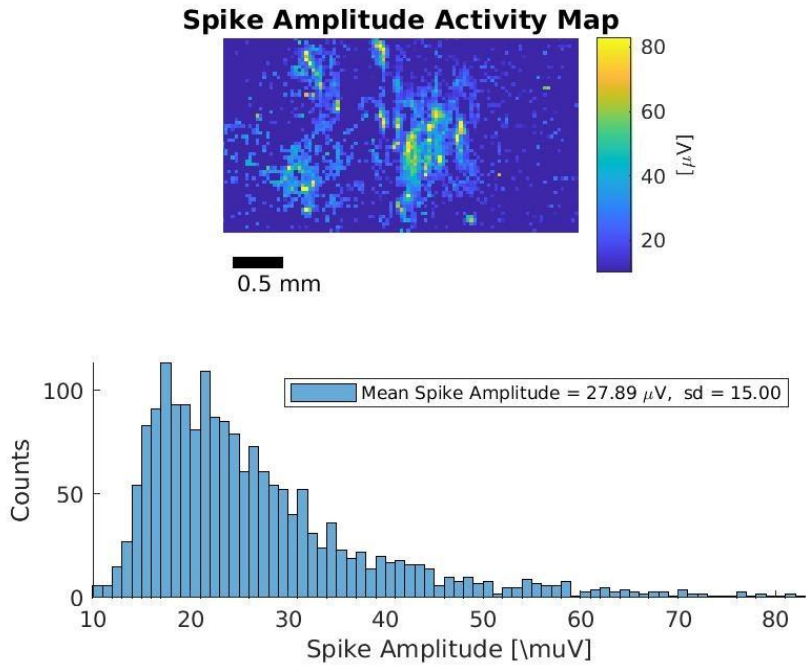

Figure 5. Spike amplitude map of a midbrain organoids plated on the HD-MEAs. Upper panel shows the position of the sliced midbrain organoid on the chip. Each pixel here refers to the average spike amplitude peak, computed after an activity scan.

Calcium imaging on organoids was performed at Prof. Mario Bortolozzi's Lab at the the Venetian Institute of Molecular Medicine (VIMM) in Padua. Three organoids of CTR2 and PARK2 were analysed through this technique.

For calcium imaging organoids between DIV 70 and 100 were incubated in BrainPhys medium with 10 μM FluoForte (Enzo Life Science, ENZ-52015), 25 μM sulfinpyrazone (Sigma-Aldrich, 57-96-5) and Pluronic F-127 0.01% (Invitrogen, P3000MP). After 1 h incubation at 37 °C, 5% CO2, organoids were transferred into the recording chamber and perfused with heated MSC solution (NaCl 140 mM, KCl 5 mM, CaCl2 2mM, MgCl2 1mM, HEPES 10 mM, Glucose 10 mM).

Ca2+ imaging was performed by a Thorlabs Bergamo microscope equipped with a Chameleon (Coherent) pulsed laser. FluoForte fluorescence was collected by a photo multiplier upon 2-photon excitation at 850 nm. Image analysis was performed by a home-made software written in Matlab. The software generates an image segmentation correspondent to individual cell soma, which permitted us to identify active cells in terms of fluorescence variation DF = F-F0, where F0 is the resting fluorescence intensity.

A gravimetric perfusion system was used to perfuse 10 μM of Kainic Acid (KA) or 10 10 μM of UBP310 into the chamber at 1-2 ml/min flux speed. The recording chamber contained around 3 ml of MSC before starting the perfusion with KA. At least 10 ml of the new solution were perfused, and 15 minutes incubation were left before starting the new image acquisition.

3.11. Statistical analyses

Statistical analysis was performed using Prism-GraphPad 9 and it was performed by t-test with p-value < 0.05 for statistical significance when two variables were compared or by ANOVA with an α-level 0.05 followed by pairwise post-hoc comparison with Tukey correction for multiple testing.

4. Results

4.1. IPSCs characterization

iPSCs used in this study have been reprogrammed in our laboratory. Karyotypes were normal in all cell lines, except for CTR 2 which was 46 XY, t (6;13) (q13; q22). This cell line was used in the experiments because the translocation was balanced (*see figure 6*).

To prove iPSCs effective staminality, they were tested for the expression of a panel of stemness markers by IF (*see figure 7*). We analysed the expression of: OCT4, SSEA-4, Nanog, SOX2, Tra181 and Tra160. OCT4 is one of the first pluripotency-related transcription factors to be downregulated upon differentiation; SSEA-4 is specifically expressed on the surface of human stem cells, Nanog is a transcriptional factor that helps embryonic stem cells maintain pluripotency; SOX2 is also a transcription factor that helps maintaining pluripotency; Tra160 and Tra181 are membrane surface markers expressed in staminal cells. All cell lines used in the experiments expressed stemness markers. The expression of two stemness markers (OCT-4 and Nanog) in all iPSCs lines used in the study was assessed also through qPCR and fibroblasts were used as negative control (*see figure 8*).

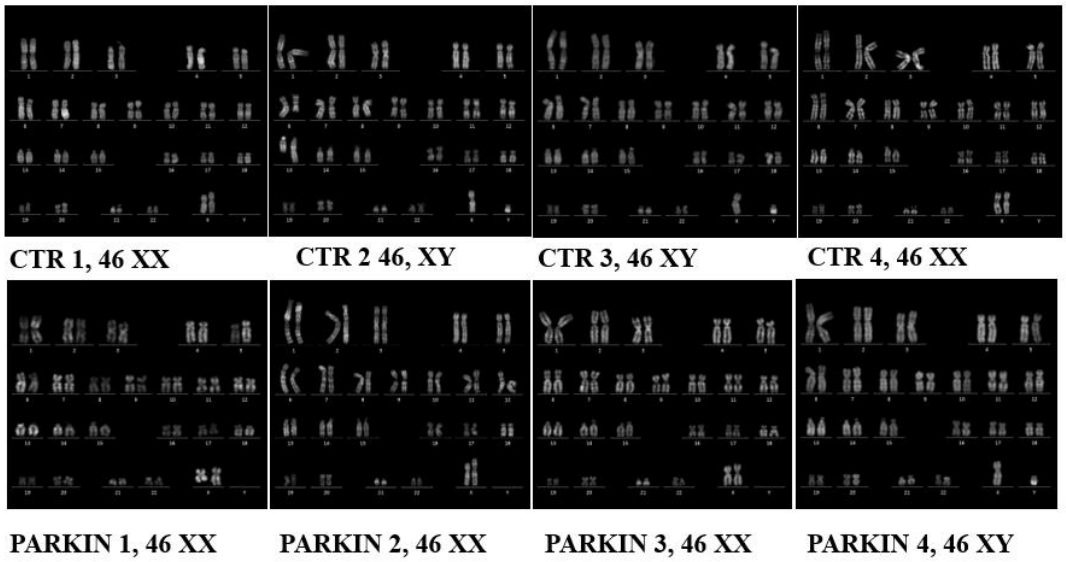

Figure 6. Karyotype analyses of cell lines used in the study

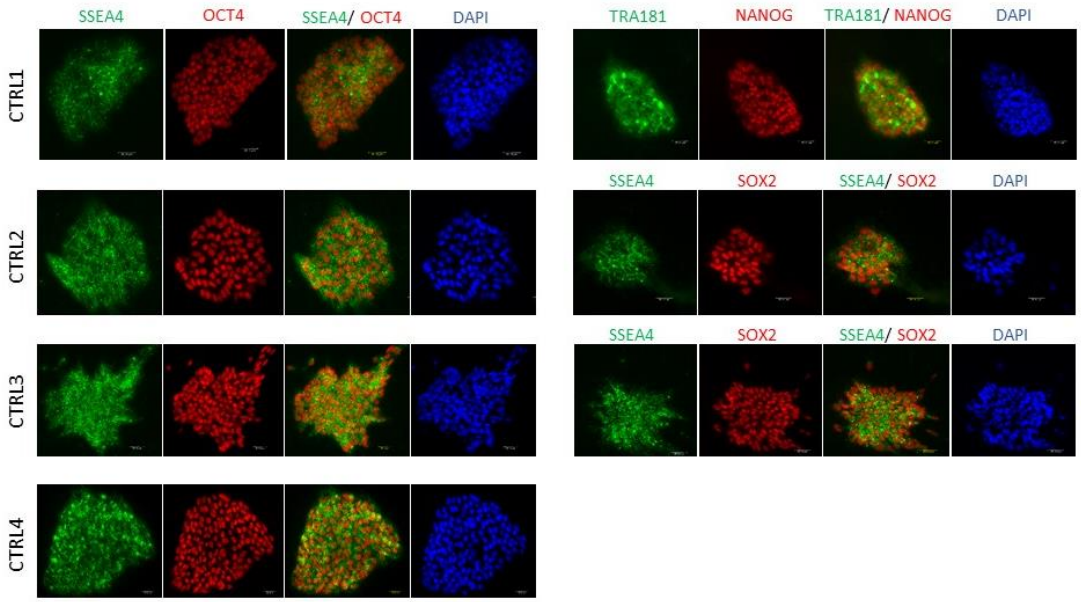

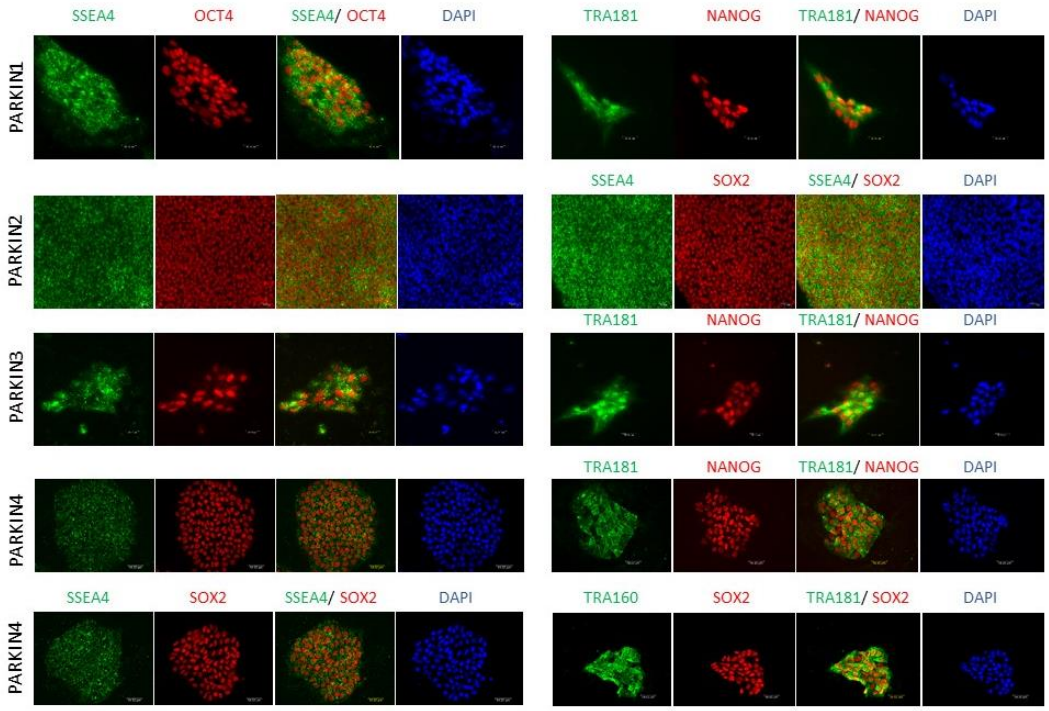

Figure 7. IF for stemness markers. All cell lines used in the experiments (both CTR and PARK2) expressed stemness markers: OCT-4, SSEA-4, Nanog, SOX2, Tra160 and Tra181.

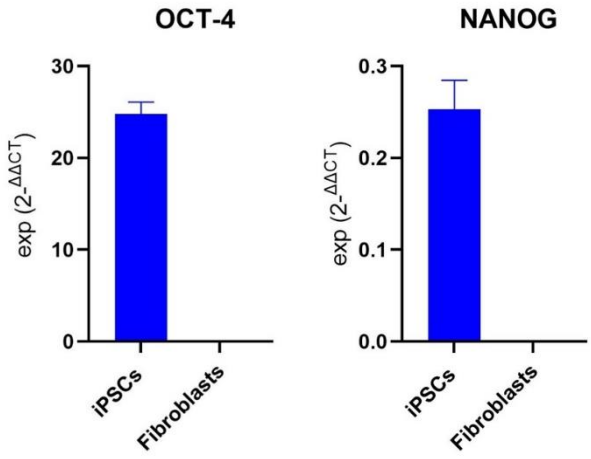

Figure 8. qPCR on iPSCs for stemness markers. OCT-4 and Nanog expression was assessed in all iPSCs lines used in the study. Fibroblasts were used as negative control. Normalization was performed on YWHAZ.

4.2. Dopaminergic neurons characterization

DA neurons of three controls (CTR 2, CTR 3 and CTR 4) and two PARK2 lines (Parkin 2 and Parkin 3) were differentiated from iPSCs using the protocol described by Zhang (Zhang P, 2014) which allowed the generation of tyrosine-hydroxilase (TH) positive neurons with high efficiency (*see table 5*).

DIV 35	TH/DAPI	TUJ1/DAPI	TH/TUJ1
PARK2	77 %	89 %	87 %
CTR	79 %	87 %	91 %

DIV 50	TH/DAPI	TUJ1/DAPI	TH/TUJ1
PARK2	78 %	86 %	91 %
CTR	80 %	88 %	91 %

Table 5. Percentage of TH/DAPI, TUJ1/DAPI and TH/TUJ1 co-staining at DIV 35 and DIV 50 in PARK2 and CTR iPSCs-derived DA neurons

The differentiation was carried out until DIV 75, but data regarding the quantification of dopaminergic markers and Gluk2 are shown only till DIV 50 because after that timepoint there was an important decrease in the expression levels of these markers, indicating that their survival in 2D culture conditions is poor.

Dopaminergic markers were quantified through IF analyses, WB and qPCR performed at two defined timepoints: DIV 35 and DIV 50. Kainate receptor levels were assesed through WB analyses and qPCR at DIV 35 and DIV 50.

At DIV 35 and at DIV 50 cells resulted positive for tubulin beta 3 (TUJ1) and the majority of them were also positive fot TH (*see figure 9*). The quantifications of IF data were performed on CTR 2, 3 and 4 and on Parkin 2 and 3 and they were obtained by analysing the normalized intensity mean for TH and the cell counting for nuclear markers, such as SOX2. TH levels were comparebale among CTR and PARK2 at DIV 35, whereas at DIV 50 TH levels resulted significantly increased in the mutated line ($p < 0.0001$). SOX 2 is a transcriptor factor which is abundant in neuronal progenitors. As a matter of fact SOX2 was expressed at higher levels at DIV 35, especially in CTR ($p < 0.05$) with a reduced expression at DIV 50 ($p < 0.001$) (*see figure 10*).

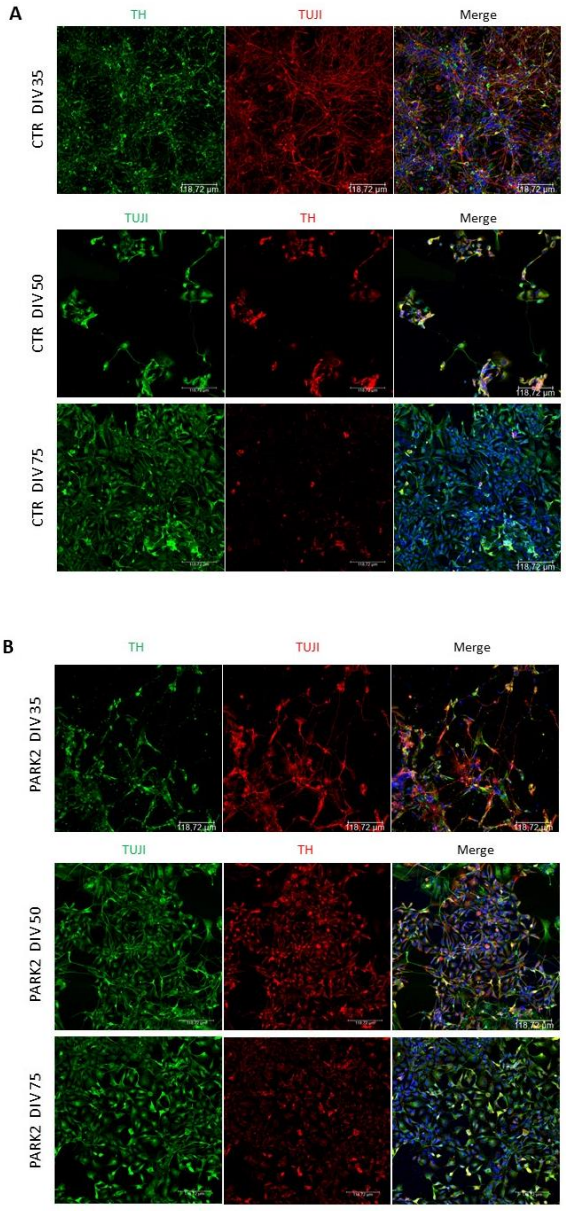

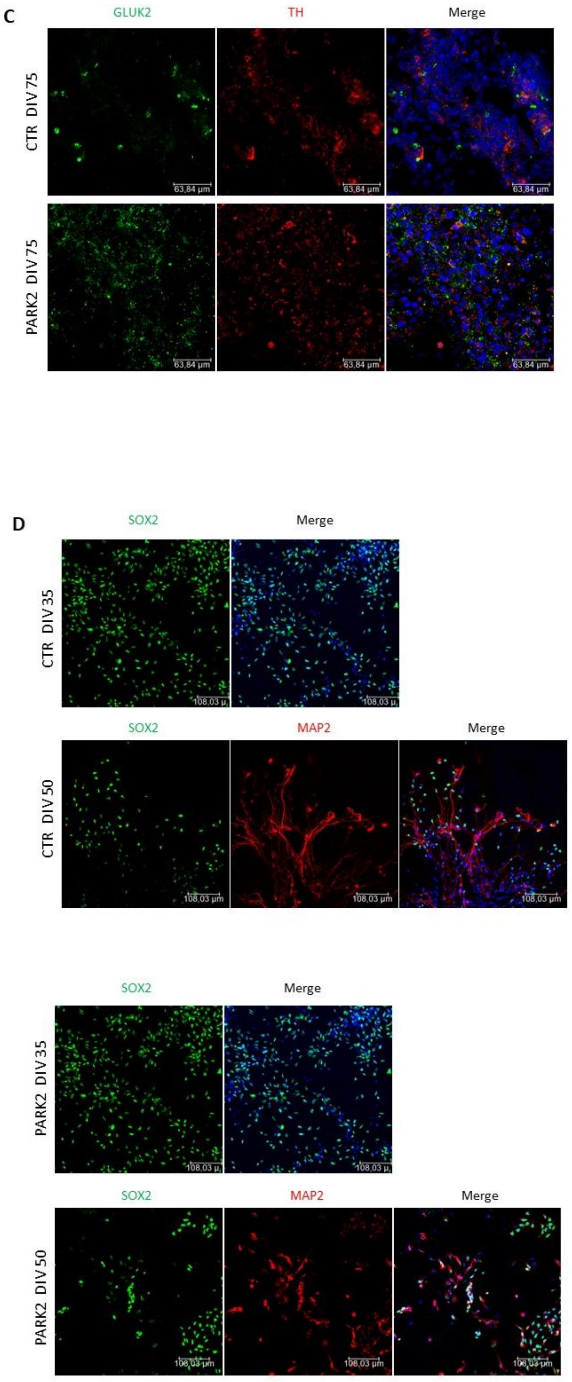

Figure 9. IF on iPSCs-derived DA neurons of CTR and PARK2. (A) TH and TUJ1 staining on CTR at DIV 35, 50 and 75; 20x, confocal microscope.Scale bar, 60 µm (B) TH and TUJ1 staining on PARK2 at DIV 35, 50 and 75; 20 x, confocal microscope. Scale bar, 60 µm (C) Gluk2 staining on CTR and PARK2 at DIV 75; 40x, oil, confocal microscope. Scale bar, 60 µm (D) SOX2 and MAP2 staining on CTR and PARK2 at DIV 35 and 50; 20 x, confocal microscope. Scale bar, 60 µm.

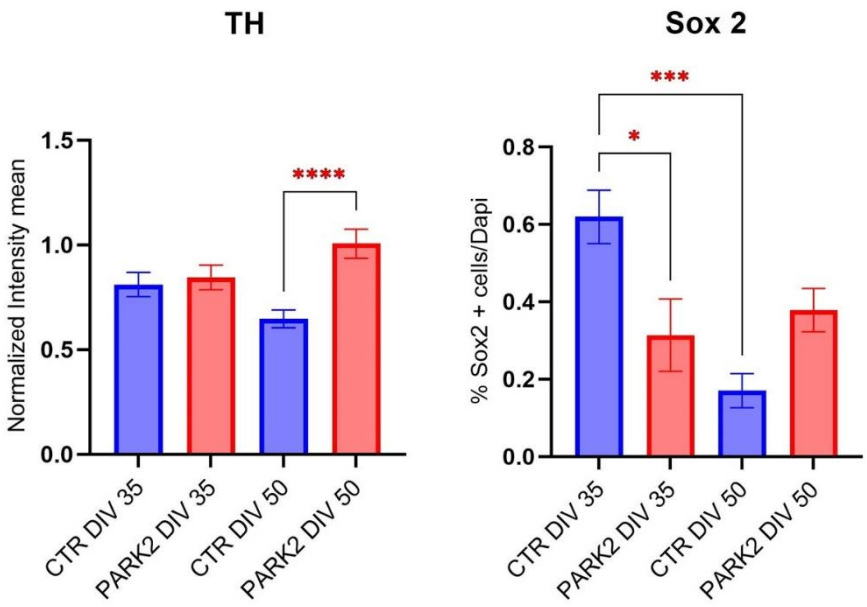

Figure 10. IF quantification on DA neurons of TH and Sox 2. Data are expressed as mean ± SEM. * p< 0.05; *** p< 0.001; **** p< 0.0001.

qPCR was performed on CTR 3, CTR 4 and Parkin 2 in order to quantify the expression of dopaminergic markers such as TH and dopamine transporter (DAT) and Gluk2 (*see figure 11*). TH levels were significantly higher in PARK2 compared to CTR at DIV 35 (p< 0.0001) with a pronounced reduction at DIV 50 (p< 0.0001). DAT showed a different trend with significantly higher levels in CTR compared to PARK2 early in the maturation process, at DIV 35 (p< 0.05). qPCR showed no difference in Gluk2 levels among CTR and PARK2.

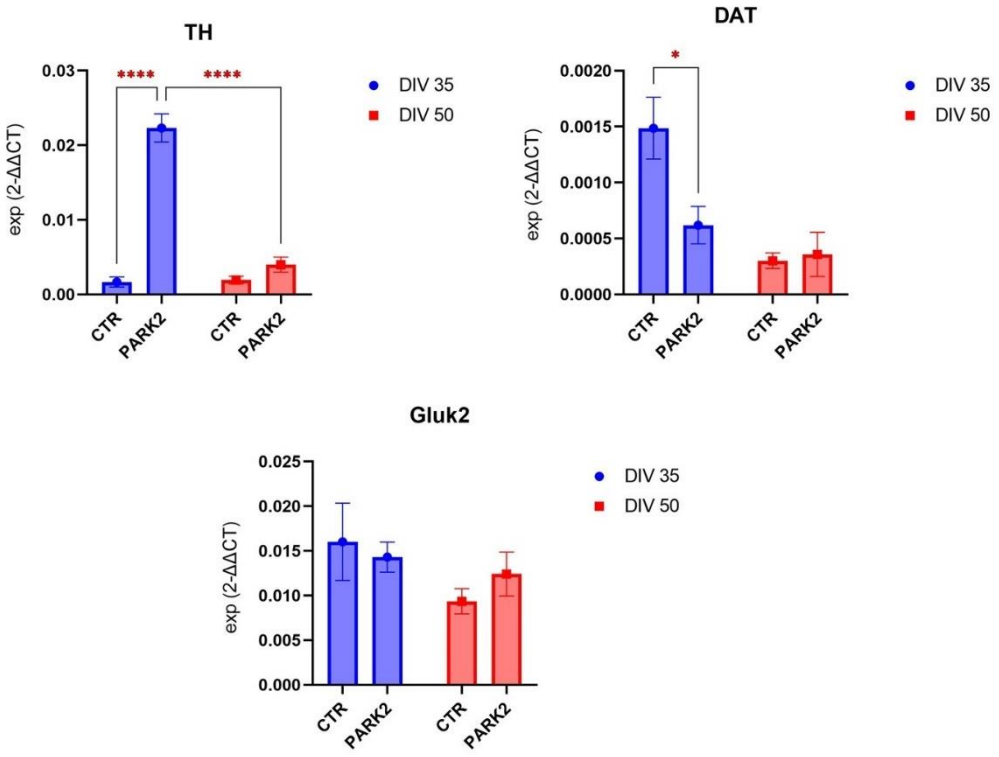

Figure 11. qPCR on DA neurons. The quantification of neuronal markers expression in DA neurons (CTR vs PARK2) was realized using the reference gene YWHAZ.

WB analyses were performed on CTR2 and Parkin 3 and showed a significantly increased expression of TH in PARK2 at DIV 50 ($p < 0.01$) and a significantly reduced expression of Parkin in PARK2 ($p < 0.05$), as expected. Dopa decarboxilase (DDC) levels were similar in PARK2 and CTR. No difference in Gluk2 levels was found in CTR and PARK2 (*see figure 12*).

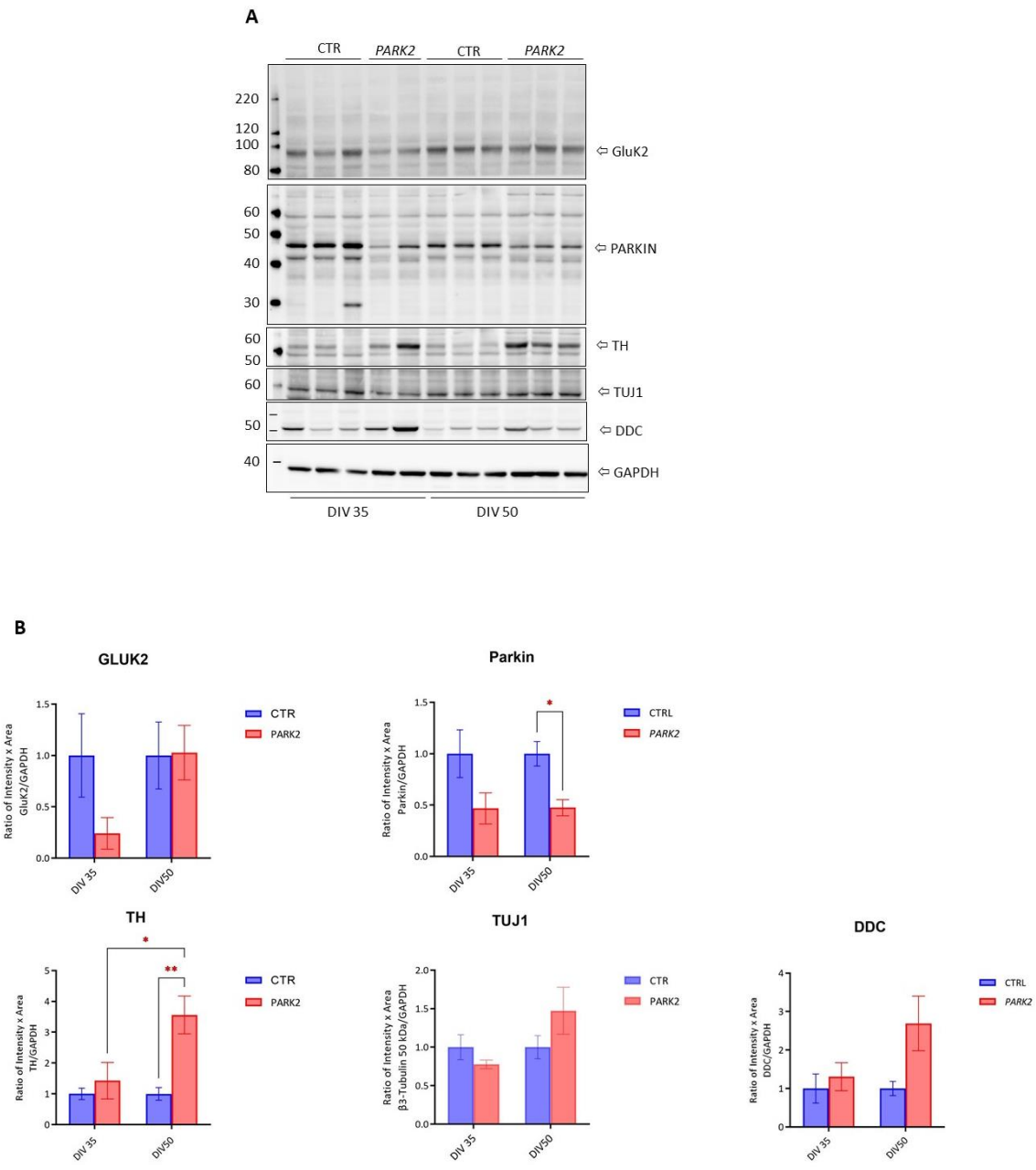

Figure 12. WB analyses on DA neurons at DIV 35 and 50 (A) showing expression of dopaminergic markers (TH, DDC), Parkin and Gluk2 expression; (B) quantification of markers normalized for GAPDH. Data are expressed as mean ± SEM. * p< 0.05; ** p< 0.01.

DA neurons of CTR 4 and Parkin 2 were also characterized by electrophisiology using the patch clamp technique (*see figure 13*). Registrations took place between DIV 40 and DIV 75. Action potentials firing in response to depolarizing current were detected both in CTR and PARK2, with a similar frequency (respectively of 25% and 23%). Analysis of current/voltage relationship did not show differences between CTR and PARK2 (only cells showing inward and outward current has been analysed). There was also no difference for input resistance, capacitance and resting membrane potential (RMP). PARK2 and CTR showed similar AP threshold, amplitude and half-width. Inward currents analyses did not reveal differences between CTR and PARK2 (58% vs 53%), as well as outward currents (86% in CTR vs 80% in PARK2). Spontaneous post-synaptic currents (sPSCs) were detected only in CTR. In conclusion, neuronal activity showed a similar rate in PARK2 and CTR. Unfortunately, sPSCs were detected only in CTR but registrations took place quite late in the differentiation timeline and that could explain the difficulty in finding this activity. As demonstrated from WB, IF and qPCR analyses, after DIV 50 the majority of neurons degenerate and the percentage of alive and active neurons is very low and difficult to detect, especially for patch-clamp recordings.

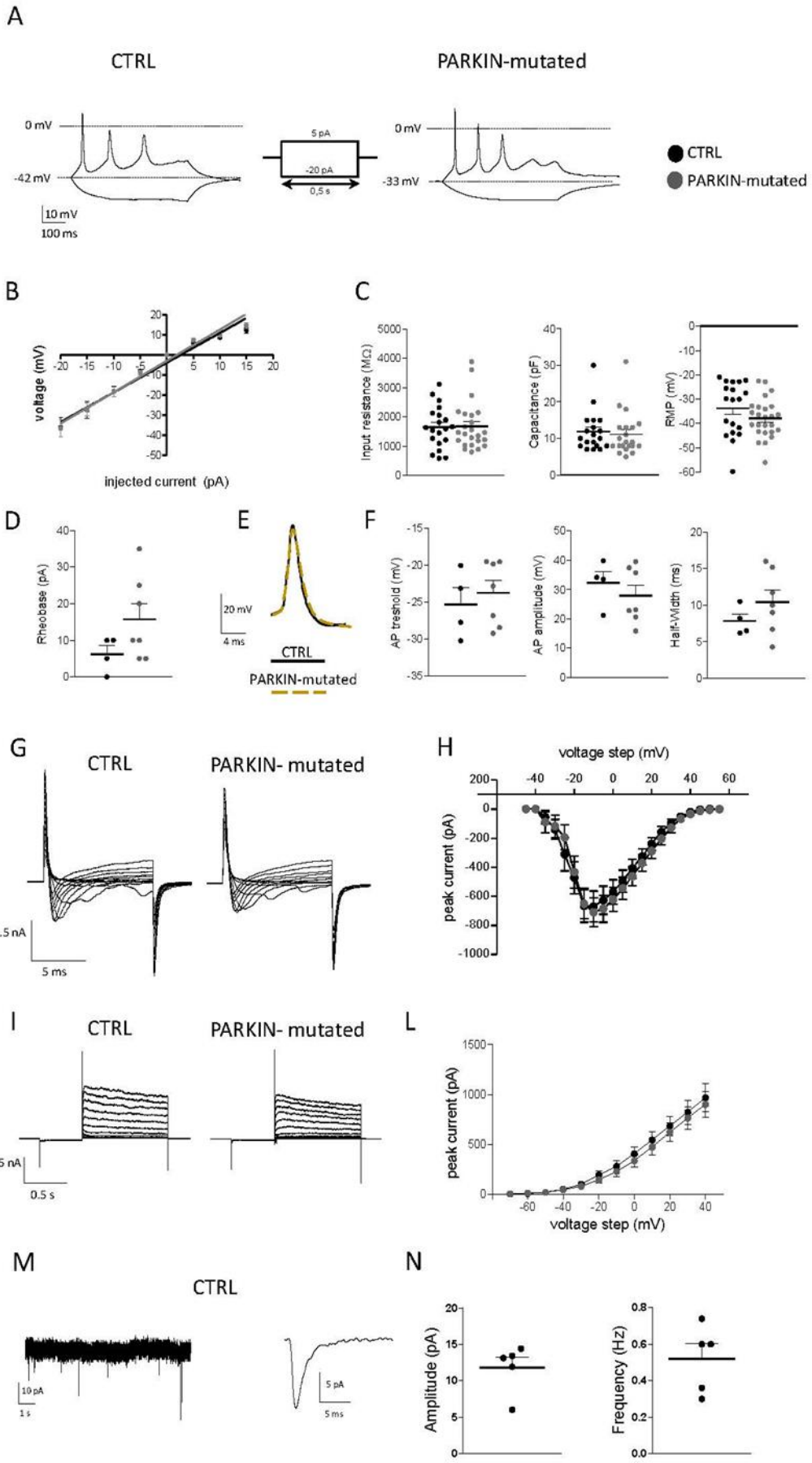
A
CTRL
PARKIN-mutated
0 mV
-42 mV
10 mV
100 ms
5 pA
-20 pA
0,5 s
0 mV
-33 mV
CTRL
PARKIN-mutated
B
voltage (mV)
injected current (pA)
C
Input resistance (MΩ)
Capacitance (pF)
RMP (mV)
D
Rheobase (pA)
E
20 mV
4 ms
CTRL
PARKIN-mutated
F
AP treshold (mV)
AP amplitude (mV)
Half-Width (ms)
G
CTRL
PARKIN- mutated
0.5 nA
5 ms
H
voltage step (mV)
peak current (pA)
I
CTRL
PARKIN- mutated
0.5 nA
0.5 s
L
peak current (pA)
voltage step (mV)
M
CTRL
10 pA
1 s
5 pA
5 ms
N
Amplitude (pA)
Frequency (Hz)

Figure 13. Electrophysiological characterization of human iPSCs-derived DA neurons using patch-clamp technique: (A) Representative current-clamp trace showing AP in response to depolarizing current; (B) Analysis of current/voltage relationship; (C) Input resistance, capacitance and RMP; (D) histogram showing the Rheobase for AP induction; (E) Representative traces showing the first AP evoked by current; (F) AP threshold, amplitude and half-width; (G) Representative traces for inward currents; (H) Analysis of inward currents; (I) Representative traces for outward currents; (L) Analysis of outward currents; (M) Representative trace of sPSCs; (N) Amplitude and frequency analyses of sPSCs.

4.3. Astrocytes characterization

Mature astrocytes of CTR2, CTR4, Parkin2 and Parkin3 were generated with high efficiency using the protocol of Santos et al. (Santos R, 2017) with mild modifications. This protocol allowed the generation of mature astrocytes starting from day 14 after the beginning of the differentiation from GPCs. Efficiency rate of the protocol was assessed through the quantification of GFAP and Aldh1l1 positive cells on totality, marked with DAPI (*see table 6*).

	Aldh1l1/DAPI DIV 14	**Aldh1l1/DAPI DIV 30**
PARK2	98 %	99 %
CTR	98 %	98 %

	GFAP/DAPI DIV 50	**GFAP/DAPI DIV 75**
PARK2	93 %	94 %
CTR	95 %	93 %

Table 6. Percentage of Aldh1l1 and GFAP positive cells in iPSCs-derived astrocytes of PARK2 and CTR.

Six timepoints (DIV 14-20-30-40, 50 and 75) were selected in order to perform the analyses. IF, qPCR and WB analyses were used to assess and quantify the expression of astrocytic markers, such as glial fibrillary acidic protein (GFAP), 10-formyltetrahydrofolate dehydrogenase (Aldh1l1) and TUJ1 and glutamate transporters with a focus on Gluk2 and the Excitatory Amino Acid Transporter-2 (EAAT2) which is the glutamate transporter more expressed in astrocytes. Aldh1l1 is a pan-astrocyte marker that stains the majority of astrocytes, whereas GFAP stains only reactive astrocytes.

IF was performed at DIV 14, 30, 50 and 75 (*see figure 14*). All cells were positive for TUJ1 with the majority of them also positive for two astrocytic markers: GFAP and Aldh1l1.

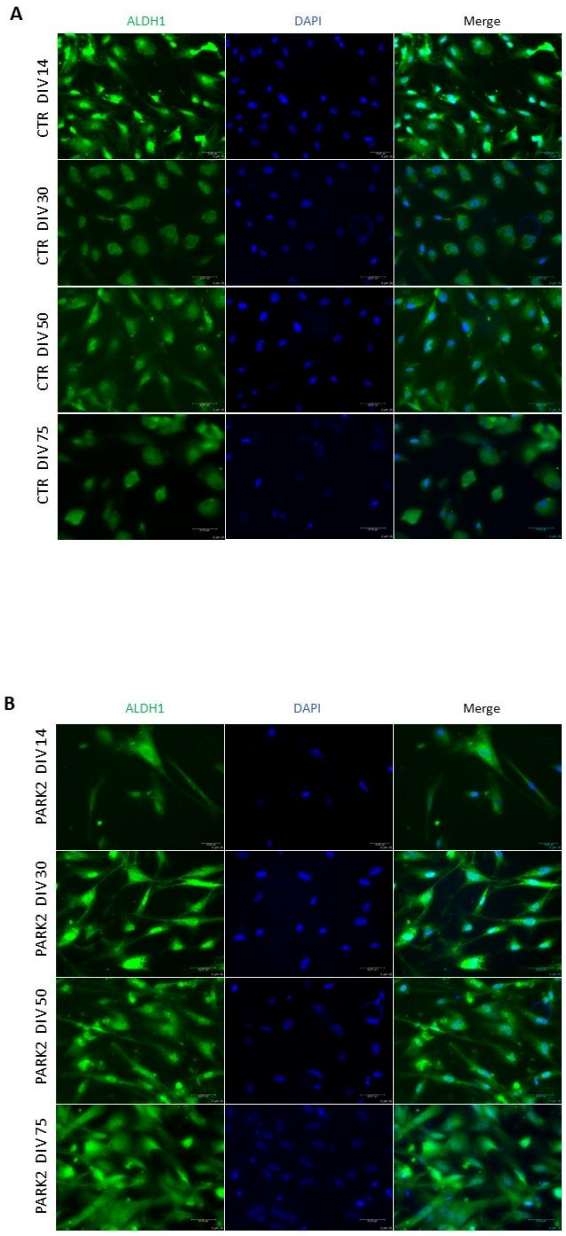

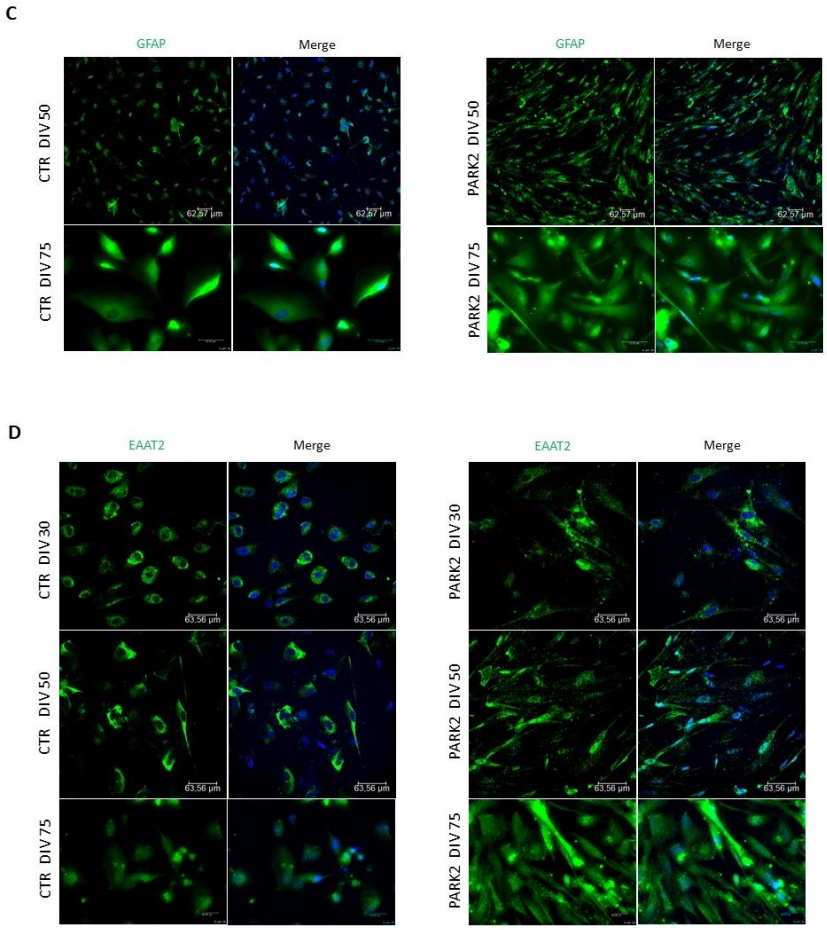

Figure 14. IF on iPSCs-derived astrocytes of CTR and PARK2. (A) Aldh1l1 staining on CTR at DIV 14, 30, 50 and 75; 20x, confocal microscope. Scale bar, 60 µm; (B) Aldh1l1 staining on PARK2 at DIV 14, 30, 50 and 75; 20x, confocal microscope. Scale bar, 60 µm; (C) GFAP staining on CTR and PARK2 at DIV 50 and 75; DIV 50 20 x; DIV 75 20X, confocal microscope. Scale bar, 60 µm; (D) EAAT2 staining on CTR and PARK2 at DIV 30, 50 and 75; 60x, oil, confocal microscope. Scale bar, 60 µm.

The intensity quantification of the signal of these two markers showed a significant increased expression in PARK2 compared to CTR starting from DIV 30 ($p < 0.001$) (*see figure 15*). IF quantification was performed on CTR2, CTR4 and on Parkin2, Parkin3.

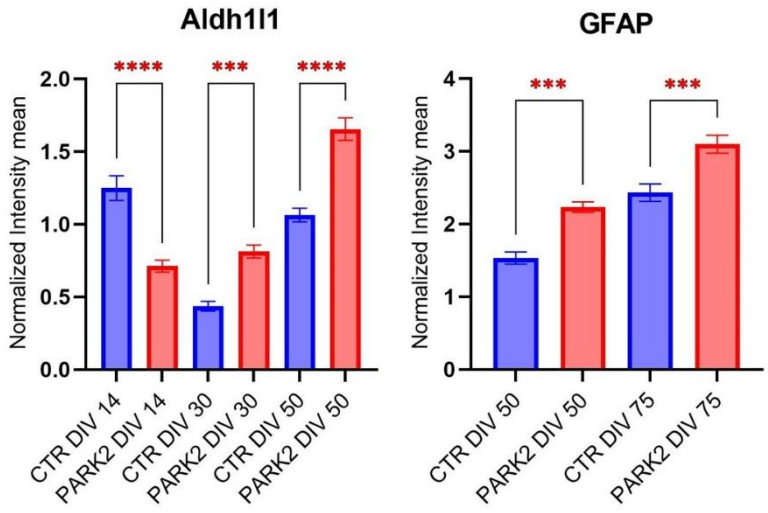

Figure 15. IF quantification of GFAP and Aldh1l1 in iPSCs-derived astrocytes. Data are represented as mean ± SEM. *** p< 0.001, **** p< 0.0001.

WB analyses performed on CTR 2 and Parkin 3 showed the expression of astrocytic markers such as GFAP and Aldh1l1 (*see figure 16*). Aldh1l1 resulted significantly more expressed in PARK2 compared to CTR only at DIV 14 (p< 0.05), whereas GFAP levels were comparable among the two groups. There was a significantly decreasing trend of both markers (GFAP and Aldh1l1) over the differentiation timeline starting from DIV 14 in PARK2 and from DIV 20/30 in CTR. EAAT2 started to be expressed in astrocytes from DIV 30 with an increasing trend until DIV 50. Gluk2 levels were significantly more expressed in PARK2 compared to CTR only at DIV 14 (p< 0.05).

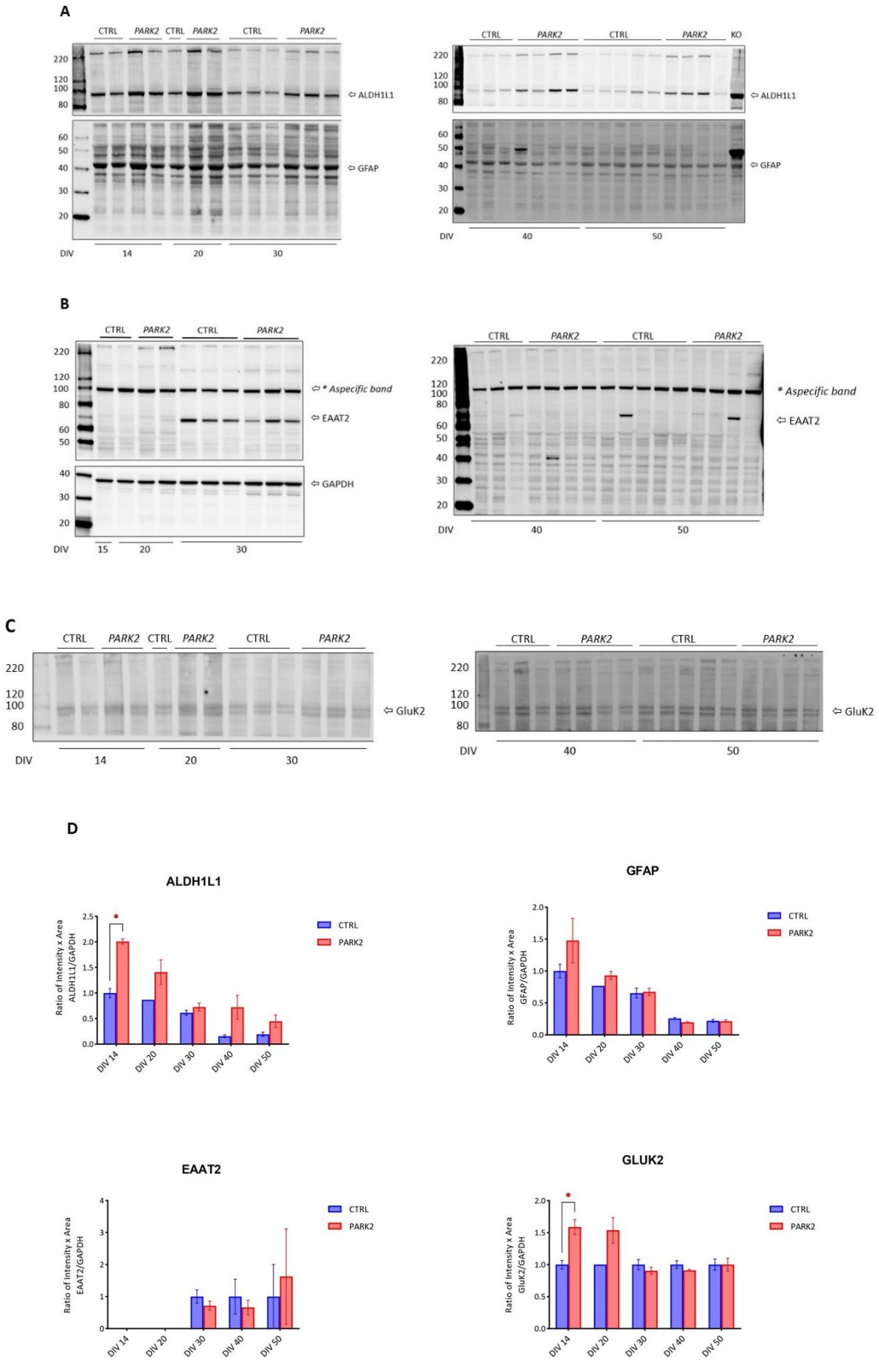

Figure 16. WB analyses on astrocytes (CTR vs PARK2). (A) WB of Aldh1l1, GFAP at DIV 14,20, 30, 40 and 50; (B) WB of EAAT2 at DIV 15, 20, 30, 40, 50; (C) Gluk2 at DIV 14, 20, 30, 40 and 50; (D) Quantification was normalized for GAPDH. Data are presented as mean ± SEM. * $p < 0.05$.

qPCR analyses were performed on CTR4 and Parkin2 in order to assess Gluk2 expression at two different timepoints: DIV 30 and DIV 50. No differences were found at DIV 30 between CTR and PARK2, whereas at DIV 50 Gluk2 levels were significantly higher in PARK2 ($p < 0.05$) (*see figure 17*).

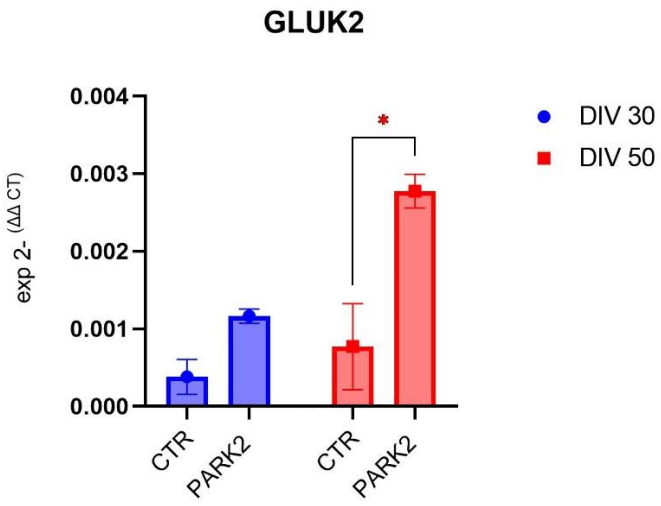

Figure 17. qPCR on astrocytes showing expression levels of Gluk2. Quantification was performed using a reference gene: YWHAZ. Data are presented as mean ± SEM. * $p < 0.05$.

4.4. Midbrain organoids characterization

Midbrain organoids of CTR1, CTR2, CTR3, CTR4 and of Parkin 1, Parkin 2, Parkin 3 and Parkin 4 were generated and differentiated following the protocol described in the methods.

Characterization of these organoids was performed through IF, qPCR and WB analyses in order to define the expression levels of dopaminergic and astrocytic markers and to evaluate the presence of other neuronal and glial populations. Electrophysiological properties of these organoids were defined using two different techniques and differences between CTR and PARK2 were checked with a focus on the excitotoxicity hypothesis in mutated organoids.

IF staining was performed on 4 CTR and 4 PARK2 and revealed the presence of TH positive neurons and GFAP positive astrocytes (*see figure 18, A and B*). The staining with glutamic acid decarboxylase-65 (GAD-65) and glutamic acid decarboxylase-67 (GAD-67) revealed also the presence of GABAergic neurons (*see figure 18, C and D*). GAD-65 and GAD-67 are two isoforms of glutamic acid decarboxylase, the key enzyme for γ-aminobutyric acid synthesis and are expressed in all neurons using GABA as neurotransmitter. The assessment of other cells identities on organoids at DIV 110 was performed also through Myelin Basic Protein (MBP) staining which revealed the presence, both in CTR and PARK2, of oligodendrocytes (*see figure 18, E*). MBP is a structural component of myelin expressed exclusively by myelinating glia and it is a marker that can be used to assess the presence of mature oligodendrocytes.

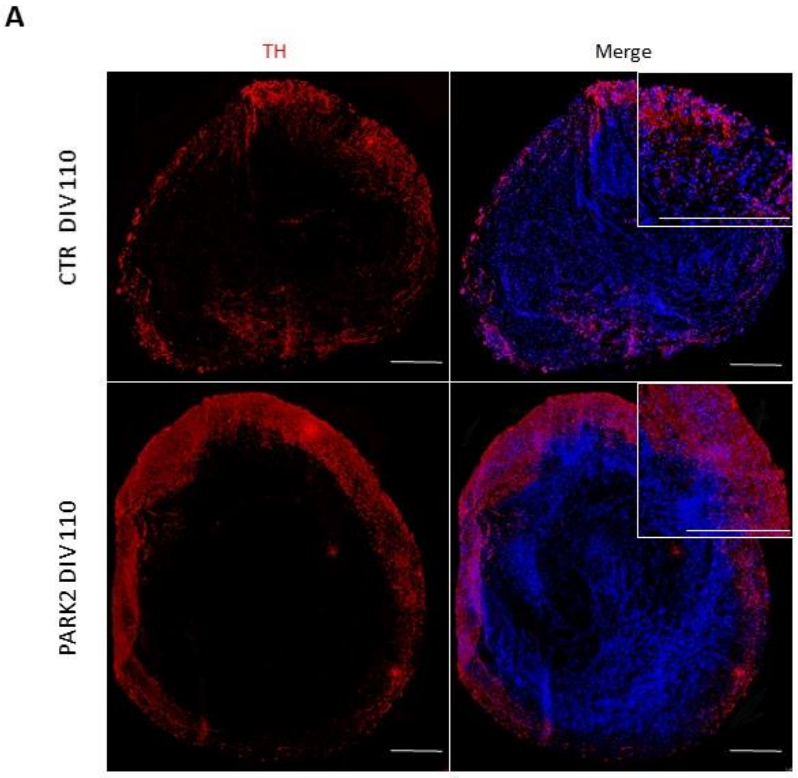
A
TH
Merge
CTR DIV110
PARK2 DIV110

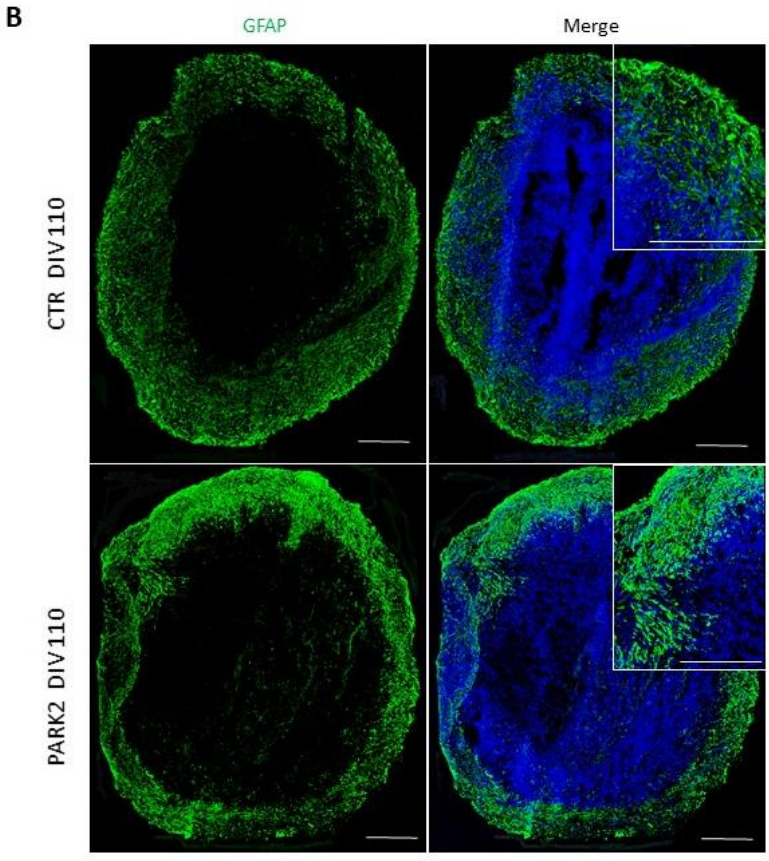
B
GFAP
Merge
CTR DIV110
PARK2 DIV110

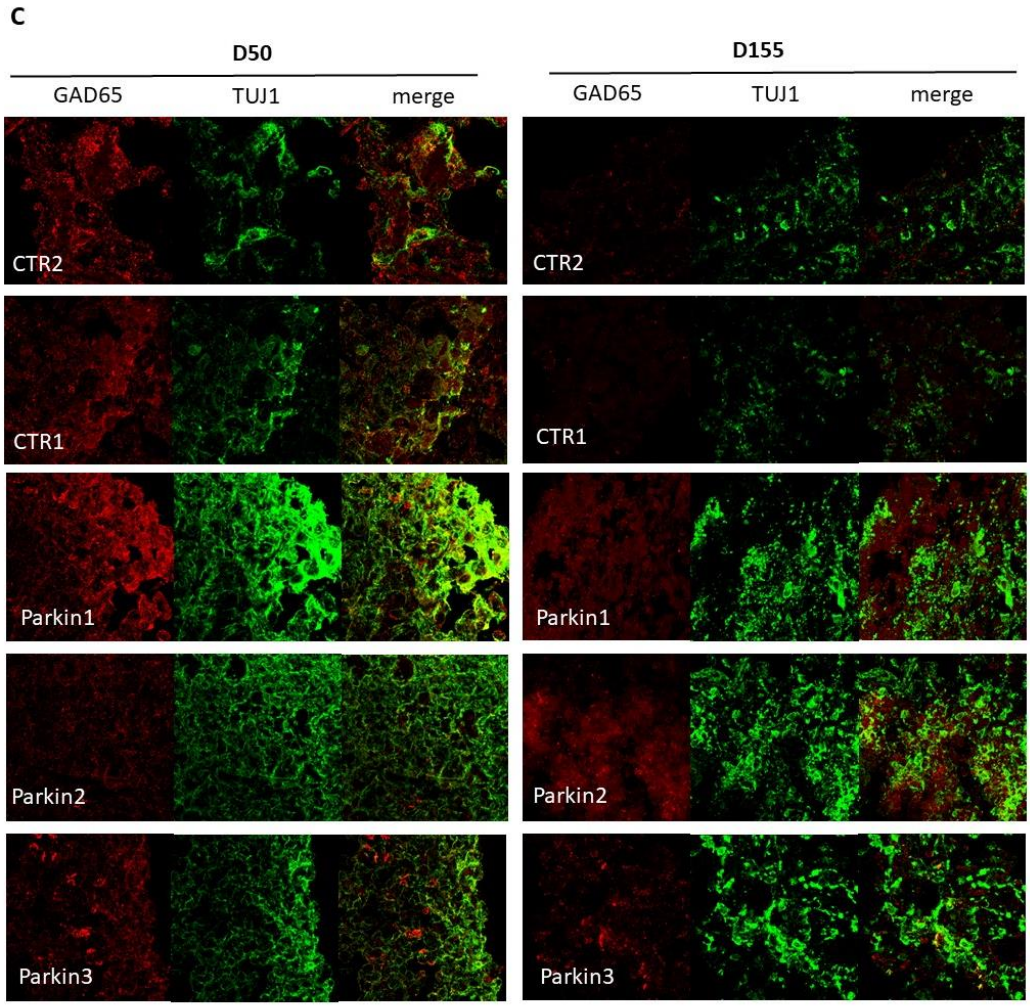
C
D50
D155
GAD65
TUJ1
merge
GAD65
TUJ1
merge
CTR2
CTR2
CTR1
CTR1
Parkin1
Parkin1
Parkin2
Parkin2
Parkin3
Parkin3

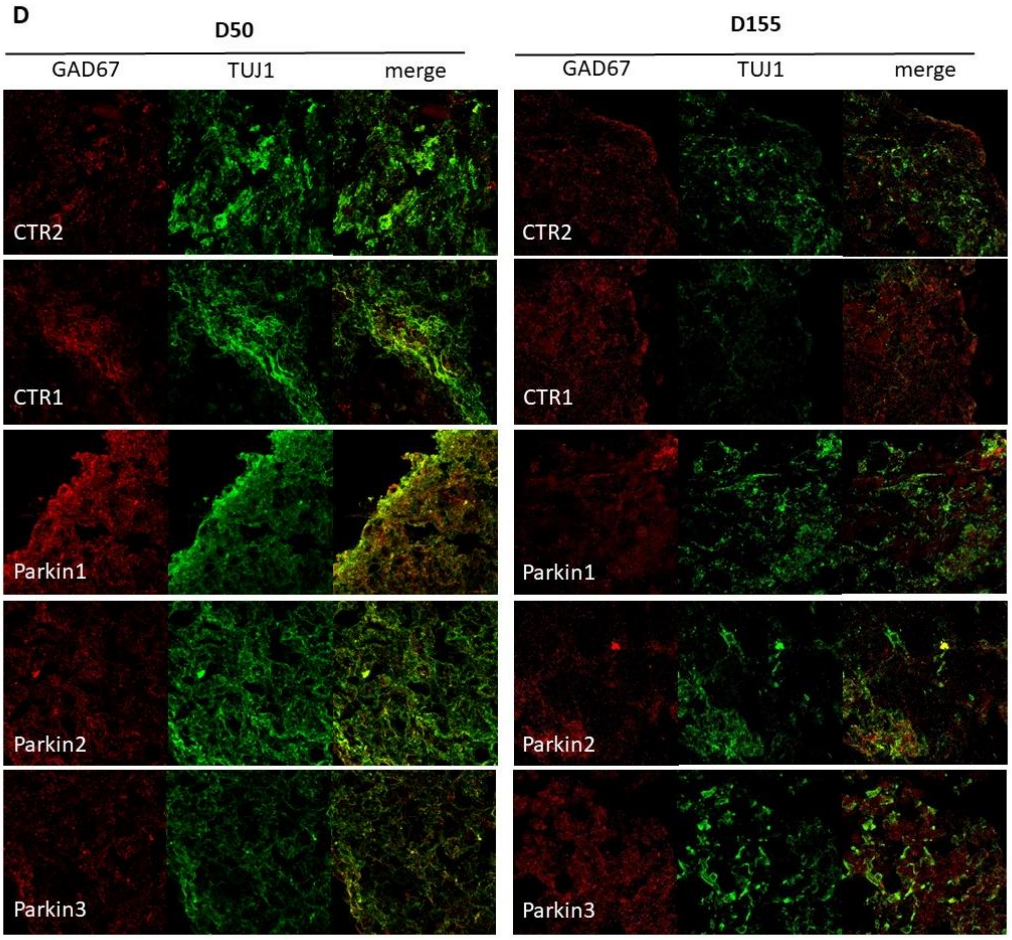
D
D50
D155
GAD67
TUJ1
merge
GAD67
TUJ1
merge
CTR2
CTR2
CTR1
CTR1
Parkin1
Parkin1
Parkin2
Parkin2
Parkin3
Parkin3

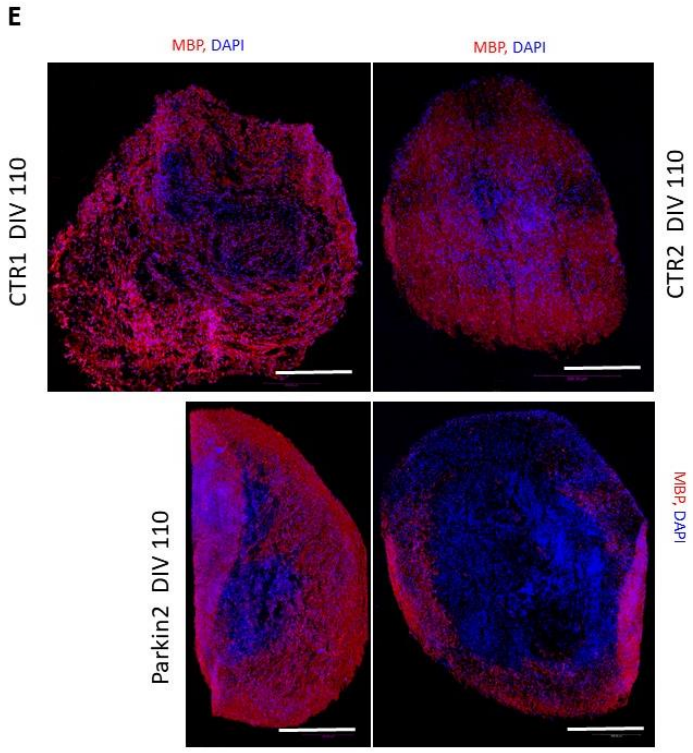
E
MBP, DAPI
MBP, DAPI
CTR1 DIV 110
CTR2 DIV 110
Parkin2 DIV 110
MBP, DAPI

Figure 18. IF on midbrain organoids. (A) TH staining on CTR (CTR1) and PARK2 (Parkin 2) at DIV 110; whole organoid images were taken at 20x on confocal microscope; squares above show a 40x, oil magnification; scale bar, 200 µm (B) GFAP staining on CTR (CTR1) and PARK2 (Parkin 2) at DIV 110; whole organoid images were taken at 20x on confocal microscope; squares above show a 40x, oil magnification; scale bar, 200 µm (C) GAD-65 and TUJ1 co-staining on CTR (CTR1 and 2) and PARK2 (Parkin 1,2 and 3) at DIV 50 and DIV 155, 20x, confocal microscope; (D) GAD-67 and TUJ1co-staining on CTR (CTR1 and 2) and PARK2 (Parkin 1,2 and 3) at DIV 50 and DIV 155, 20x, confocal microscope; (E) MBP staining on CTR1, CTR2 and Parkin2 at DIV 110, whole organoid images were taken at confocal microscope at 20x. Scale bar, 300 µm.

IF intensity signal analyses were performed on midbrain organoids of CTR1 and Parkin2 at DIV 110 (*see figure 19*). Two cytoplasmic markers were quantified: TH and GFAP. TH levels resulted significantly increased in PARK2 compared to CTR ($p < 0.0001$), as well as GFAP ($p < 0.01$).

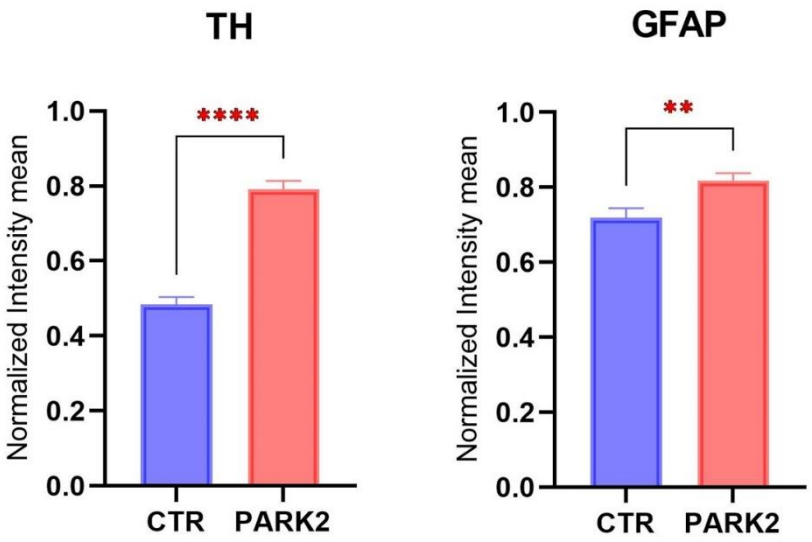

Figure 19. IF intensity analyses on midbrain organoids of CTR and PARK2 at DIV 110. The two graphs show the normalized intensity mean of TH and GFAP. Data are presented as mean ± SEM. ** p< 0.01; **** p< 0.0001.

Quantification of GFAP as GFAP positive area on total organoid area was analysed on CTR1, CTR2, CTR3 and CTR4 and on Parkin1, Parkin2, Parkin3 and Parkin4 on two timepoints: DIV 50 and DIV 155. GFAP resulted significantly increased in PARK2 compared to CTR at DIV 155 (p< 0.05) (*see figure 20*).

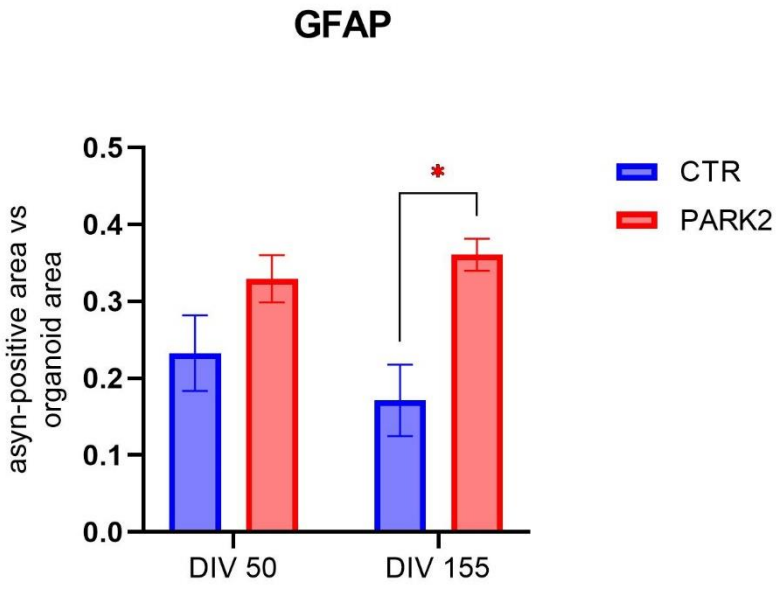

Figure 20. GFAP positive area on total organoid area. Quantification of positive area /total organoid area on 4 CTR and 4 PARK2 lines. Confocal images of 2 organoids/line and 2 sections/organoid were analysed using Imaris from Prof. Bellucci's team. Data are presented as mean ± SEM. * p< 0.05.

An IHC characterization was performed as well on midbrain organoids of CTR and PARK2 (*see figure 21*). IHC was particularly useful to assess the presence of myelin using the Klüver-Barerra method and neuromelanin through a direct observation of the pigmentation on eosin hematoxylin staining and with Scmorl technique. IHC was also

performed on markers such as TH and GFAP. Neuromelanin pigmentation was observed both in CTR and PARK2 but quantification was not performed.

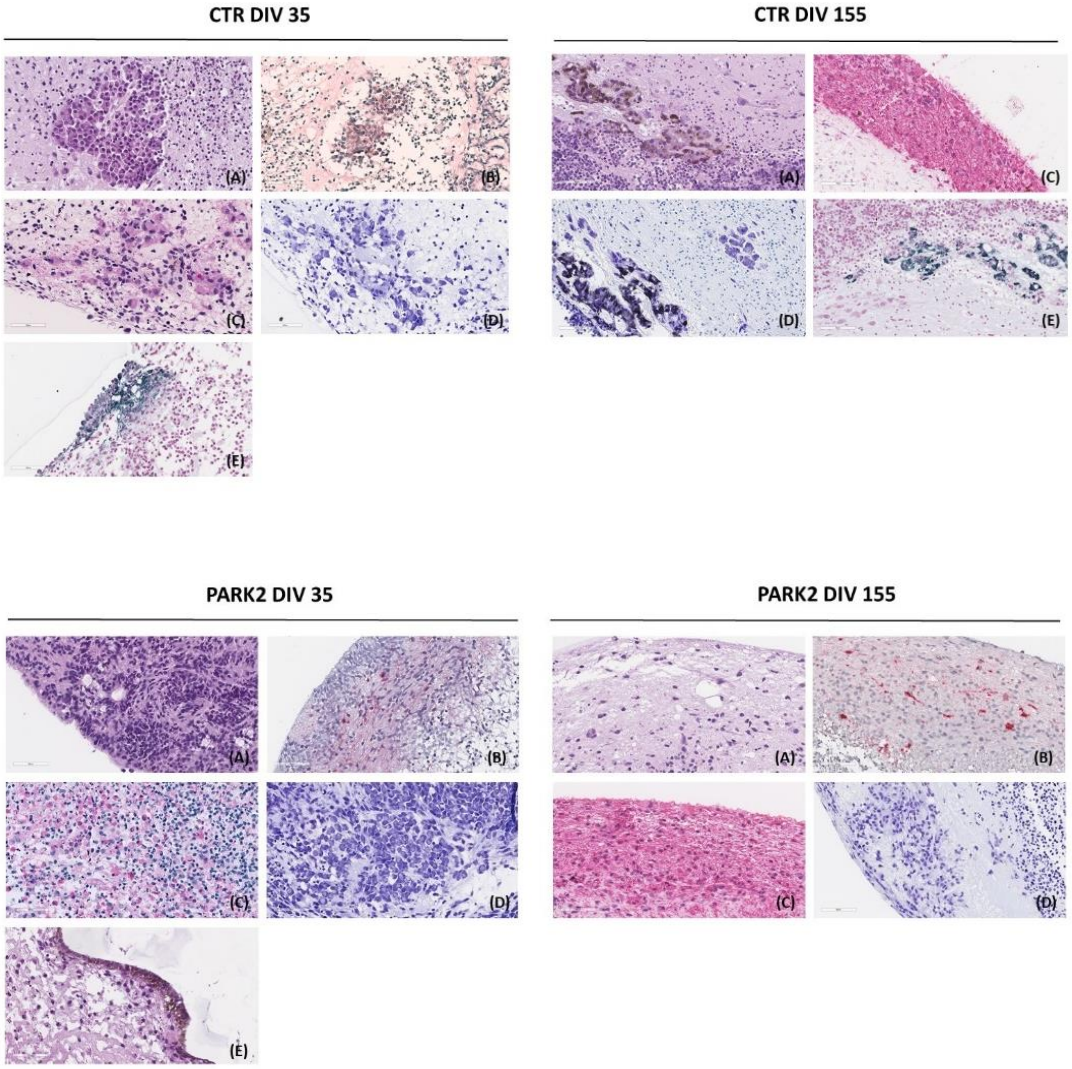

Figure 21. IHC on midbrain organoids of CTR and PARK2. (A) Eosin hematoxylin staining, 20x, brightfield microscope. Scale bar, 60 µm; (B) TH staining, 20x, brightfield microscope. Scale bar, 60 µm; (C) GFAP staining, 20x, brightfield microscope. Scale bar, 60 µm; (D) Klüver-Barerra staining, 20x, brightfield microscope. Scale bar, 60 µm; (E) Neuromelanin pigment +/- Schmorl staing, 20x, brightfield microscope. Scale bar, 60 µm.

In order to quantify gene expression of dopaminergic markers (TH and DAT) and Gluk2 qPCR was performed on midbrain organoids of CTR2, CTR3, Parkin 1, Parkin 2, Parkin 3 and Parkin 4 at two defined timepoints: DIV 35 and DIV 110 (*see figure 22*). TH levels resulted significantly higher in PARK2 at DIV 35 compared to CTR ($p < 0.0001$). DAT showed a similar trend to DA neurons and resulted increased in CTR at DIV 35 ($p < 0.0001$). Gluk2 levels were significantly higher in PARK2 at DIV 110 compared to CTR ($p < 0.001$).

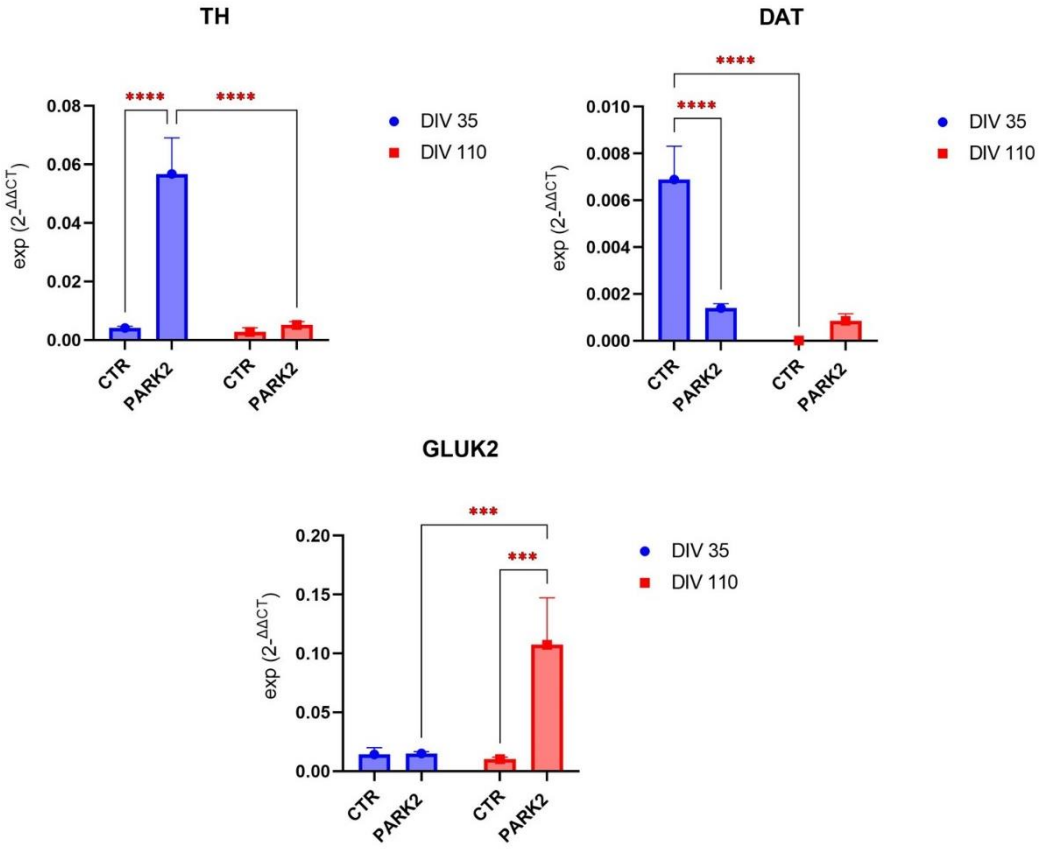

Figure 22. qPCR on midbrain organoids of CTR and PARK2 at DIV 35 and 110. Quantification was performed using a reference gene: YWHAZ. Data are presented as mean ± SEM. *** $p < 0.001$, **** $p < 0.0001$.

WB analyses were performed on CTR1, CTR2, Parkin1, Parkin2 and Parkin3 and they evaluated the expression of dopaminergic and astrocytic markers, including also Gluk2

(*see figure 23*). Protein quantification was performed with normalization to GAPDH, a housekeeping protein abundantly distributed in cells (*see figure 24*). TUJ1 levels are similar in CTR and PARK2 with a significantly increasing trend from DIV 35 to DIV 110. TH levels are higher in PARK2 compared to CTR with significance ($p< 0.01$) at DIV 110. DDC has a different trend compared to TH, showing increasing levels both in CTR and PARK2 from DIV 35 to DIV 110 ($p< 0.0001$), although this data has to be valued carefully because there was a high variability in CTR at DIV 35. As expected we found Parkin levels reduced in PARK2, compared to CTR. Considering the astrocytic markers, we evaluated Aldh1l1 expression as a pan-astrocytic marker and we found that in PARK2 its levels raised significantly from DIV 35 to DIV 110 ($p< 0.0001$). At DIV 110 Aldh1l1 levels resulted higher in PARK2 compared to CTR although not significant. Interestingly, GFAP levels are higher in PARK2 compared to CTR both at DIV 35 and DIV 110 with significance at DIV 110 ($p< 0.001$). EAAT2 showed a different trend with higher levels in CTR, especially at DIV 35 where this difference resulted significant ($p< 0.01$). In the end we evaluated expression of Gluk2 and we found that expression levels raised from DIV 35 to DIV 110 and that it showed a significant higher expression in PARK2 at DIV 110 ($p< 0.0001$).

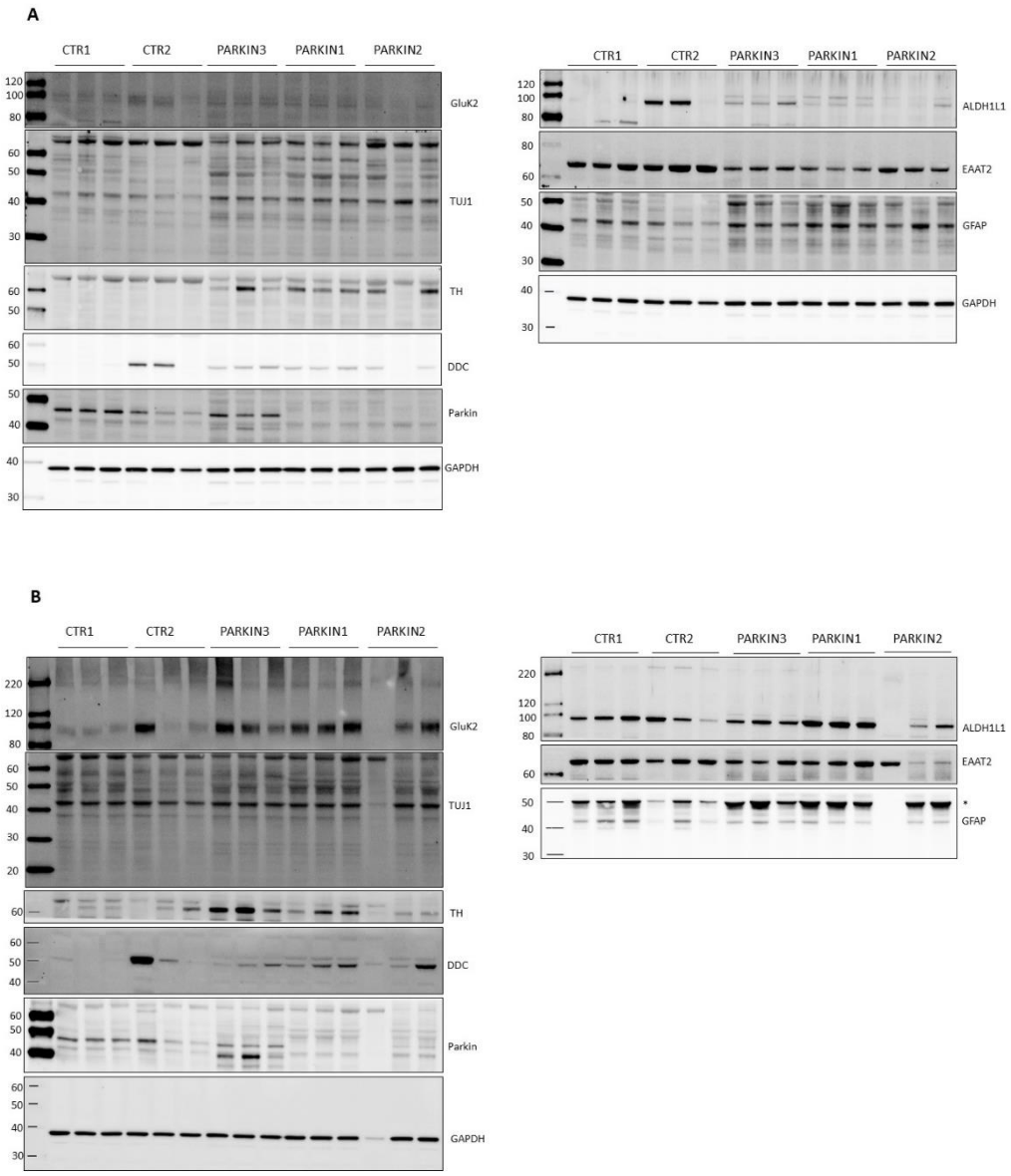

Figure 23. WB analyses performed on midbrain organoids of CTR1, CTR2, Parkin1, Parkin 2 and Parkin 3 showing the expression of TUJ1, TH, DDC, Aldh1l1, GFAP, EAAT2, Gluk2 and Parkin. Normalization was performed on GAPDH. (A) WB on midbrain organoids at DIV 35; (B) WB on midbrain organoids at DIV 110. GFAP has an aspecific band at 50kDa (*).

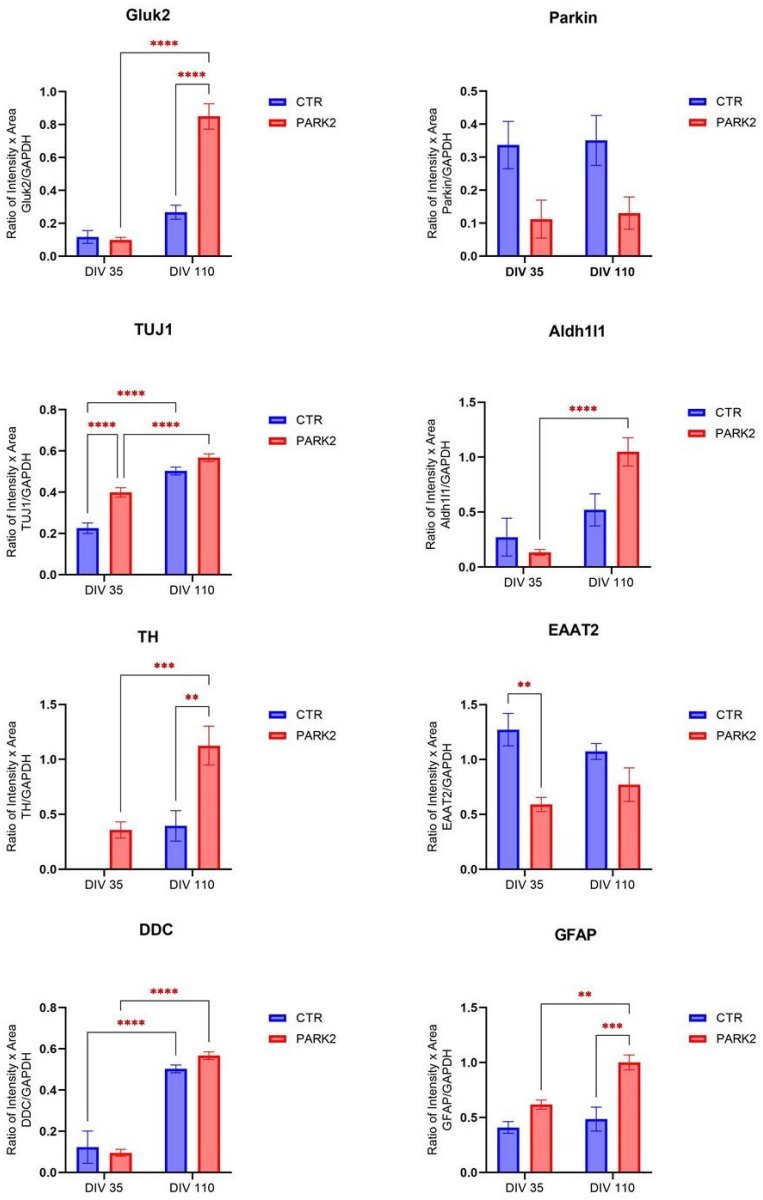

Figure 24. WB quantification of neuronal and astrocytic markers. Each marker is normalized for GAPDH. Data are presented as mean ± SEM. ** p< 0.01; *** p<0.001; **** p< 0.0001.

HD-MEAs recordings were performed on CTR2, CTR3 and CTR4 and on Parkin 1, Parkin 2, Parkin 3 and Parkin 4.

HD-MEA recordings of sliced CTR and PARK2 organoids (> DIV60), demonstrated very robust spontaneous neuronal activity (*see figure 25*) with slow, but regular network bursts (average burst rate < 0.1Hz). PARK2 organoids also showed bursts, but they had a significantly higher overall firing rate compared to CTR ($p<0.001$). Moreover, the bursts of this mutant line were much longer (~1min) compared to the CTR, and resembled epileptiform activity. The exact mechanism underlying these network activities warrant further investigations (*see figure 26*).

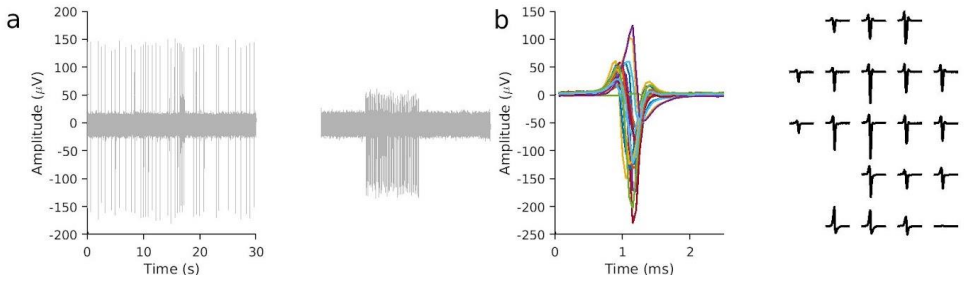

Figure 25. Example traces for spontaneous activity in midbrain organoids. (a) wide range of firing dynamics of single neurons, from less to very regular burst firing (traces are filtered between 0.15-9.50 kHz)). (b) neuronal footprint of one neuron (after spike sorting) using spike-triggered averaging on the chip.

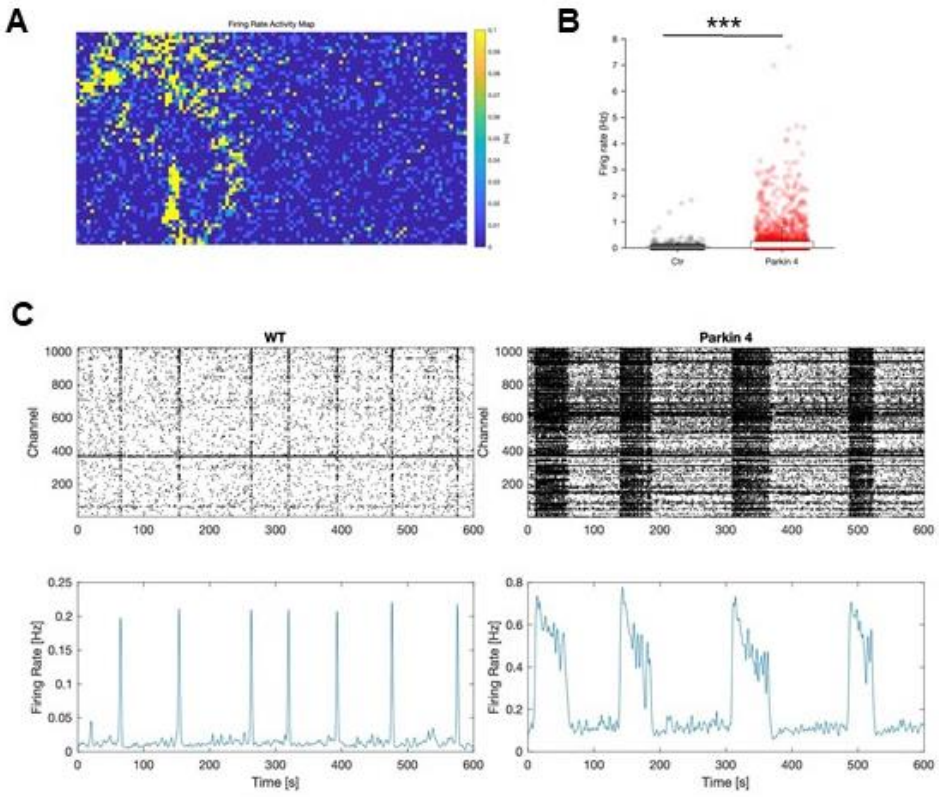

Figure 26. HD-MEAs of midbrain organoids. (A) activity scan of CTR2 organoid (WT); (B) comparison of the firing rate of 5 CTR2 (WT) to 6 Parkin 4 slices, *** $p<0.001$; (C) raster plot for 10 min activity recording in a CTR2 (WT) on the left and a Parkin4 organoid on the right (~ 3 weeks after plating on the HD-MEA)

Calcium imaging was performed on CTR2 and Parkin2 (*see figure 27*). Both CTR and PARK2 presented calcium oscillations with significantly longer latency in CTR compared to PARK2 ($p= 0.01$). In PARK2 we observed a second Ca+ peak, just after the first one, meaning that the threshold for triggering Ca+ oscillations is reduced in PARK2. By the stimulation of organoids with kainite we observed an increased frequency in Ca+ oscillation both in CTR and PARK2, but especially in CTR. An explanation of this phenomenon could be that KAR at basal conditions is already overstimulated in PARK2. The link between Ca+ oscillations and KAR was demonstrated through the administration of UBP310 (a KAR inhibitor) that abolished organoids activity both in CTR and PARK2. Further studies are needed in order to clarify the link between KAR and Ca+ oscillations in organoids and to better understand the augmented reactivity in PARK2.

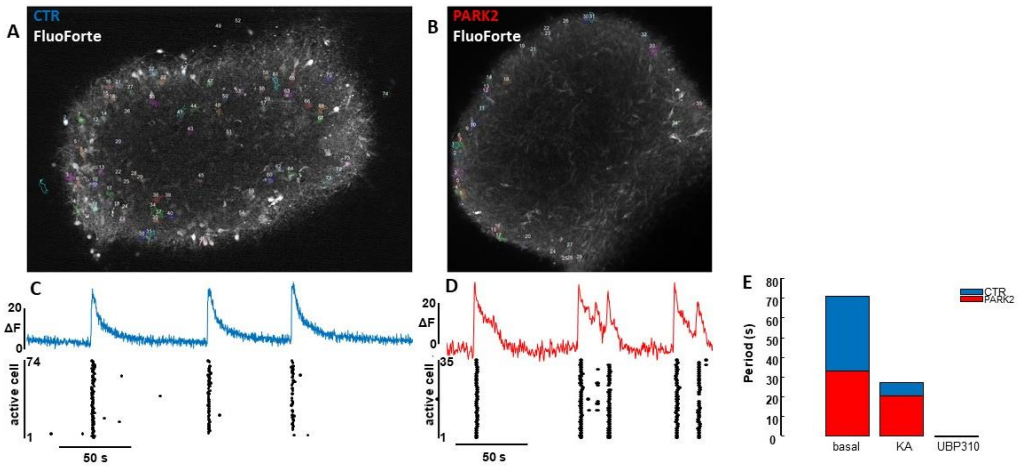

Figure 27. Calcium imaging in midbrain organoids. (A-B) FluoForte signal acquired by 2-photon microscopy in CTR and PARK2 organoids. Fluorescence signals of active cells were averaged in the correspondent pixel regions (numbered). (C) Fluorescence variation (ΔF) averaged over the whole organoid (upper blue trace) and individual active cell activity summarized in a raster plot (lower panel), where each dot corresponds to a Ca2+ peak. (D) Same as panel C for Parkin2. E) Ca2+ oscillation period calculated in basal condition or with addition of kainic acid (KA, 10 µM) or UBP310 (10 µM).

5. Discussion

5.1. Increased TH expression in PARK2

Considering clinical and neuropathological aspects of *Park2* PD, it is evident that the pathogenesis of this disease is different from the one of classic idiopathic PD. Yamamura (Yamamura, 2010) observed that these patients presented diurnal fluctuations and that parkinsonian symptoms were alleviated by sleep. On the basis of this peculiar aspects he supposed that the consumption of some dopamine-related substance was reverted by rest and because of hereditary and early-onset he thought that an inborn error in the metabolism could be the cause. By making these considerations he was on the right path to *Park2* pathogenesis discovery.

One curious finding that emerged from this study and that has never been reported before is that TH levels are significantly higher in PARK2 compared to CTR, both in dopaminergic neurons and midbrain organoids. The study we performed on DA neurons revealed that at DIV 35 TH mRNA levels were significantly increased in PARK2. We also found that PARK2 DA neurons at DIV 50 had significantly higher TH protein levels, assessed through WB and IF intensity analyses. The percentage rate of TH-positive cells was similar in PARK2 and CTR DA neurons. Although quantification of TH+ cells in midbrain organoids has not been performed yet, a similar result was found in PARK2 midbrain organoids. At DIV 35 TH mRNA levels resulted significantly increased in PARK2 at qPCR analyses and at DIV 110 TH protein levels, assessed by WB and IF analyses, were also significantly enhanced in PARK2. This could mean that in *Park2* there might be an altered TH transcription and translation.

TH is an enzyme that catalyses the conversion of L-tyrosine to L-3,4-dihydroxyphenylalanine (L-DOPA), which is the initial and rate-limiting step in the

biosynthesis of catecholamines, including dopamine. TH activity is regulated at different levels. There is a short term regulation induced directly through a feedback inhibition by catecholamines, such as dopamine. There is also a medium/long-term regulation that occurs at different phases of gene expression, such as transcription, alternative splicing, translation and post-translational modifications (Nagatsu T, 2019). TH was found markedly decreased in catecholamine-rich brain regions of PD patients (Nagatsu T., 1977). Furthermore, TH mRNA levels were found reduced in SNpc of PD patients (Ichinose H, 1994). TH reduction is associated with dopamine decreased production but there are some compensatory mechanisms, such as an increased D2 receptor sensitivity and TH activation by phosphorylation of its N-terminal serine residues. This compensatory activation may promote TH proteasomal degradation with consequent reduced levels and this sequence of events may promote neurodegeneration in PD (Nakashima A, 2013). In addition to that there are familiar forms of PD such as the rare EOPD caused by *DJ-1* mutations, where the gene is directly implicated in TH transcription, suggesting that *DJ-1* mutations may reduce TH expression (Ishikawa S, 2010). It is evident that there is a link between TH and PD and that a dysregulation of enzymatic levels and activity is an important contributor in neurodegeneration associated to PD. As *Park2* PD differs from other forms of PD, also the relationship between *Park2* mutations and TH expression might be different and further studies are certainly needed to elucidate this link.

In this study both TH mRNA and protein levels resulted increased in PARK2 meaning that *Park2* mutations could lead to a long-term regulation of TH expression. A hypothesis that can be formulated by this observation is that TH mRNA and protein are augmented to probably compensate an increased dopamine release and a reduced dopamine uptake. As a matter of fact, a study published by Jiang et al. (Jiang H., 2012) demonstrated that *Park2* mutations were associated with increased MAOs levels with consequent enhanced oxidative stress, and calcium-independent dopamine release. They reported also a reduced dopamine uptake. *Park2* mutations also reduce the binding sites of DAT (Jayaramayya K, 2020). Taken together, these results suggested the key role of Parkin in regulating dopamine utilization and suppressing dopamine oxidation. In addition to that it has been proved Parkin role in transcriptional regulation by acting as transcription factor

(Alves da Costa C., 2019). The DNA-binding properties of Parkin and its nuclear localization may play a key role in controlling the expression of several genes.

Midbrain organoids are the right model to study disorders where alterations in neurodevelopment may play a key function. Taking into account all the pathogenic roles played by *Park2* discovered until now, we might consider *Park2* PD a neurodevelopment disorder. Increased TH mRNA and protein levels both in PARK2 DA neurons and midbrain organoids indicate that such alterations happen early in the neurodevelopment. Cellular models can only recapitulate early features of the disease because of their limited lifespan. Considering our results and results from previous studies we can speculate that early in the disease there is an impairment in dopamine release which is increased and dopamine re-uptake which is decreased. These alterations may lead probably through an indirect mechanism to an augmented TH expression in order to compensate this rapid dopamine turnover. As a result, oxidative stress is enhanced and this sums up to all the other dysregulations caused by *Park2* mutations, leading to dopaminergic neuron death. Further studies are needed in order to assess whether TH transcription factors are substrates of Parkin and which is exactly *Park2* role in regulating TH expression. In order to better prove that TH expression is increased in *Park2* DA neurons we aim to perform a TH signal analyses using FACS which is a technique that provides an objective and quantitative recording of fluorescent signal from individual cells. In addition to that through this technique we could perform a more objective quantification of TH+ cells on the total amount of neuronal cells derived from each samples (both bi-dimensional DA neurons culture and midbrain organoids).

5.2. Increased astrocytes reactivity in PARK2

Another interesting result that emerged from this research is that PARK2 is associated to increased GFAP: a reactive astrocytes marker. Both in our astrocytes cultures but especially in our midbrain organoids we found significantly increased levels of GFAP at WB and IF analyses. It can be hypothesized that *Park2* mutations are associated to an astrogliosis and increased astrocytic reactivity.

Neuroinflamation has been widely studied over the past decades and it has been linked to different neurodegenerative diseases, including PD. Neuroinflammation involves the synthesis and release of pro-inflammatory mediators, such as cytokines and chemokines, but also the infiltration of immune cells. When this process becomes uncontrolled it exacerbates neurodegeneration. The attention over the past years has been focused especially on microglia, which are resident macrophages of the CNS that contribute to the parenchymal homeostasis. Their role in neurodegereative diseases has been widely studied as they are capable of initiating inflammation in response of pro-inflammatory molecules. Neuroinflammation induced by 'reactive' microglia has been recognized in the pathogenic process leading to PD (McGeer PL, 1988).

Astrocytes are the most abundant cell population in the CNS but their role in neurodegeneration associated to PD has been less extensively studied. Astrocytes play different physiological roles, including the synaptic transmission regulation, the ionic and water homeostasis maintenance, neuron survival and differentiation through the secretion of GDNF and BDNF. Astrocytes are also fundamental during brain development. They regulate neurogenesis by guiding and supporting neuronal migration, survival and process formation. For all this reasons it is clear that the loss of astrocytic function may contribute to neurodegeneration in different diseases, including PD. Astrocytes become reactive in response to a stimulus and may initiate or promote the pathogenesis of PD (Sofroniew MV, 2010). There are two types of astrocytes in response to exogenous stimuli: an A1-type which is pro-inflammatory and an A2-type which is anti-inflammatory. A1 astrocytes have been found in post-mortem brains of neurodegenerative diseases

including PD (Liddelow SA, 2017). In addition to that there are regional differences in astrocytes and this may contribute to selective vulnerability in PD. For example, striatal astrocytes exhibit less gap-junction and neuronal interactions compared to astrocytes of other brain regions (Chai H, 2017).

Parkin deficient astrocytes display endoplasmic reticulum stress, inflammation with increased cytokines release and reduced secretion of neurotrophic factors (Singh K, 2018). In addition to that they are more susceptible to neurotoxins, proliferate less and have an increased expression of proapoptotic proteins (Solano RM, 2008). Parkin expression results increased in reactive astrocytes of diseased human brains (Witte ME, 2009), suggesting that this protein somehow regulates glial immune responses. *Park2* mutations are linked to a pro-inflammatory profile, exacerbating inflammation, promoting activated microglia survival and spreading neurodegeneration (de Léséleuc L, 2013).

The generation and differentiation of *Park2* iPSCs-derived astrocytes might be a useful tool to investigate astrocytic pathogenic mechanisms associated to *Park2* mutations although they might be not exhaustive. Neurodegeneration is a complex process where glia-neurons interactions are fundamentals. For this reason, we generated *Park2* midbrain organoids as they are a complex system made of not just dopaminergic neurons but also of other neuronal types and also glia, including an abundant quote of astrocytes.

In our *Park2* midbrain organoids we found that there could be an impaired astrocytic glutamate re-uptake as EAAT-2, the major astrocytic glutamate transporter, resulted significantly reduced.

EAAT-2 is the major glutamate transporter responsible for 95% of glutamate uptake and it is mainly expressed on astrocytes, but to a lesser extent it is expressed also in other glial cells, such as microglia and oligodendrocytes. EAAT-2 expression in neurons is controversial. EAAT-2 mRNA was found in neurons of several rat models although protein expression was variable (Berger U. V., 2005) (Schmitt A., 1996). Most human

studies suggest that EAAT-2 is only expressed in astrocytes (Simpson J. E., 2010) (Rothstein J. D., 1994) whereas few others provide evidence of neuronal expression (Rimmele T. S., 2016). These controversial data might be the result of technical problems that can lead to misleading results. Defining spatial distribution of glutamate transporters, including EAAT-2, and cellular localization can help understanding glutamate recycling and possible alteration in glutamatergic homeostasis.

Supposing that the majority of EAAT-2 is expressed in astrocytes, reduced levels of this transporter might lead to a consequent glutamate synaptic overload that can contribute to excitotoxicity. Astrocytes play an important role at the synaptic cleft as they regulate synaptic function and plasticity (Blanco-Suárez E, 2017). At the excitatory synapse, through glutamate transporters such as EAAT-2, they provide excess glutamate elimination in order to prevent excitotoxicity. Astrocytes transform glutamate in glutamine and released it back to neurons pre-synaptic terminal where it is then re-converted into glutamate.

We did not find the same result in astrocytic cultures and there could be three possible considerations that can be made upon this finding. The first one is that in PARK2 astrocytic cultures, although EAAT-2 protein expression is unchanged, it might not properly localize to cellular membrane and might not clear properly extracellular glutamate. In IF it is difficult to distinguish if EAAT-2 signal is properly localized to the cellular membrane or if it is mainly cytoplasmic. One possibility would be to perform an IF co-staining with another membrane marker (such as E-Cadherin, CD98 etc) in order to check the co-localization of the two markers. Another observation that can be made is that the midbrain organoid is a more complex model where glial cells differentiate and grow along with neuronal cells. In such models cellular development resembles human midbrain development, so that the astrocytic phenotype in midbrain organoids might be different from the one of astrocytic cultures. As a matter of fact, the pathogenic process leading to neurodegeneration implies the interaction of glia with neurons and midbrain organoids seem to be the perfect model to study it in PD. A third consideration upon this finding is that EAAT-2 is also expressed by other glial cells and also by neurons, even if at a lower rate, so that our finding in midbrain organoids might summarize alterations that

could happen in all these cell types. In order to test this hypothesis, midbrain organoids might be disaggregated and EAAT-2 expression could be checked in different glial and neuronal populations through IF and FACS.

It is not known yet whether EAAT-2 is a substrate of Parkin and which is exactly Parkin role in regulating EAAT-2 expression. It would be very interesting to investigate how *Park2* mutations affect EAAT-2 transcription, translation and ubitiquination. We have only assessed EAAT-2 expression through WB, so at a protein level and we have not yet assessed mRNA levels through qPCR. If mRNA levels are high, it means that *Park2* mutations may affect EAAT-2 translation.

A study on astrocytes of *Park2* PD patients and their iPSCs-derived midbrain organoids was published recently by Kano et al. (Kano M, 2020). They found reduced GFAP and vimentin-positive astrocytes in the SNpc of *Park2*-mutated subjects and in *Park2* iPSCs-derived midbrain organoids. The neuropathological study compared *Park2* SNpc with the ones of sporadic disease that present a reduced disease time course and the astrocytic quantification on midbrain organoids was performed only at DIV 35 and only through IF analyses. In addition, they used a different protocol for the generation of midbrain organoids.

In conclusion, it is evident that astrocytes play a key role in neurodegeneration associated to PD and also to *Park2* PD. Further studies, especially on *Park2* midbrain organoids, may elucidate their involvement in the pathogenesis of this disease and may lead to the identification of new molecular target for future disease-modifying therapies.

5.3. Gluk2 overexpression in PARK2

As the focus of this study was the assessment of KAR impairment in *Park2*, we assessed Gluk2 levels in all our *in vitro* cellular models, using WB analyses and qPCR. We found significantly increased Gluk2 levels in PARK2 midbrain organoids at DIV 110, both on WB and qPCR. As Gluk2 is also expressed in glial cells, especially in astrocytes, we assessed Gluk2 levels also in these cells and we found significantly enhanced levels in PARK2, both on WB and qPCR.

It has been demonstrated that Gluk2 is a substrate of Parkin and that when *Park2* is mutated Gluk2 levels arise (Maraschi A, 2014). Parkin loss-of-function enhances the efficacy of glutamatergic synapses. Maraschi et al. in their paper specified that Parkin regulates KAR current by binding Gluk2 C-terminal, a binding that is transiently induced by KAR activation. This action may take place both at pre and post-synaptic sites and contribute to excitoxicity. SNpc receives glutamatergic inputs from different brain areas, including the cortex, the pedunculopontine nuclei, the thalamus, the superior colliculus, and the subthalamic nucleus. When *Park2* is mutated SNpc dopaminergic neurons become very vulnerable to excitotoxicity and this can lead or contribute to neurodegeneration which is extremely marked in *Park2* patients. Excessive glutamate at the synaptic cleft cause an increase of intracellular calcium levels and bioenergetics changes that enhance the oxidative burden and cause apoptosis. At the synaptic cleft astrocytes contribute to buffer glutamate excess through EAATs. Glutamate toxicity is recognized as a common feature of many neurodegenerative diseases, including PD (Ambrosi G, 2014).

Increased Gluk2 levels in astrocytes represent another novelty coming from this study. When Gluk2 expression is increased, there is an increased glutamate influx in astrocytes, meaning that excitotoxicity related to *Park2* mutations affect also these glial cells. *Park2* astrocytes might incur in a glutamate overload due to increased Gluk2 levels. As we found EAAT-2 reduced in *Park2* midbrain organoids, another explanation of this finding could be a compensatory downregulation of this glutamate transporter. It would be interesting to check also the expression in *Park2* astrocytes of the glutamine synthase (GS), the

limiting enzyme in the conversion of glutamate to glutamine which is then release in the synaptic cleft. Increased GS levels could be in line with an increased glutamate influx in *Park2* astrocytes, but decreased GS could happen at some point if oxidative stress prevails.

Astrocytes do not fire action potentials but are excitable and can respond to stimuli such as glutamatergic ones. Astrocytes respond to Gluk2 activation with an increase in intracellular Ca2+ and a downregulation of extracellular signal-regulated kinase (ERK) 1/2 phosphorylation. Intracellular Ca2+ overload leads to a series of events: glutamate transporters regulation; increased GFAP and other reactive markers expression, pro-inflammatory cytokines release; increased expression of synaptogenic molecules and increased release of gliotransmitters (glutamate, ATP, GABA etc..) (Shigetomi E, 2019). On the other side a downregulation of ERK1/2 has important consequences on astrocytic and neuronal function as well. As a matter of fact, ERK1/2 are a group of Ser or Thr kinases that regulate different substrates such as cytoplasmic phospholipase A2 (PLA2), cytoskeletal elements and intracellular domains of membrane receptors. ERK1/2 have also intranuclear targets such as transcription factors (Elk1, c-Fos, c-Jun) (Wortzel, 2011). An overexpression of Gluk2 in astrocytes may lead to an intracellular overload of Ca2+ that causes an astrocytic reactive pro-inflammatory state that combined with ERK1/2 downregulation results in astrocytic dysfunction and consequent neuronal damage.

This finding indicate that excitotoxicity involves also astrocytes and as a matter of fact GFAP, a marker of reactive astrocytes, resulted increased in PARK2. As glia-neurons interactions are fundamental in the neurodegenerative process, it would be extremely interesting to study astrocytes and DA neurons straightly from *Park2* dissociated midbrain organoids. This would provide a better insight in the pathogenesis of *Park2* PD and clarify how exactly excitotoxicity arises.

5.4. Increased neuronal activity in PARK2 midbrain organoids

Considering that *Park2* alters KAR function we looked further into neuronal excitability through electrophysiological experiments both in our iPSCs-derived DA neurons and midbrain organoids.

We did not find significant differences between PARK2 and CTR in bi-dimensional cultures, but we found an increased spontaneous neuronal activity in PARK2 midbrain organoids. Midbrain organoids were studied through different electrophysiological techniques: HD-MEAs and calcium imaging using two-foton microscope.

Through HD-MEA recordings we found a robust spontaneous neuronal activity both in CTR and PARK2 with regular bursts organized in an oscillatory pattern. Interestingly, PARK2 showed a significantly higher overall firing rate compared to CTR and longer bursts duration meaning that they displayed an abnormal neuronal hyperactivity compared to CTR.

Similar results were obtained from an independent experiment: the calcium imaging of these midbrain organoids. Latency between Ca2+ oscillations was significantly shorter in PARK2 midbrain organoids and they displayed also a second Ca2+ peak, meaning that the threshold for triggering Ca2+ oscillations was reduced in PARK2. Interestingly, kainate stimulation produced only a little increase in Ca2+ oscillations frequency, meaning that in PARK2 KAR, at basal conditions, is already overstimulated. From these recordings emerged the link between Ca2+ oscillations and KAR, because after the administration of a KAR antagonist, organoids activity was abolished both in CTR and PARK2.

It can be speculated also that the reduced latency in Ca2+ oscillations in PARK2 organoids could be partly due to overactive astrocytes that are dysfunctional and could not properly

clear the excessive glutamate at the synaptic cleft. In addition to that they also release more glutamate, contributing to neuronal overstimulation. KAR antagonists are expected to be beneficial both on neurons and astrocytes, reducing their distress.

Further studies are needed in order to understand, first of all, network activities in midbrain organoids but also to clarify the link between KAR and Ca2+ oscillations and better understand the augmented reactivity in PARK2.

To better isolate only KAR mediated currents a non-competitive AMPA antagonist could be used along with kainite during the recordings.

This typical oscillatory neuronal activity that we observed in our PARK2 midbrain organoids have been already described in basal ganglia of PD patients (Wichmann T, 2011). It was demonstrated that this activity could be disrupted by levodopa administration (Brown P, 2005). In addition to that, increased rhythmic, oscillatory burstings in *Park2* DA neurons have been already reported by Zhong et al. (Zhong P., 2017). From their experiments emerged that *Park2* iPSCs-derived DA neurons had a delayed increase of spontaneous Excitatory Postsynaptic Current (EPSCs) in response to dopamine with concomitant increase in quantal dopamine release. A selective D2-receptors inhibition or D1-receptors activation induced a large rhythmic bursting of EPSCs in *Park2* DA neurons. This rhythmic EPSCs bursting reminded of the oscillatory neuronal activities of PD basal ganglia. This results suggested that *Park2* mutations could potentiate presynaptic glutamatergic transmission through D1-receptors stimulation.

In conclusion, the increased oscillatory neuronal activity and Gluk2 overexpression found in our *Park2* midbrain organoids support the hypothesis that *Park2* mutations may lead to excitotoxicity. Further studies are need to elucidate how *Park2* neuronal activity is increased and this could be demonstrated pharmacologically by defining neuronal networks through the use of neurotransmitter stimulants and blockers which is something that we aim to do.

6. Strengths and limitations of the study and future perspectives

One of the major strengths of this study is that the investigation of the pathogenic mechanisms behind *Park2* mutations, with a focus on the glutamatergic excitotoxicity hypothesis, was performed on iPSC-derived cellular models obtained straight from the patients affected by this disease. This constitutes a unique opportunity to investigate the underling *Park2* neurophysiopathology in models that recapitulate features of human neurons and glial cells. Through the generation and differentiation of dopaminergic neurons, astrocytes and especially midbrain organoids we could be able to observe the development of the pathogenic processes that lead to the disease. iPSC-derived midbrain organoids are an extremely valuable tool that recapitulates neurodevelopmental characteristics of human midbrain and that is particularly useful in modelling *Park2* PD as its pathology is presumed to start early in the neurodevelopment. Another advantage of using these models is the possibility of testing experimental drugs that could modify the disease course and observe positive and negative responses to it as these cell share human metabolisms.

Another strength of the study is that different methodologies were used in order to define and quantify specific markers expression. As a matter of fact, we processed our samples through WB, qPCR and IF/IHC. We were also able to perform an electrophysiological characterization of both DA neurons and midbrain organoids. The electrophysiological study of *Park2* midbrain organoids has never been published before and gave interesting insights into the pathologic phenotype associated to this mutation.

Considering the limitations of this study, one of the biggest is the high variability that cellular models present. We tried to overcome this problem by increasing the number of

iPSC lines of both CTR and PARK2 and by producing multiple batches of the same line for all differentiation protocols, especially for midbrain organoids.

Another limitation of these models is that they cannot be kept in culture for long period of time, especially for 2D cultures. 2D DA neurons survival is limited with important cellular loss from DIV 50 to DIV 75 and exponentially decreasing survival after that timepoint. Midbrain organoids starts to show mature features from DIV 35 with a peak between DIV 75 and DIV 110. After DIV 110 a cellular decay process starts and especially the central part of these organoids dies because without vascularization this part cannot receive nutritional elements. Fortunately, as reminded before, *Park2* PD is a disease that is suspected to start early in the neurodevelopment and the vital period of these organoids could be sufficient to see some pathologic alterations. For this reason, we may consider midbrain organoids the most suitable model to study this disease as it is able to recapitulate human midbrain neurodevelopment during which pathologic modifications may arise.

Another limitation of this study is that we were not able at the moment to generate an isogenic CTR line, but this will be created in the future using the CRISPR-Cas9 technique. The possibility of genetically correct *Park2* mutations in patients-derived iPSCs allows the generation of an ideal control line which shares the same genetic background of the mutated line except for the mutation itself. As a matter of fact, genetic background affects the cellular phenotype of both healthy and patient lines, generating a noise that could influence the results.

Another limitation that can be taken into account concerns cell counting methods used. DA neurons would be more accurately quantified by using a TH-NeuN co-staining and by performing a quantification of TH-positive cells out of NeuN-positive cells. In this study the quantification of TH-positive cells was obtained through the TH-TUJ1 co-staining by calculating TH/DAPI and TH/TUJ1 ratio. TUJ1 is a neuronal cytoplasmic marker, whereas NeuN is a neuronal nuclear marker which is more suitable to quantify the percentage of dopaminergic neurons out of the whole neuronal population present in

the sample. In addition to that, the quantification of TH+ neurons in midbrain organoid has not been performed yet but this is something we plan to do through a TH-NeuN co-staining.

Quantification of IF signal in our cellular models was mainly performed through an intensity analyses. A better method, especially to quantify IF markers in midbrain organoids, is the assessment of a marker positive area/total organoid area. We performed this analyses for GFAP and we are going to do it also for other markers, especially TH.

An important finding of this project is TH increased levels in PARK2. Although DA neurons number was similar in PARK2 and CTR we need to perform further experiments in order to confirm that TH expression is increased in a singular PARK2 DA neuron. FACS would be the ideal technique that could be used to record and quantify the fluorescent signal from individual cells. This method could also be very useful to easily count TH-positive cells out of NeuN-positive cells.

No potentially disease-modifying drugs have been tested yet in our *Park2* midbrain organoids. We aim, in the future, to test a KAR antagonist (such as UBP-310) in our *Park2* midbrain organoids to see if the drug is able to reduce neuronal hyperactivity and to rescue *Park2* phenotype.

As already argued in the discussion, *Park2* astrocytes would be better studied in midbrain organoids as glia-neuron interaction is fundamental in the neurodegenerative process. We aim to perform all the analyse we did on 2D astrocytes, also on astrocytes from dissociated midbrain organoids. This would certainly give a more accurate insight in what happens early in the neurodegeneration associated to *Park2* mutation, where astrocytes seem to be co-protagonists.

In the end, we aim also to better define the cellular population of our midbrain organoids and especially to quantify neuronal groups, other than dopaminergic ones, such as:

GABAergic neurons and glutamatergic neurons. Studying the neuronal networks of these organoids and how they change over time can help us in understanding pathogenic mechanisms related to neurological disease, especially, in our case, to *Park2* PD.

7. Conclusions

Park2 PD, for clinical and neuropathological aspects, could be considered a disease distinct from classic idiopathic PD and seems to differ in the pathogenesis as well. Diurnal fluctuations and alleviation of parkinsonian symptoms by sleep are unique features of this form of PD. That may result from an excessive oxidative stress that dopaminergic neurons experience, probably due to a glutamate overstimulation. This is accompanied by an impaired dopamine release, re-uptake and production. As a matter of fact, it is known that Parkin regulates dopamine utilization and suppress dopamine oxidation through a MAOs downregulation. A calcium-independent dopamine release and reduced dopamine re-uptake has been reported by Jiang et al. (Jiang H., 2012). In addition to that Parkin has DNA-binding properties (Alves da Costa C., 2019) and regulate the transcription of a multitude of genes, most of which are still unknown.

We found both TH mRNA and protein levels increased in PARK2 DA neurons and midbrain organoids. Although further studies are needed to assess single cell TH increased expression, these results could suggest that Parkin might be implicated in the long-term regulation of TH expression. According to this consideration enhanced TH mRNA levels could result from an indirect feedback caused by an excessive dopamine loss and reduced dopamine re-uptake. Future investigations should clarify if TH transcription factors are substrates of Parkin and which is exactly *Park2* role in regulating TH expression.

Another important finding that emerged from this study is the increased astrocytic reactivity in *Park2 in vitro* models. It has been established that neuroinflammation is implicated in neurodegeneration associated to PD and that *Park2* mutations are linked to a pro-inflammatory profile (de Léséleuc L, 2013) but not many investigations have been made on the role played by astrocytes in *Park2* neurodegeneration. Astrocytes are the most abundant cell population in the CNS and are fundamental for neurons survival and

differentiation. For this reason, they were studied in this project as well. We also discovered in *Park2* astrocytes reduced glutamate transporter EAAT-2 and increased Gluk2 levels, meaning that astrocytes may play an active role in a possible excitoxic mechanism related to *Park2* mutations.

It has already been demonstrated that Gluk2 is a substrate of Parkin and that when *Park2* is mutated Gluk2 levels arise (Maraschi A, 2014). Parkin loss-of-function enhances the efficacy of glutamatergic synapses and dopaminergic neurons become very vulnerable to excitotoxicity which contributes to neurodegeneration. Although we did not find increased Gluk2 levels in *Park2* DA neurons, we did find an enhanced expression in *Park2* midbrain organoids. Unfortunately, we do not know if increased Gluk2 levels in midbrain organoids belong to astrocytes, to DA neurons or other neuronal types. Further studies are required to assess it. Overexpression of Gluk2 both in astrocytes and DA neurons would probably contribute to an excitotoxic, reactive, pro-inflammatory state that leads to neurodegeneration in the end. KAR inhibition would probably be beneficial on both cell types.

In the end we observed a significantly increased firing rate with an oscillatory pattern in *Park2* midbrain organoids. These oscillatory activity remains even after stimulation with kainite, meaning that when *Park2* is mutated, at basal conditions, KAR is already overstimulated. On the contrary, the oscillatory activity is suppressed by a kainite antagonist, indicating that these oscillations are somehow controlled by KAR. Dysfunctional astrocytes might take part in this process as well. Further studies are needed to better clarify their role.

In conclusion, these results, taken together with the Gluk2 overexpression in midbrain organoids, could support the hypothesis that *Park2* mutations may cause excitotoxicity. Additional research is needed to elucidate how *Park2* neuronal activity is increased and how this is associated to excitotoxicity and neurodegeneration.

Midbrain organoids contain a complex glia-neurons network and recapitulate key neurodevelopment features of human midbrain. For this reason, they should be considered the most suitable model to study monogenic early-onset diseases such as

Park2 PD. All these findings that emerged from preliminary results of this project may lay the basis for the identification of molecular targets that could be used for the detection of novel therapeutic strategies. Considering that they are generated straight from *Park2* patients, organoids share the same metabolism of the patient, and, in the era of personalized medicine, they constitute a unique model suitable for testing new disease-modifying drugs.

Midbrain organoids could be a useful tool to study also other forms of PD such as sporadic late-onset PD, in which PD susceptibility seems to have a neurodevelopment component. Such forms of PD are certainly more challenging to study using organoids, as aging plays an important role. To overcome this problem, overexpression of progerin can be induced in iPSC-derived cell cultures, allowing the generation of an aged phenotype (Miller J.D., 2013) although it may not capture all aspects of normal aging. It is known that PD pathology in sporadic late-onset cases seems to arise in the gastrointestinal tract where microbiota is determinant in the development of the disease. In order to recreate these multifaceted aspects, more complex organoid models such as "assembloids" made of different brain areas, vasculature, immune cells as well as other organs such as intestine would be the ideal *in vitro* model to study such forms of PD (Reiner O., 2021).

Midbrain organoids, besides being a useful tool to investigate pathogenic mechanisms leading to neurodegeneration associated to sporadic and genetic forms of PD, are certainly relevant in studying the response to new drugs in order to tailor the treatment in a "personalized medicine" approach. This would allow to avoid possible side effects and reduce non-responders frequency (Doss M.X., 2019).

In the future, more complex organoid systems, so called "assembloids", would be able to recreate the complicated interactions in the human brain and would be suitable to model a wider spectrum of neurologic diseases.

8. Bibliography

Aboud AA., Tidball AM., Kumar KK. et al. PARK2 patient neuroprogenitors show increased mitochondrial sensitivity to copper. *Neurobiol Dis.* (2015): 204-12.

Ahfeldt T., Ordureau A., Bell C. et al. Pathogenic Pathways in Early-Onset Autosomal Recessive Parkinson's Disease Discovered Using Isogenic Human Dopaminergic Neurons. *Stem Cell Reports* (2020): 4(1):75-90.

Alves da Costa C., Duplan E., Rouland L. et al. The Transcription Factor Function of Parkin: Breaking the Dogma. *Front Neurosci.* (2019): 12:965.

Ambrosi G., Cerri S., Blandini F. et al. A further update on the role of excitotoxicity in the pathogenesis of Parkinson's disease. *J Neural Transm* (2014): 121(8):849-59.

Asakawa S., Tsunematsu K., Takayanagi A. et al. The genomic structure and promoter region of the human Parkin gene. *Biochem. Biophys. Res. Commun* (2001): 863-868.

Asanuma M, Miyazaki I, Murakami S, Diaz-Corrales FJ, Ogawa N. Striatal astrocytes act as a reservoir for L-DOPA. *PLoS One* (2014): 9(9):e106362.

Beach TG., Adler CH., Sue LI. et al. Multi-organ distribution of phosphorylated alpha-synuclein histopathology in subjects with Lewy body disorders. *Acta Neuropathol* (2010): 119: 689–702.

Beasley SA., Hristova VA., Shaw GS. et al. Structure of the parkin in-between-ring domain provides insights for E3-ligase dysfunction in autosomal recessive Parkinson's disease. *Proc. Nat. Acad.* (2007): 3095-3100.

Bendotti C, Guglielmetti F, Tortarolo M, Samanin R, Hirst WD. Differential expression of S100β and glial fibrillary acidic protein in the hippocampus after kainic acid-induced lesions and mossy fiber sprouting in adult rat. *Experimental Neurology.* (2000): 317-329.

Berger U. V., DeSilva T. M., Chen W., Rosenberg P. A. Cellular and subcellular mRNA localization of glutamate transporter isoforms GLT1a and GLT1b in rat brain by in situ hybridization. *J. Comp. Neurol.* (2005): 78-79.

Bernardini J., Lazarou M. & Dewson G. Parkin and mitophagy in cancer. *Oncogene* (2017): 1315–1327 .

Bezard E, Przedborski S. A tale on animal models of Parkinson’s disease. *Mov Disord* (2011): 26: 993–1002.

Blanco-Suárez E., Caldwell AL., Allen NJ. Role of astrocyte-synapse interactions in CNS disorders. *J Physiol.* (2017): 1903-1916.

Blandini F., Porter RH. and Greenamyre JT. Glutamate and Parkinson's disease. *Mol Neurobiol* (1996): 73-94.

Bogetofte H., Jensen P., Okarmus J. et al. Perturbations in RhoA signalling cause altered migration and impaired neuritogenesis in human iPSC-derived neural cells with PARK2 mutation. *Neurobiol Dis.* (2019): 132:104581.

Bonifati V. Autosomal recessive parkinsonism. *Parkinsonism and Relat Disord* (2012): S4–S6.

Booth HDE., Hirst WD and Wade-Martins R. The Role of Astrocyte Dysfunction in Parkinson's Disease Pathogenesis. *Trends Neurosci.* (2017): 40, 358–370.

Braak H., Del Tredici K., Rüb U. et al. Staging of brain pathology related to sporadic Parkinson's disease. *Neurobiol Aging* (2003): 24: 197–211.

Brown P., Williams D. Basal ganglia local field potential activity: character and functional significance in the human. *Clin Neurophysiol.* (2005): 2510-9.

Burns MPL., Zhang GW.,Rebeck HW. et al. Parkin promotes intracellular Aβ1-42 clearance. *Human Molecular Genetics* (2009): vol. 18, no. 17, pp. 3206–3216.

Cakir B., Xiang Y., Tanaka Y. et al. Engineering of human brain organoids with a functional vascular-like system. *Nat Methods* (2019): 16(11):1169-1175.

Cardozo D L. Midbrain dopaminergic neurons from postnatal rat in long-term primary culture. *Neuroscience.* (1993): 409-21.

Cartelli D., Amadeo A., Calogero AM. et al. Parkin absence accelerates microtubule aging in dopaminergic neurons. *Neurobiol Aging.* (2018): 61:66-74. .

Casarejos MJ., Menendez J., Solano RM. et al. Susceptibility torotenone is increased in neurons from parkin null mice and isreduced by minocycline. *J. Neurochem.* (2006): 97, 934–946.

Cerri S., Blandini F. Role of Autophagy in Parkinson's Disease. *Curr Med Chem* (2019): 26(20):3702-3718.

Cesari R., Martin ES., Calin GA. et al. Parkin, a gene implicated in autosomal recessive juvenile parkinsonism, is a candidate tumor suppressor gene on chromosome 6q25-q27. *Proceedings of the National Academy of Sciences of the U.S.A.* (2003): vol. 100, no. 10, pp. 5956–5961.

Chai H., Diaz-Castro B., Shigetomi E. et al. Neural Circuit-Specialized Astrocytes: Transcriptomic, Proteomic, Morphological, and Functional Evidence. *Neuron* (2017): 531-549.

Chambers SM., Fasano CA., Papapetrou EP. et al. Highly efficient neural conversion of human ES and iPS cells by dual inhibition of SMAD signaling. *Nat Biotechnol.* (2009): 275-80.

Chan NC., Salazar AM., Pham AH. et al. Broad activation of the ubiquitin-proteasome system by Parkin is critical for mitophagy. *Human Molecular Genetics* (2011): 1726–1737.

Chlebanowska P., Tejchman A., Sułkowski M. et al. Use of 3D Organoids as a Model to Study Idiopathic Form of Parkinson's Disease. *Int J Mol Sci* (2020): 21(3):694; doi:10.3390/ijms21030694.

Choi D.W. Glutamate neurotoxicity and diseases of the nervous system. *Neuron* 1 (1988): 623–634.

Choi SH., Kim YH., Hebisch M. et al. A three-dimensional human neural cell culture model of Alzheimer's disease. *Nature* (2014): 274-8.

Chung SY., Kishinevsky S., Mazzulli JR. et al. Parkin and PINK1 Patient iPSC-Derived Midbrain Dopamine Neurons Exhibit Mitochondrial Dysfunction and α-Synuclein Accumulation.» *Stem Cell Reports.* (2016): 664-677.

Cipriani S., Chen X., Schwarzschild MA. Urate: a novel biomarker of Parkinson's disease risk, diagnosis and prognosis. *Biomark Med* (2010): 4: 701–12.

Cremer JN., Amunts K., Schleicher A. et al. Changes in the expression of neurotransmitter receptors in Parkin and DJ-1 knockout mice—a quantitative multireceptor study. *Neuroscience* (2015): 539–51.

Cullen DK., Wolf JA., Vernekar VN. et al. Neural tissue engineering and biohybridized microsystems for neurobiological investigation in vitro (Part 1). *Crit Rev Biomed Eng* (2011): 201-40.

Darstein M., Petralia RS., Swanson GT. et al. Distribution of kainate receptor subunits at hippocampal mossy fiber synapses. *J Neurosci.* (2003): 8013-9.

Dawson TM. and Dawson VL.The role of parkin in familial and sporadic Parkinson's disease. *Mov. Disord.* (2010): S32–S39.

De Léséleuc L., Orlova M., Cobat A. et al. PARK2 mediates interleukin 6 and monocyte chemoattractant protein 1 production by human macrophages. *PLoS Negl Trop Dis.* (2013): 7(1):e2015.

Dickson DW. Parkinson's disease and parkinsonism: neuropathology. *Cold Spring Harb Perspect Med* (2012): 2: a009258.

Doss MX, Sachinidis A. Current Challenges of iPSC-Based Disease Modeling and Therapeutic Implications. *Cells* 8.5 (2019): 403.

Dutta D., Heo I., Clevers H. Disease Modeling in Stem Cell-Derived 3D Organoid Systems. *Trends Mol Med.* (2017): 393-410.

Falkenburger BH., Saridaki T., Dinter E. Cellular models for Parkinson's disease. *J Neurochem.* (2016): 121-130.

Fallon L., Moreau F., Croft BG. et al. Parkin and CASK/LIN-2 associate via a PDZ-mediated interaction and are co-localized in lipid rafts and postsynaptic densities in brain. *J Biol Chem* (2002): 486–91.

Gautier CA., Erpapazoglou Z., Mouton-Liger F. et al. The endoplasmic reticulum-mitochondria interface is perturbed in PARK2 knockout mice and patients with PARK2 mutations. *Hum Mol Genet.* (2016): 2972-2984.

Gibb WR., Lees AJ. The relevance of the Lewy body to the pathogenesis of idiopathic Parkinson's disease. *J Neurol Neurosurg Psychiatry* (1988): 51: 745–52.

Glessner JT., Wang K., Cai G et al. Autism genome-wide copy number variation reveals ubiquitin and neuronal genes. *Nature* (2009): vol. 459, no. 7246, pp. 569–573.

Greene JC., Whitworth AJ., Kuo I. et al. Mitochondrial pathology and apoptotic muscle degeneration in Drosophila parkin mutants. *Proc Natl Acad Sci U S A.* (2003): 4078-83.

Haas A. Dopaminergic differentiation of the Nurr1-expressing immortalized mesencephalic cell line CSM14.1 in vitro. *J. Anat.* (2002): 61-69.

Han D.W., Tapia N., hermann A. et al. Direct reprogramming of fibroblasts into neural stem cells by defined factors. *Cell stem cell* (2012): 465-72.

Hattori N., Kitada T., Matsumine H., et al. Molecular genetic analysis of a novel Parkin gene in Japanese families with autosomal recessive juvenile parkinsonism: evidence for variable homozygous deletions in the Parkin gene in affected individuals. *Ann Neurol* (1998): 44(6):935–941.

Hattori N., Mizuno Y. Twenty years since the discovery of the parkin gene. *J Neural Transm* (2017): 1037-1054.

Helton TD., Otsuka T., Lee MC. et al. Pruning and loss of excitatory synapses by the parkin ubiquitin ligase. *Proc. Natl Acad. Sci. USA* (2008): 19492–19497.

Hely MA., Reid WGJ., Adena MA. et al. The Sydney multicenter study of Parkinson's disease: the inevitability of dementia at 20 years. *Mov Disord* (2008): 23: 837–44.

Hermanson E., Joseph B., Castro D. et al. Nurr1 regulates dopamine synthesis and storage in MN9D dopamine cells. *Exp. Cell Res.* (2003): 324–334.

Hirsch EC., Standaert DG. Ten Unsolved Questions About Neuroinflammation in Parkinson's Disease. *Mov Disord.* (2021): 36(1):16-24.

Hirsch EC. Why are nigral catecholaminergic neurons more vulnerable than other cells in Parkinson's disease?. *Ann Neurol* (1992): S88–S93.

Humbert J., Beyer K., Carrato C. et al. Parkin and synphilin-1 isoform expression changes in Lewy body diseases. *Neurobiol Dis* (2007): 26(3):681–687.

Ichinose H., Ohye T., Fujita K. et al. Quantification of mRNA of tyrosine hydroxylase and aromatic L-amino acid decarboxylase in the substantia nigra in Parkinson's disease and schizophrenia. *J Neural Transm Park Dis Dement Sect* (1994): 149-58.

Ikeuchi, K., Marusawa, M., Fujiwara, M. Attenuation of proteolysis-mediated cyclin E regulation by alternatively spliced Parkin in human colorectal cancers. *International Journal of Cancer* (2009): 2029–2035.

Imai, Y., Soda, M., Takahshi, R. Parkin suppresses unfolded protein stress-induced cell death through its E3 ubiquitin-protein ligase activity. *The Journal of Biological Chemistry* (2000): 35661–35664.

Imaizumi Y., Okada Y., Akamatsu W., et al. Mitochondrial dysfunction associated with increased oxidative stress and α-synuclein accumulation in PARK2 iPSC-derived neurons and postmortem brain tissue. *Mol Brain* (2012): 5:35.

Ishikawa A., Tsuji S. Clinical analysis of 17 patients in 12 Japanese families with autosomal-recessive type juvenile parkinsonism. *Neurology* (1996): 47(1):160–166.

Ishikawa S., Taira T., Takahashi-Niki K. et al. Human DJ-1-specific transcriptional activation of tyrosine hydroxylase gene. *J Biol Chem* (2010): 39718-31.

Iwasawa C., Kuzumaki N., Suda Y. et al. Reduced expression of somatostatin in GABAergic interneurons derived from induced pluripotent stem cells of patients with parkin mutations. *Mol Brain.* (2019): 12(1):5.

Jankovic J., McDermott M., Carter J. et al. Variable expression of Parkinson's disease: a base-line analysis of the DATATOP cohort. The Parkinson Study Group. *Neurology* (1990): 40: 1529–34.

Jayaramayya K., Iyer M., Venkatesan D. et al. Unraveling correlative roles of dopamine transporter (DAT) and Parkin in Parkinson's disease (PD) - A road to discovery? . *Brain Res Bull.* (2020): 169-179.

Jiali P., Ting G., Ran Z. et al. Parkin mutation decreases neurite complexity and maturation in neurons derived from human fibroblasts. *Brain Research Bulletin* (2020): 9-15.

Jiang H., Jiang Q., LiuW. et al. Parkin suppresses the expression of monoamine oxidases. *J Biol Chem* (2006): 281, 8591-8599.

Jiang H., Ren Y., Yuen EY. et al. Parkin controls dopamine utilization in human midbrain dopaminergic neurons derived from induced pluripotent stem cells. *Nat Commun* (2012): 3:668.

Jo J., Xiao Y., Sun AX. et al. Midbrain-like Organoids from Human Pluripotent Stem Cells Contain Functional Dopaminergic and Neuromelanin-Producing Neurons. *Cell Stem Cell* (2016): 19(2):248–257. doi:10.1016/j.stem.2016.07.005.

Kalia LV., Lang AE. Parkinson's disease. *Lancet* (2015): 386(9996):896-912.

Kano M., Takanashi M., Oyama G. et al. Reduced astrocytic reactivity in human brains and midbrain organoids with PRKN mutations. *NPJ Parkinsons Dis.* (2020): 6(1):33.

Kano M., Takanashi M., Oyama G. et al. Reduced astrocytic reactivity in human brains and midbrain organoids with PRKN mutations. *NPJ Parkinsons Dis.* (2020): 6(1):33.

Kasten M., Klein C. The many faces ofalpha-synucleinmutations. *Mov Disord* (2013): 697–701.

Kim H., Park HJ., Choi H. et al. Modeling G2019S-LRRK2 Sporadic Parkinson's Disease in 3D Midbrain Organoids. *Stem Cell Reports* (2019): 12(3):518–531. doi:10.1016/j.stemcr.2019.01.020.

Kim HS., Kim J., Jo Y. et al. Direct lineage reprogramming of mouse fibroblasts to functional midbrain dopaminergic neuronal progenitors. *Stem Cell Res* (2013): 60-68.

Kim CY. and Alcalay RN. Genetic Forms of Parkinson's Disease. *Semin Neurol* (2017): 135–146.

Kirkeby A., Grealish S., Wolf DA. et al. Generation of regionally specified neural progenitors and functional neurons from human embryonic stem cells under defined conditions. *Cell Rep.* (2012): 703-14.

Kitada T., Asakawa S., Hattori N. et al. Mutations in the parkin gene cause autosomal recessive juvenile parkinsonism. *Nature* (1998): 392(6676):605-608.

Klein C., Lohmann-Hedrich K., Rogaeva E. et al. Deciphering the role of heterozygous mutations in genes associated with parkinsonism. *Lancet Neurol* (2007): 6: 652–62.

Klein C., Lohmann Hedrich K., Rogaeva E. et al. Deciphering the role of heterozygous mutations in genes associated with parkinsonism. *Lancet Neurol* (2007): 652–662.

Konovalova EV., Lopacheva OM., Grivennikov IA. et al. Mutations in the Parkinson's Disease-Associated PARK2 Gene Are Accompanied by Imbalance in Programmed Cell Death Systems. *Acta Naturae.* (2015): 146-9.

Krebs CE., Karkheiran S., Powell JC. et al. The Sac1 domain of SYNJ1 identifi ed mutated in a family with early-onset progressive parkinsonism with generalized seizures. *Hum Mutat* (2013): 34: 1200–07.

Kriks S., Shim JW., Piao J. et al. Dopamine neurons derived from human ES cells efficiently engraft in animal models of Parkinson's disease. *Nature* (2011): 547-51.

Kubo SI., Kitami T., Noda S. et al. Parkin is associated with cellular vesicles. *J Neurochem* (2001): 78: 42–54.

La Cognata V., Iemmolo R., D'Agata V. et al. Increasing the coding potential of genomes through alternative splicing: the case of PARK2 gene. *Curr Genomics* (2014): 15(3):203–216. .

Lancaster MA., Corsini NS., Burkard TR. et al. Guided self-organization recapitulates tissue architecture in a bioengineered brain organoid model. *BioRxiv* (2016).

Lancaster MA., Knoblich JA. Generation of cerebral organoids from human pluripotent stem cells. *Nat Protoc.* (2014): 2329-40.

Lancaster MA., Knoblich JA. Organogenesis in a dish: modeling development and disease using organoid technologies. *Science* (2014): 345(6194):1247125.

Lancaster MA., Renner M., Martin CA. Cerebral organoids model human brain development and microcephaly. *Nature* (2013): 373–379.

Lewerenz J., Maher P. Chronic glutamate toxicity in neurodegenerative diseases-what is the evidence? *Front Neurosci* (2015): 469.

Liddelow SA., Guttenplan KA., Clarke LE. et al. Neurotoxic reactive astrocytes are induced by activated microglia. *Nature* (2017): 481-487.

Liu B., Traini R., Killinger B. et al. Overexpression of parkin in the rat nigrostriatal dopamine system protects against methamphetamine neurotoxicity. *Exp Neurol* (2013): 59–372.

Lotharius J., Falsig J., van Beek J. et al. Progressive degeneration of human mesencephalic neuron-derived cells triggered by dopamine-dependent oxidative stress is dependent on the mixed-lineage kinase pathway. *Neurosci* (2005): 6329–6342.

Lücking CB., Dürr A., Bonifati V. et al. Association between early-onset Parkinson's disease and mutations in the parkin gene. *N Engl J Med* (2000): 342: 1560–67.

Malik AR., Willnow T.E. Excitatory amino acid transporters in physiology and disorders of the central nervous system. *Int J Mol Sci* (2019): 20-22.

Mallet N., Delgado L., Chazalon M. et al. Cellular and Synaptic Dysfunctions in Parkinson's Disease: Stepping out of the Striatum. *Cells.* (2019): 8(9):1005.

Mansour AA., Gonçalves JT., Bloyd CW. et al. An in vivo model of functional and vascularized human brain organoids. *Nat Biotechnol* (2018): 36(5):432-441.

Maraschi A., Ciammola A., Folci A. et al. Parkin regulates kainate receptors by interacting with the GluK2 subunit. *Nat Commun.* (2014): 5:5182.

Marongiu R., Ferraris A., Ialongo T. et al. PINK1 heterozygous rare variants: prevalence, significance and phenotypic spectrum. *Human Mutat* (2008): (4):565.

Marote A., Pomeshchik Y., Goldwurm S. et al. Generation of an induced pluripotent stem cell line (CSC-44) from a Parkinson's disease patient carrying a compound heterozygous mutation (c.823C>T and EX6 del) in the PARK2 gene. *Stem Cell Res.* (2018): 27:90-94.

Marras C., Lang A. Parkinson's disease subtypes: lost in translation? *J Neurol Neurosurg Psychiatry* (2013): 84: 409–15.

Matsumine H., Saito M., Shimoda-Matsubayashi S. et al. Localization of a gene for an autosomal recessive form of juvenile Parkinsonism to chromosome 6q25.2-27. *Am J Hum Genet* (1997): 60(3):588–596.

Matsumine H., Yamamura Y., Kobayashi T. et al. Early onset parkinsonism with diurnal fluctuation maps to a locus for juvenile parkinsonism. *Neurology* (1998b): 1340–1345.

McGeer PL., Itagaki S., Boyes BE. et al. Reactive microglia are positive for HLA-DR in the substantia nigra of Parkinson's and Alzheimer's disease brains. *Neurology* (1988): 1285-1291.

Mehta A., Prabhakar M., Kumar P. et al. Excitotoxicity: bridge to various triggers in neurodegenerative disorders. *Eur J Pharmacol.* (2013): 698(1-3):6-18.

Mellick GD., Siebert GA., Funayama M. et al. Screening PARK genes for mutations in early-onset Parkinson's disease patients from Queensland, Australia. *Parkinsonism Relat Disord* (2009): 15:105-9.

Miller JD, Ganat YM, Kishinevsky S, Bowman RL, Liu B, Tu EY, Mandal PK, Vera E, Shim JW, Kriks S, Taldone T, Fusaki N, Tomishima MJ, Krainc D, Milner TA, Rossi DJ, Studer L. Human iPSC-based Modeling of Late-Onset Disease via Progerin-induced Aging. *Cell Stem Cell.* 13.6 (2013): 691–705.

Mira MT., Alca¨ıs A., van Thuc H. et al. Susceptibility to leprosy is associated with PARK2 and PACRG. *Nature* (2004): 636-640.

Monzel AS., Smits LM., Hemmer K., et al. Derivation of Human Midbrain-Specific Organoids from Neuroepithelial Stem Cells. *Stem Cell Reports* (2017): 8(5):1144–1154. doi:10.1016/j.stemcr.2017.03.010.

Mori H., Kondo T., Yokochi M. et al. Pathologic and biochemical studies of juvenile parkinsonism linked to chromosome 6q. *Neurology* (1998): 890–892.

Moussawi K., Riegel A., Nair S. and Kalivas P.V. Extracellular glutamate: functional compartments operate in different concentration ranges. *Front Syst Neurosci* 5 (2011): 94.

Murabe Y., Ibata Y. e Sano Y. Proliferative response of non-neuronal elements in the hippocampus of the rat to kainic acid-induced lesions. *Cell Tissue Res* (1982): 223-226.

Nagatsu T., Nakashima A., Ichinose H. et al. Human tyrosine hydroxylase in Parkinson's disease and in related disorders. *J Neural Transm (Vienna)* (2019): 397-409.

Nagatsu T., Kato T., Numata Y. et al. Phenylethanolamine N-methyltransferase and other enzymes of catecholamine metabolism in human brain. *Clin Chim Acta* (1977): 221-32.

Nakashima A., Kaneko YS., Kodani Y. et al. Intracellular stability of tyrosine hydroxylase: phosphorylation and proteasomal digestion of the enzyme. *Adv Pharmacol* (2013): 68:3-11.

Nalls MA., Pankratz N., Lill CM. et al. Large-scale meta-analysis of genome-wide association data identifi es six new risk loci for Parkinson's disease. *Nat Genet* (2014): 46: 989–93.

Narendra D., Tanaka A., Suen DF. et al. Parkin is recruited selectively to impaired mitochondria and promotes their autophagy. *J Cell Biol.* (2008): 795-803.

Nolbrant S., Giacomoni J., Hoban DB. et al. Direct Reprogramming of Human Fetal- and Stem Cell-Derived Glial Progenitor Cells into Midbrain Dopaminergic Neurons. *Stem Cell Reports* (2020): 869-882.

Noyce AJ., Bestwick JP., Silveira-Moriyama L. et al. Meta-analysis of early nonmotor features and risk factors for Parkinson disease. *Ann Neurol* (2012): 72: 893–901.

Nuytemans K., Theuns J., Cruts M. et al. Genetic etiology of Parkinson disease associated with mutations in the SNCA, PARK2, PINK1, PARK7, and LRRK2 genes: a mutation update. *Hum Mutat.* (2010): 763-80.

Okarmus J., Bogetofte H., Schmidt SI. et al. Lysosomal perturbations in human dopaminergic neurons derived from induced pluripotent stem cells with PARK2 mutation. *Sci Rep.* (2020): 10(1):10278.

Okarmus J., Havelund JF., Ryding M. et al. Identification of bioactive metabolites in human iPSC-derived dopaminergic neurons with PARK2 mutation: Altered mitochondrial and energy metabolism. *Stem Cell Reports* (2021): 1510-1526.

Oyama G., Yoshimi K., Natori S. et al. Impaired in vivo dopamine release in parkin knockout mice. *Brain Res* (2010): 1352:214-22.

Pajares M., I Rojo A., Manda G. et al. Inflammation in Parkinson's Disease: Mechanisms and Therapeutic Implications. *Cells* (2020): 9(7):1687.

Palacino JJ., Sagi D., Goldberg MS. et al. Mitochondrial dysfunction andoxidative damage in parkin-deficient mice. *J. Biol. Chem.* (2004): 279, 18614–18622.

Paşca AM., Sloan SA. , Clarke LE. et al. Functional cortical neurons and astrocytes from human pluripotent stem cells in 3D culture. *Nat Methods* (2015): 12(7):671-8.

Pawlyk AC., Giasson BI., Sampathu DM. et al. Novel monoclonal antibodies demonstrate biochemical variation of brain parkin with age. *J Biol Chem* (2003): 278(48): 48120–48128.

Perez FA., Palmiter RD. Parkin-deficient mice are not a robust model of parkinsonism. *Proc Natl Acad Sci U S A.* (2005): 102(6):2174-9.

Periquet M., Latouche M., Lohmann ., et al. Parkin mutations are frequent in patients with isolated early-onset parkinsonism. *Brain* (2003): 126: 1271–78.

Petrucci S., Ginevrino M., Trezzi I. et al. GBA-Related Parkinson's Disease: Dissection of Genotype-Phenotype Correlates in a Large Italian Cohort. *Mov Disord* (2020): 35(11):2106-2111.

Pham MT., Pollock KM., Rose MD. et al. Generation of human vascularized brain organoids. *Neuroreport* (2018): 9(7):588-593.

Phani S., Loike JD., Przedborski S. Neurodegeneration and infl ammation in Parkinson's disease. *Parkinsonism Relat Disord* (2012): 18: S207–09.

Pickrell AM., Youle RJ. The roles of PINK1, parkin, and mitochondrial fidelity in Parkinson's disease. *Neuron* (2015): 257-73.

Polymeropoulos MH., Lavedan C., Leroy E. et al. Mutation in the alpha-synuclein gene identified in families with Parkinson's disease. *Science* (1997): 276(5321):2045-7.

Postuma RB., Aarsland D., Barone P. et al. Identifying prodromal Parkinson's disease: pre-motor disorders in Parkinson's disease. *Mov Disord* (2012): 27: 617–26.

Poulopoulos M., Levy OA., Alcalay RN. The neuropathology of genetic Parkinson's Disease. *Mov Disord* (2012): 831–42.

Prensa L., Giménez-Amaya JM., Parent A. et al. The nigrostriatal pathway: axonal collateralization and compartmental specificity. *J Neural Transm Suppl.* (2009): (73):49-58.

Pu J., Gao T., Zheng R. et al. Parkin mutation decreases neurite complexity and maturation in neurons derived from human fibroblasts. *Brain Res Bull.* (2020): 9-15.

Puschmann A. Monogenic Parkinson's disease and parkinsonism: clinical phenotypes and frequencies of known mutations. *Parkinsonism Relat Disord* (2013): 19: 407–15.

Qian X., Nguyen HN., Song MM. et al. Brain-Region-Specific Organoids Using Mini-bioreactors for Modeling ZIKV Exposure. *Cell* (2016): 165(5):1238–1254. doi:10.1016/j.cell.2016.04.032.

Quinn N., Critchley P., Marsden CD. Young onset Parkinson's disease. *Mov Disord* (1987): 73-91.

Raja WK., Mungenast AE., Lin YT. et al. Self-Organizing 3D Human Neural Tissue Derived from Induced Pluripotent Stem Cells Recapitulate Alzheimer's Disease Phenotypes. *PLoS One.* (2016): 11(9):e0161969.

Regoni M., Cattaneo S., Mercatelli D. et al. Pharmacological antagonism of kainate receptor rescues dysfunction and loss of dopamine neurons in a mouse model of human parkin-induced toxicity. *Cell Death Dis.* (2020): 11(11):963.

Reiner O., Sapir T. & Parichha A. Using multi-organ culture systems to study Parkinson's disease. . *Mol Psychiatry* 26 (2021): 725–735.

Reinhardt P., Glatza M., Hemmer K. et al. Derivation and expansion using only small molecules of human neural progenitors for neurodegenerative disease modeling. *PLoS One.* (2013): 8(3):e59252.

Ren Y., Jiang H., Hu Z. et al. Parkin mutations reduce the complexity of neuronal processes in iPSC-derived human neurons. *Stem Cells.* (2015): 33(1):68-78.

Rimmele T. S., Rosenberg P. A. GLT-1: The elusive presynaptic glutamate transporter. *Neurochem. Int.* (2016): 18-28.

Ring KL., Tong LM., Balestra ME. et al. Direct reprogramming of mouse and human fibroblasts into multipotent neural stem cells with a single factor. *Cell stem cell* (2012): 100-9.

Rothstein J.D., Martin L., Levey A.I., Dykes-Hoberg M., Jin L., Wu D., et al. Localization of neuronal and glial glutamate transporters. *Neuron* (1994): 713–725.

Rubio de la Torre E., Luzon-Toro B., Forte-Lago I. et al. Combined kinase inhibition modulates parkin inactivation. *Hum. Molec. Genet.* (2009): 809-823.

Sánchez-Danés A., Richaud-Patin Y., Carballo-Carbajal I. et al. Disease-specific phenotypes in dopamine neurons from human iPS-based models of genetic and sporadic Parkinson's disease. *EMBO Mol Med.* (2012): 4(5):380-395.

Santos R., Vadodaria KC., Jaeger BN. et al. Differentiation of Inflammation-Responsive Astrocytes from Glial Progenitors Generated from Human Induced Pluripotent Stem Cells. *Stem Cell Reports.* (2017): 1757-1769.

Sassone J., Serratto G., Valtorta F. et al. The synaptic function of parkin. *Brain* (2017): 40(9):2265-2272.

Schmitt A., Asan E., Puschel B., Jons T., Kugler P. Expression of the glutamate transporter GLT1 in neural cells of the rat central nervous system: non-radioactive in situ hybridization and comparative immunocytochemistry. *Neuroscience* (1996): 989–1004. .

Scholz D., Poeltl D., Genewsky A. et al. Rapid, complete and large-scale generation of post-mitotic neurons from the human LUHMES cell line. *J. Neurochem.* (2011): 957–971.

Schrag A., Schott JM. Epidemiological, clinical, and genetic characteristics of early-onset parkinsonism. *Lancet Neurol* (2006): 355–363.

Shaltouki A., Sivapatham R., Pei Y. Mitochondrial alterations by PARKIN in dopaminergic neurons using PARK2 patient-specific and PARK2 knockout isogenic iPSC lines. *Stem Cell Reports* (2015): 847-59.

Shigetomi E., Saito K., Sano F., Koizumi S. Aberrant Calcium Signals in Reactive Astrocytes: A Key Process in Neurological Disorders. *Int J Mol Sci.* 20.4 (2019): 996.

Shimura H., Hattori N., Kubo S. Immunohistochemical and subcellular localization of Parkin protein: absence of protein in autosomal recessive juvenile parkinsonism patients. *Annals of Neurology* (1999): 668–672.

Sidransky E., Nalls MA., Aasly JO. et al. Multicenter analysis of glucocerebrosidase mutations in Parkinson's disease. *N Engl J Med* (2009): 361: 1651–61.

Sidransky E., Lopez G. The link between the GBA gene and parkinsonism. *Lancet Neurol* (2012): 11: 986–98.

Simpson J.E., Ince P.G., Lace G., Forster G., Shaw P.J., Matthews F., et al. . Astrocyte phenotype in relation to Alzheimer-type pathology in the ageing brain. *Neurobiol. Aging* 31 (2010): 578–590.

Singh K., Han K., Tilve S. et al. Parkin targets NOD2 to regulate astrocyte endoplasmic reticulum stress and inflammation. *Glia* (2018): 2427-2437.

Singleton AB., Farrer MJ., Bonifati V. The genetics of Parkinson's disease: progress and therapeutic implications. *Mov Disord* (2013): 28: 14–23.

Sironi .F, Primignani P., Zini M. et al. Parkin analysis in early onset Parkinson's disease. *Parkinsonism Relat Disord* (2008): 14:326-33.

Sliter DA., Martinez J., Hao L. et al. Parkin and PINK1 mitigate STING-induced inflammation. *Nature* (2018): 258–262.

Smits LM., Reinhardt L., Reinhardt P. et al. Modeling Parkinson's disease in midbrain-like organoids. *NPJ Parkinsons Dis.* (2019): 5:5; doi:10.1038/s41531-019-0078-4.

Sofroniew MV., Vinters HV. Astrocytes: biology and pathology. *Acta Neuropathol.* (2010): 7-35.

Solano RM., Casarejos MJ., Menéndez-Cuervo J. et al. Glial dysfunction in parkin null mice: effects of aging. *J Neurosci.* (2008): 598-611.

Song P., Trajkovic K., Tsunemi T. et al. Parkin Modulates Endosomal Organization and Function of the Endo-Lysosomal Pathway. *J Neurosci.* (2016): 2425-37.

Sossi V., De la Fuente-Fernández R., Schulzer M. Age-related differences in levodopa dynamics in Parkinson's: implications for motor complications. *Brain* (2006): 1050-8.

Staropoli JF., McDermott C., Martinat C. et al. Parkin is a component of an SCF-like ubiquitin ligase complex and protects postmitotic neurons from kainate excitotoxicity. *Neuron* (2003): 735-49.

Stichel CC., Augustin M., Kuhn K. et al. Parkin expression in the adult mouse brain. E. *Eur J Neurosci* (2000): 12(12):4181–4194.

Suzuki S., Akamatsu W., Kisa F. et al. Efficient induction of dopaminergic neuron differentiation from induced pluripotent stem cells reveals impaired mitophagy in PARK2 neurons. *Biochem Biophys Res Commun.* (2017): 483(1):88-93.

Tabata Y., Imaizumi Y., Sugawara M. et al. T-type Calcium Channels Determine the Vulnerability of Dopaminergic Neurons to Mitochondrial Stress in Familial Parkinson Disease. *Stem Cell Reports.* (2018): 1171-1184.

Takahashi H., Ohama E., Suzuki S. et al. Familial juvenile parkinsonism: clinical and pathologic study in a family. *Neurology* (1994): 437–441.

Takahashi K., Yamanaka S. Induction of pluripotent stem cells from mouse embryonic and adult fibroblast cultures by defined factors. *Cell.* (2006): 126(4):663–676. doi:10.1016/j.cell.2006.07.024.

Tang, Y. Microglial Polarization in the Pathogenesis and Therapeutics of Neurodegenerative. *Front. Aging Neurosci.* (2018): 10, 154.

Tariq M., Liu H., Ibañez DP. et al. Generation of three induced pluripotent stem cell lines from a Parkinson's disease patient with mutant PARKIN (p. C253Y). *Stem Cell Res.* (2020): 45:101822.

Terada T., Yokokura M., Yoshikawa E. et al. Extrastriatal spreading of microglial activation in Parkinson's disease: a positron emission tomography study. *Ann Nucl Med* (2016): 579-587.

Thomas M., Beal B. Parkinson's disease. *Hum. Mol. Genet.* (2007): 16 Spec No. 2, R183–R194.

Thomson JA., Itskovitz-Eldor J., Shapiro SS. et al. Embryonic stem cell lines derived from human blastocysts. *Science* (1998): 1145-7.

Thomson JA., Kalishman J., Golos TG. et al. Isolation of a primate embryonic stem cell line. *Proc Natl Acad Sci U S A.* (1995): 7844-8.

Tieng V., Stoppini L., Villy S. et al. Engineering of midbrain organoids containing long-lived dopaminergic neurons. *Stem Cells Dev.* (2014): 1535-47.

Verkhratsky M., Nedergaard A. Physiology of astroglia. *Physiol Rev* (2018): 239-389.

Vincow ES., Merrihew G., Thomas RE. et al. The PINK1-Parkin pathway promotes both mitophagy and selective respiratory chain turnover in vivo. *Proc Natl Acad Sci U S A.* (2013): 6400-5.

Wang Q., Yu S., Simonyi A., Sun G.Y., Sun A.Y. Kainic acid-mediated excitotoxicity as a model for neurodegeneration. *Mol Neurobiol.* 31 (2005): 3-16.

Wang Y., Chen J., Hu JL. et al. Reprogramming of mouse and human somatic cells by high-performance engineered factors. *EMBO Rep.* (2011): 373-8.

Warren Olanow C., Kieburtz K. Factors predictive of the development of Levodopa-induced dyskinesia and wearing-off in Parkinson's disease. *Mov Disord* (2013): 1064-71.

Wichmann T., Dostrovsky JO. Pathological basal ganglia activity in movement disorders. *Neuroscience* (2011): 232-44.

Wilson GR., Sim JC., McLean C., et al. Mutations in RAB39B cause X-linked intellectual disability and early-onset Parkinson disease with α-synuclein pathology. *Am J Hum Genet* (2014): 95: 729–35.

Witte ME., Bol JGJM., Gerritsen WH. et al. Parkinson's disease-associated parkin colocalizes with Alzheimer's disease and multiple sclerosis brain lesions. *Neurobiol Dis* (2009): 445–452.

Wortzel I., and Seger R. The ERK Cascade: Distinct Functions within Various Subcellular Organelles. *Genes & cancer* 2,3 (2011): 195-209.

Yamamura Y., Kohriyama T., Kawakami H. et al. Early-onset parkinsonismwith diurnal fluctuation – clinicopathological studies. *RinshoShinkeigaku (Tokyo)* (1993): 33: 491-496.

Yamamura Y., Sobue I., Ando K. et al. Paralysis agitans of early onset with marked diurnalfluctuation of symptoms. *Neurology* (1973): 23: 239–244.

Yamamura Y. The long journey to the discovery of PARK2: The 50th Anniversary of Japanese Society of Neuropathology. *Neuropathology*. (2010): 30(5):495-500.

Yamamura Y., Kuzuhara S., Kondo K. et al. Clinical, pathologic and genetic studies on autosomal recessive early-onset parkinsonism with diurnal fluctuations.» *Parkinsonism Relat Disord* (1998): 4: 65-72.

Yamamura Y., Iida M., Ando K. et al. Juvenile familial disorder with rigidospasticity, bradykinesia andminor dystonia alleviated after sleep. *Rinsho Shinkeigaku (Tokyo)* (1968): 8:233-238.

Yetnikoff L., Lavezzi HN., Reichard RA. et al. An update on the connections of the ventral mesencephalic dopaminergic complex. *Neuroscience* (2014): 282:23-48.

Yokota M., Kakuta S., Shiga T. et al. Establishment of an in vitro model for analyzing mitochondrial ultrastructure in PRKN-mutated patient iPSC-derived dopaminergic neurons. *Mol Brain.* (2021): 14(1):58.

Zanon A., Riekschnitz D., Von Troyer M. et al. Generation of an induced pluripotent stem cell line (EURACi005-A) from a Parkinson's disease patient carrying a homozygous exon 3 deletion in the PRKNgene. *Stem Cell Res.* (2019): 41:101624.

Zhang H., Sulzer D. Glutamate spillover in the striatum depresses dopaminergic transmission by activating group I metabotropic glutamate receptors. *J Neurosci* (2003): 10585-10592.

Zhang P., Xia N., Reijo Pera RA. Directed dopaminergic neuron differentiation from human pluripotent stem cells. *J Vis Exp.* (2014): (91):51737.

Zhong P., Hu Z., Jiang H. et al. Dopamine Induces Oscillatory Activities in Human Midbrain Neurons with Parkin Mutations. *Cell Rep.* (2017): 1033-1044.